# CORRELATING NONLINEAR STATIC AND DYNAMIC ANALYSES OF REINFORCED CONCRETE FRAMES

By
Janelle N. Marsh
JoAnn Browning

A Report on Research Sponsored by

National Science Foundation Grant No. CMS-9904090

Structural Engineering and Engineering Materials
SM Report No. 64

UNIVERSITY OF KANSAS CENTER FOR RESEARCH, INC.
LAWRENCE, KANSAS
July 2001

## ABSTRACT

Nonlinear static and dynamic analyses for the design of reinforced concrete frames for strong ground motion are explored in the study. The objectives of the study are to determine 1) the correlation between results from nonlinear static and dynamic analyses, 2) the optimal lateral loading distribution for static analysis, 3) the simplest lateral load distribution that provides adequate results, and 4) the parameters that are reasonably calculated using static analysis for use in design. Parameters included in the study were four number of stories, three frame configurations, four lateral loading distributions for use in static analysis, and ten strong ground motion records for use in dynamic analysis. The key design items were base shear, location of member yielding, column ductility, controlling mechanism, distorted shape of the frame, story drift ratio, and shear and rotation in the members. Results indicated that static analysis provided fair estimates of base shear, general member yielding, distorted shape, and story drift, but gave insufficient estimates of member shear and rotation and the exact location of the controlling mechanism in the frames. The uniform loading distribution best estimated base shear and member shear and rotation, whereas the loading distribution based on provisions in FEMA-356 best estimated the distorted shape, story drift, and column ductility. Overall, precise results from static analysis can not be expected because the results from dynamic analysis vary widely.

## AKNOWLEDGEMENTS

This report is based on a thesis submitted by Jenelle N. Marsh in partial fulfillment of the requirements of the M.S.C.E. degree. Support for this research was provided by the National Science Foundation under NSF Grant No. CMS-9904090.

## TABLE OF CONTENTS

## LIST OF TABLES

## LIST OF FIGURES

# CHAPTER 1

# INTRODUCTION

## 1.1 STATEMENT OF THE PROBLEM

Analysis of buildings subjected to earthquakes can be time-consuming and costly. In some areas of the country, experience in earthquake design is limited, and the analysis of buildings is even more time-consuming and costly. The most difficult task of building analysis for earthquake design is predicting the correct earthquake ground motion. Simplified methods are advantageous because they eliminate the need for selecting ground motion data. However, the confidence level as to the accuracy of the simplified methods over more detailed methods is questionable.

Current design codes encourage the use of nonlinear static analysis as a simplified method for the earthquake resistant design of building structures (ATC40, 1996; FEMA, 1997; FEMA, 2000). However, few studies have addressed and compared the effects that different static loading patterns have on structures in nonlinear static analysis. More information also is needed concerning which key criteria should be emphasized in static analysis, such as member shear and rotation, building drift, and story drift ratio.

## 1.2 BACKGROUND OF NONLINEAR STATIC ANALYSIS

Several researchers have conducted studies involving static nonlinear analyses. The results of these studies are summarized in the following section.

Fajfar and Fischinger (1987 and 1988) proposed a method for the nonlinear analysis of regular buildings oscillating predominantly in the first mode. First, a multi-degree of freedom (MDOF) system is analyzed statically using a uniform and linear loading distribution. Next, the MDOF system is converted into an equivalent single degree of freedom (SDOF) system and analyzed dynamically. The nonlinear characteristics of the system are based on the base shear-displacement relationship obtained in the static analysis. A validation of the method was performed on a 7-story reinforced concrete frame-wall building in Tsukuba, Japan. The building was analyzed with the proposed method and with nonlinear dynamic analysis using the El Centro record of 1940

amplified by 1.5. The resulting displacements from the MDOF system analyzed statically and the SDOF system analyzed dynamically matched reasonably well with the MDOF system analyzed dynamically. The locations of plastic hinges found in the static analysis matched the locations found in the dynamic analysis very well.

Yoshimura (1997) investigated a reinforced concrete building with a tall first story collapsed by the Hyogoken-Nanbu earthquake of 1995. The building was a 7-story apartment house, and the first story was used for parking lots. The building contained both structural and non-structural walls in the north-south direction, whereas the east-west direction was a frame structure. Actual damage to the building was concentrated in the first story of the north-south direction, and a first story mechanism formed in this direction. Two models of the building, considering the walls structural and non-structural, were analyzed statically and dynamically. The static analysis performed on the building used a linear load with extra force at the roof as described in the Japanese building code provisions. For both the static and dynamic analyses of the building, almost all the displacement concentrated on the first story. The hinge formation in the static and dynamic analyses was similar. The building model considering the walls non-structural matched the actual building response better.

Kim and D'Amore (1999) reviewed the nonlinear static analysis capacity spectrum method outlined in ATC40 (ATC, 1996). The method uses the first mode shape forcing function to push the model. A 6-story steel commercial building built in 1997

located in Burbank, California was used to evaluate the accuracy of the capacity spectrum method. The welded moment connections were assumed to displace 0.02 radians in plastic rotation without failure. A nonlinear static analysis was performed on one frame. The most severe damage that was calculated occurred in the base of the ground level columns and the third level girders. The maximum plastic rotation of 0.02 radians was not surpassed at a roof drift of 35 cm. A nonlinear dynamic analysis was performed on the building using three unscaled near-source earthquake records: two records from the Northridge event and a record from the Kobe event of 1995. The maximum base shear force and roof drift was nearly the same from the static and dynamic analyses. The hinge distribution for the three earthquakes was greater in the dynamic than in the static analysis

Kunnath and Gupta (1999) introduced a new spectra-compatible nonlinear static analysis procedure for regular buildings that takes higher mode effects into consideration. The procedure incorporates ground motion characteristics and a changing load pattern from one step to the next to account for changes in member stiffness. The procedure estimates the location of plastic hinges and distribution of story drift along the height of the building. A step-by-step analysis method was described:

1) Compute a spectrum using both several ground motions and a smooth NEHRP-type design spectrum.

2) Compute the story forces at each level for the modes to be included in the analysis.
3) Combine the modal base shears using a square root of the sum of the squares combination.
4) Perform a static analysis of the structure using scaled incremental story forces corresponding to each mode independently.
5) Compute element forces, displacements, story drifts, and member rotations by a square root of the sum of the squares combination of the respective modal quantities for each step and add to the previous step.

A validation of the method was performed using a 14-story model. The proposed method was compared to a nonlinear dynamic analysis using Northridge earthquake records from 1994. The static analysis both using smooth spectra and actual spectra compared well to results from the dynamic analysis in terms of identification of plastic hinging locations and estimated the story drift to within 1%.

Lew and Kunnath (2000) modeled the 7-story Holiday Inn building located in Los Angeles, California. Twenty ground motions were selected to perform linear and nonlinear dynamic analyses of the building, lateral forces according to Equation 3-7 in FEMA-273 (Equations 3-11 and 3-12 in FEMA-356) were selected to perform a linear static analysis, and a triangular loading distribution was selected to perform a

nonlinear static analysis. The equations in FEMA-273 and FEMA 256 combine to produce the following equation:

$$Fx = \frac{w_x h_x^{\,k}}{\sum_{i=1}^{n} w_i h_i^{\,k}} \tag{1.1}$$

where:

$F_x$ = lateral load applied at any floor level $x$

$h_i$ = height from the base to floor level $i$

$h_x$ = height from the base to floor level $x$

$W_i$ = portion of the total building weight $W$ assigned to floor level $i$

$W_x$ = portion of the total building weight $W$ assigned to floor level $x$

$k$ = 2.0 for $T \geq 2.5$ seconds

= 1.0 for $T \leq 0.5$ seconds

Results from the four analyses were compared to the acceptance criteria specified in the NEHRP Guidelines, including shear, axial, and plastic rotation demands in the members. In the linear static procedure, the demands on the columns in the lower stories of the building were found to be unacceptable, whereas most beam demands were acceptable. In the linear dynamic procedure, most column and beam demands were unacceptable. In both the nonlinear static and dynamic procedures, beam demands in the middle stories and most column demands were unacceptable. Generally, the linear static procedure resulted in low demands. Thus, it is more likely to pass acceptance criteria. Although the linear and nonlinear dynamic procedures

generally exceeded acceptance criteria, the distribution of demands differed. In comparing the nonlinear static and dynamic analyses, the average column and beam demands from the dynamic analysis matched to within 0.03 radians of plastic rotation in the static analysis, but the static analysis underestimated the maximum demands by 0.12 radians.

Yang and Wang (2000) performed a study on the improvement of nonlinear static analysis. Three different loading patterns were used to evaluate three structures varying in number of stories and configuration. A 12-story structure with discontinuous upper columns and a tall seventh story and 8- and 16-story stepped structures were used in the study. Results from static analyses using the loading patterns were compared to results from dynamic analyses. The first pattern was a linear load. The second was found using Equation 1.1. The third pattern utilizes story shear forces calculated using a square root of the sum of the squares combination of three modes when the period and modes are known at a previous load step. For structures whose fundamental period is less than two seconds, all three patterns compared well with results from dynamic analysis in terms of elasto-plastic displacement rotation in members. Although the third pattern best approximates the behavior of the structures during strong ground motion, the linear and FEMA-based loading distributions provide sufficient estimates of roof displacement, rotation, and story shear force.

In summary, researchers have analyzed buildings statically using linear, linear with extra force at the roof, uniform, first mode-shaped, FEMA-based, and story shear force-based loading patterns. They have also used more complex loading patterns that change shape with each load step. Most of the researchers found satisfactory correlation between results from static and dynamic analyses in terms of member rotation, shear force, axial force, displacement, story drift, and location of plastic hinges.

## 1.3 ADVANTAGES AND LIMITATIONS OF NONLINEAR STATIC ANALYSIS

Krawinkler and Seneviratna (1998) identified two main advantages of nonlinear static analysis. First, it encourages design engineers to recognize key factors in seismic response and use good judgment concerning the force and deformation demands and capacities that control the seismic response of a structure. Second, it can uncover design weaknesses, such as excessive deformation demands, story mechanisms, strength irregularities, and overloads on potentially brittle elements, which may not otherwise surface in a linear analysis.

Kim and D'Amore (1999) identified several limitations of simple nonlinear static analysis. Nonlinear static analysis implies that structural capacity and earthquake demand separate. It assumes that damage of a structure is dependent upon lateral

deformation but not cumulative effects over time. It is simply a static analysis, and does not take into account the dynamics of a structure; kinetic and viscous damping energy are significant. Nonlinear static analysis creates a two-dimensional view of a structure, and ignores three-dimensional effects. The vertical loading on a structure is neglected. It oversimplifies the response of a structure by reducing its behavior to the base shear-roof drift relationship of the structure. It does not account for the progressive change in the modal properties of a structure throughout its response.

Although the theoretical basis for nonlinear static analysis has flaws, it remains a popular tool for analysis and design of structures. It provides a practical solution for estimating building response in the absence of a known ground motion. Nevertheless, it is important to clearly understand the benefits and limitations of using the method.

## 1.4 OBJECT AND SCOPE

The objectives of the study are to determine 1) the correlation between results from nonlinear static and dynamic analyses, 2) the optimal lateral loading distribution, 3) the simplest lateral load distribution that provides adequate results, and 4) the key design items needed to be considered in design and analysis.

Only bare reinforced concrete frames without walls or bracing were considered. The study includes regular frames, regular frames with a tall first story, and irregular

stepped frames varying from 4 to 16 stories. The bay widths of the frames, girder dimensions, and story heights were kept constant.

Only earthquakes recorded in high seismicity zones were included. "Near source" ground motions were not included in the study.

## 1.5 ORGANIZATION

Chapter 2 further describes the parameters chosen for the study. Among the parameters are the characteristics of the frames and structural members. The three frame configurations analyzed in the study are described. The four lateral loading distributions commonly used in static analysis for design purposes are introduced. The ten earthquake records selected for the dynamic analysis and their properties are discussed.

Chapter 3 outlines the analysis procedure and reports the results of the analyses. The correlation between the static and dynamic analyses for several key design criteria is also discussed. Base shear strength, member yielding, distorted shapes of the frames, and shear and rotation within the members are among the key design items considered.

A summary of the results and conclusions developed in the study are presented in Chapter 4.

# CHAPTER 2

# PARAMETERS

## 2.1 INTRODUCTION

Chapter 2 discusses the parameters used in the parametric analysis. A set of parameters was selected in order to simulate a variety of typical existing reinforced concrete building characteristics. The parametric analysis was conducted in order to compare static and dynamic nonlinear analysis results using frames with these various characteristics. The results are compared to determine the adequacy of the static analysis to represent the actual dynamic response of a building to a particular earthquake.

The selected parameters include characteristics of the frames, characteristics of the structural members, and three building geometries selected to represent typical existing reinforced concrete buildings. In addition, four loading distributions commonly used in analysis and design are chosen for use in the static analysis, and ten earthquakes representing a variety of earthquake characteristics are chosen for use in the dynamic analysis.

## 2.2 FRAME CHARACTERISTICS

In order to correlate static and dynamic analysis, representative frames having 6-m (20-ft.) bays and 3-m (10 ft.) story heights were considered (Figure 2.1). For all frames, the base was fixed, and the joints were assumed rigid. The loading on each floor considered effective during response to strong ground motion was 7.65 kPa (160 psf). Each story had a total weight of 285 kN. The number of stories considered in the analysis was varied to represent mid- and high-rise buildings and included 4, 8, 12, and 16 stories.

## 2.3 MEMBER CHARACTERISTICS

Material properties, dimensions, and strength of the members were consistent for all frames. The buildings were modeled as bare reinforced concrete frames, neglecting

the addition of any non-structural components. Only reinforced concrete frames were considered in the study.

The assumed material properties included a concrete strength of 27.5 MPa (4 ksi), modulus of elasticity of 27,500 MPa (4,000 ksi), and shear modulus of 11,000 MPa (1,600 ksi). The ultimate strain in the concrete was defined as 0.004. The yield strength of the steel was assumed to be 420 MPa (60 ksi), and the modulus of elasticity was 200,000 MPa (29,000 ksi). The shear area of the members was defined as the total area of the member divided by 1.2.

The girders were modeled with a depth of 510 mm (20 in.), a bottom width of 305 mm (12 in.), and an effective flange width of 915 mm (36 in.). The positive-moment region of the girder was assumed to have a reinforcement ratio of 0.5 %, whereas the negative-moment reinforcement ratio was 1.0 %. The initial moment of inertia was calculated using uncracked sections. A sketch of the girder is shown in Figure 2.2.

The column sizes used in the frames were selected considering the effects of gravity and lateral load demands. The column sizes were based on the equation:

$$\frac{P_{max}}{A_{clm}} \leq 0.35 f'_c \qquad (2.1)$$

where

$P_{max}$ = maximum axial load on column

$A_{clm}$ = total area of column

The maximum axial load was calculated using a uniform dead load of 7.65 kPa (160 psf) and a tributary area of 37 $m^2$. Using Equation 2.1, the maximum level of axial stress was approximately equal to the balanced condition. The equation resulted in 405, 510, 610, 710 mm (16, 20, 24, and 28 in.) square columns in the 4-, 8-, 12-, and 16-story frames, respectively. All columns were assumed to have a reinforcement ratio of 1.0 %.

The moment-curvature behavior of all members was modeled using the tri-linear representation developed by Takeda (1970). The intersection points were defined as the cracking, yield, and ultimate conditions. The ultimate moment and curvature was estimated using a 1.0 % post-yield slope based on the research of others (Yoshimura, 1997; Kunnath and Gupta, 1999; Yang and Wang, 2000). An example of the tri-linear relationship of the elements is shown in Figure 2.3.

The member characteristics are summarized in Table 2.1.

## 2.4 FRAME GEOMETRIES

Three frame configurations were chosen in order to correlate the results of this study to a wider variety of existing buildings. A regular, tall first story, and irregular stepped frame was used in the parametric analysis. Drawings of the various frame

geometries are shown in Figure 2.4. The regular frame maintains a constant story height and four full bays throughout the height of the frame. The tall first story frame is equivalent to the regular frame, except the height of the first-story columns was increased to 5 m (16 ft.). The irregular frame is equivalent to the regular frame in the bottom half of the building, and has only two bays in the top half of the building.

The fundamental period and mode shapes of the frames were calculated. These modal characteristics are summarized in Tables 2.2 through 2.5.

## 2.5 LOADING DISTRIBUTIONS

In static nonlinear analysis, an assumed lateral loading distribution is applied to the modeled structure, and the relationship between increasing lateral loads and lateral displacement of the structure is determined. Therefore, the calculated relationship is dependent on the selected lateral load distribution. Engineers may use many different loading distributions to design and analyze structures. The choice of the distribution depends on the complexity of the modeled frame and the desired simplicity of the analysis.

Four lateral load distributions were selected for use in the nonlinear static analysis in the study to fulfill three goals:

1. To determine the correlation between results from nonlinear static and dynamic analyses
2. To determine the optimal lateral loading distribution
3. To determine the simplest lateral loading distribution that provides adequate results

As described in Chapter 1, the level of complication involved in the loading distribution may vary between a constant uniform load pattern to a pattern that is adjusted as the stiffness in the building changes. In the interest of goal 3, only lateral loading distributions that remain constant in form were considered in the analysis.

The four loading distributions used in the static analysis were chosen based on the research of others and provisions in design and analysis codes (Fajfar and Fischinger, 1987 and 1998; Krawinkler and Seneviratna, 1998; Kim and D'Amore, 1999; Lew and Kunnath, 2000; Kunnath and Gupta, 1999; Yang and Wang, 2000; Federal Emergency Management Agency, 2000). Sketches of the various loading distributions are shown in Figure 2.5. The four distributions are 1) a linear load, 2) a load based on the first fundamental mode shape of the frame, 3) a uniform load, and 4) the loading pattern described in Equation 1.1. The linear load increases from zero to a maximum at the roof; it is often described as an inverted triangular distribution. The shape of the first mode was determined using modal analysis with uncracked sections. The uniform loading pattern consists of the same load on every floor. Note

that when $k$ = 1.0 and the weight and height of each floor is uniform, the loading pattern described in the FEMA provisions is equivalent to the linear load.

## 2.6 EARTHQUAKE RECORDS

A method to obtain more detailed results in seismic analysis and design is to use earthquake ground motion data in a dynamic analysis. Unfortunately, knowing which particular earthquake will occur at a site is difficult. In the study, a representative sample of ten earthquake records was selected for the dynamic nonlinear analysis.

The ten selected earthquake records were chosen to represent a variety of peak ground accelerations, durations, epicentral distances, focal depths, and locations. A list of the ten earthquake records and their properties is shown in Table 2.6. The peak ground accelerations range from 260 cm/s$^2$ to 970 cm/s$^2$. The event durations range from 3 sec to 48 sec. The epicentral distances range from 7 km to 90 km. The focal depths range from 6 km to 33 km. The earthquakes represent major fault lines in California (El Centro, Loma Prieta, and Tarzana), Chile (Llolleo and two records from Valparaiso), Turkey (Erzincan), Japan (Kobe and Sendai), and Canada (Nahinni). Acceleration records for the ten ground motions considered are shown in Figure 2.6.

Fourier amplitude spectra were calculated for each of the ten earthquake records to determine their frequency contents (Figure 2.7). From these spectra, it is shown that a wide variety of frequencies are represented within the selected earthquakes. The primary frequencies range from 1.0 sec to 3.0 sec. The earthquakes may be grouped into three categories based on their primary frequency: 1) Sendai and Loma Prieta near 1.0 sec, 2) El Centro, Kobe, Erzincan, and the first and second records from Valparaiso near 1.5 sec, and 3) Tarzana, Llolleo, and Nahinni over 2.0 sec. Spikes are present in four of the Fourier amplitude spectra. If a spike is present, it indicates that the response of buildings near that particular period will be amplified under that earthquake loading. Llolleo exhibits three spikes at 1.9 sec, 2.2 sec, and 3.3 sec; Sendai exhibits a spike at 1.1 sec; the first Valparaiso record exhibits spikes at 0.8 sec and 1.5 sec; and the second Valparaiso record exhibits a spike at 1.4 sec. Since some of these values are close to the first fundamental period of some of the selected frames, the responses of these frames due to these earthquakes are amplified.

Table 2.8 summarizes the first three frequencies of the frames analyzed in the study and $2^{0.5}$ times the frequencies to estimate the frequencies during the inelastic response of the frames. The frequencies are then compared to the earthquake record(s) with a dominant frequency that most closely matches (within 0.3 Hz). In addition to the presence of spikes, the table may also explain why some earthquake records amplify the response of the frames and may lead to higher modes affecting the response.

The displacement, velocity, and acceleration response spectra were calculated for the ten earthquake records (Figures 2.8 through 2.17). The characteristic period of the ground motion, $T_g$, is noted on each of the figures and is found by estimating the point at which the nearly constant acceleration range ends and the nearly constant velocity region begins as defined by Newmark and Hall (1982). From these response spectra, it is evident that buildings with a variety of characteristic periods of vibration will have amplified responses when subjected to the earthquakes. The characteristic periods range from 0.35 sec to 0.95 sec.

The earthquake records were scaled to generate more consistent displacement response from the frames and produce yielding in all the frames. Since the amplification for response in the longer period range (greater than 1.5 sec) is reduced for many of the selected records, a larger scale factor was used for the frames with longer fundamental periods (12- and 16-story frames). The 4- and 8-story frames were subjected to earthquakes scaled to fit the target spectrum, $S_d = \frac{80}{3} * T$ cm (10*T in.), shown in Figure 2.18, whereas the 12- and 16-story frames were subjected to earthquakes scaled to fit the simplified spectrum, $S_d = 40 * T$ cm (15*T in.), shown in Figure 2.19. The records were scaled by multiplying the ground accelerations by a calculated scaling factor, *SF*, found using the following equation:

$$SF = \frac{T_g * TS}{S_d} \tag{2.3}$$

where

$T_g$ = characteristic period of ground motion

$TS$ = target slope of simplified displacement response spectrum, $\frac{80}{3}$ cm/sec or 40 cm/sec (10 in/sec or 15 in/sec)

$S_d$ = spectral displacement at $T_g$ and 2% damping

The unscaled acceleration values of each earthquake record were then multiplied by the scaling factor to obtain the scaled acceleration values. The values used for scaling of the records are summarized in Table 2.7.

## 2.7 SUMMARY

Chapter 2 discussed the parameters used in the parametric analysis. Characteristics of the frames, characteristics of the structural members, and the three building geometries were described. Also, the four loading distributions chosen for use in the static analysis and the ten earthquakes records chosen for use in the dynamic analysis were introduced.

A representative frame was created using consistent bay lengths, story heights, and floor loading. The material properties, such as concrete and steel strength, remained constant. The slab contributed to the moment of inertia of the girders, which were consistent for all frames. The size of the columns varied within the four frame heights based on the maximum axial load to be carried by the columns. The moment-

curvature behavior of the members was modeled using a tri-linear relationship. Twelve frames varying in height and geometry were chosen for the analysis.

The four loading distributions chosen for use in the static analysis were described, and reasons for their use were based on the research of others and provisions in design and analysis codes

The ten earthquake records chosen for use in the dynamic analysis were described, and their range of properties conveyed. The method of scaling the records to produce yielding during response was outlined.

# CHAPTER 3

# ANALYSIS AND RESULTS

## 3.1 INTRODUCTION

Chapter 3 outlines the procedure followed for analysis and reports the results of the analysis. The study will determine the correlation between results from nonlinear static and dynamic analyses, optimize the lateral load distribution, and determine the simplest lateral load distribution that provides adequate results. The parameters described in Chapter 2 are used to create notional frames, and the frames are analyzed both statically and dynamically to determine the location and distribution of plastic hinges, deformed shape at different levels of demand, and maximum rotation and shear in the members.

Twelve frames were created using the parameters. These frames vary in geometry; regular, irregular stepped, and tall first story frames are considered. The frames also vary in number of stories; 4-, 8-, 12-, and 16-story frames are considered. The bay length, story height, floor loading, girder dimension, column proportion, and concrete and steel properties remain constant. All parameters are discussed in Chapter 2. The moment-curvature relationship of the members is also described in Chapter 2.

## 3.2 STATIC ANALYSIS

The twelve frames were modeled in the static version of the nonlinear analysis routine LARZ, developed by Otani (1974) and later modified by Saiidi (1979a and 1979b) and Lopez (1988). The program has been proven to provide good representations of the displacement response of reinforced concrete structures during strong ground motion (Saidii, 1979b; Eberhard, 1989; Lopez, 1988; LePage, 1997; Browning et al, 1997). The frames were subjected to four separate loading distributions: linear, uniform, first mode shape, and FEMA-based loading. These loading distributions are described in Chapter 2. The loads were held constant in shape and increased incrementally. The loading increment was kept small so that the progression of yielding in the frames could be carefully followed. Loads that change shape were not studied; the loading distributions were kept relatively simple for ease of design and analysis by practicing engineers.

The frames were pushed to several levels of deformation to provide complete and thorough results. The frames were pushed to the controlling mechanism, 1% and 2% of the deformation induced by the dynamic analysis, and to the maximum roof drift as defined by the dynamic results.

A multitude of results were recorded. The study of other researchers served as a guide for results that were deemed important in this study. The progression of yielding was monitored, and the controlling mechanism for each frame was noted. The magnitudes and locations of maximum shear and rotation in the members were recorded. Maximum story drift ratios were calculated from the distorted shapes of the frames during loading. The distorted shape at the maximum roof drift was noted. The maximum roof drift recorded in the dynamic analysis defined the maximum roof drift in the static analysis. These results were recorded for each frame and each loading distribution separately.

## 3.3 DYNAMIC ANALYSIS

The twelve frames, modeled in the dynamic version of the nonlinear analysis routine LARZ (Otani, 1974; Saiidi, 1979a and 1979b; and Lopez, 1988), were subjected to ten separate earthquake records. These earthquake records are described in Chapter 2.

Ten earthquake records were chosen to represent a variety of peak ground accelerations, epicentral distances, focal depths, and locations. The effects of the earthquakes on the twelve chosen frames were expected to produce a variety of results. Since the earthquake records were scaled, the frames were expected to show sufficient yielding in order to provide meaningful results.

The acceleration records were scaled according to Equation 2.3 to induce yielding in the members. The 4- and 8-story frames were subjected to earthquakes scaled to fit a simplified displacement response spectrum of $\frac{80}{3} * T$ cm, whereas the 12- and 16-story frames were subjected to earthquakes scaled to fit a spectrum of $40 * T$ cm. The amplification for response in the longer period range is reduced for many of the selected records; therefore, the 12- and 16-story frames were subjected to a greater demand. Chapter 2 describes the scaling procedure in more detail.

Many results were recorded from the dynamic analysis. The progression of yielding was monitored, and the controlling mechanism, if reached, for each frame was noted. Maximum story drift ratios were calculated from the distorted shapes of the frames during loading. The distorted shape at the maximum roof drift was noted. The magnitudes and locations of maximum shear and rotation in the members were recorded. These results were recorded for each frame and each earthquake loading separately.

## 3.4 STATIC ANALYSIS RESULTS

### 3.4.1 Base Shear, Member Yielding, and Controlling Mechanism

The first set of results observed in the static nonlinear analysis was the location and progression of member yielding, noting where and when the controlling mechanism was reached. Figures 3.1 through 3.12 show member yielding of the frames associated with the mechanism. Table 3.1 summarizes the location of column yielding for each of the frames and indicates the percentage of the total height of the frame that is represented. Table 3.2 summarizes the total base shear in the frames associated with the controlling mechanism. For the purposes of the study, this total base shear is referred to as the base shear strength of the frame.

As observed in Figures 3.1 through 3.12, yielding generally occurred lowest in the tall first story frames, followed by the regular and the irregular frames. A lesser total load is required to yield the girders in the upper portion of the irregular frames than of the regular frames. The yielding in the tall first story frames was similar to the pattern of yielding in the regular frames, except that the yielding in the tall first story frames tended to occur one or two stories lower and at a lesser total load as shown in Table 3.2.

Generally, the more demand on the bottom of the frame, the lower the controlling mechanism occurred in the frame. Therefore, the selected shape of the force

distribution is critical for determining where yielding may occur. The load distribution based on the FEMA provisions caused the highest level of column yielding, followed by the linear load, the load shape based on the first mode, and lastly the uniform load. This is evident in Figures 3.1 through 3.12, and shown in Table 3.1.

In general, the mechanism for the regular frames occurred consistently at 68% of the total frame height. This is evident in Table 3.1. Although in the taller frames (12- and 16-story) the first mechanism actually occurred in the first floor; additional column yielding occurred at approximately 70% of the total frame height at either the same load or a load slightly greater than the load that caused a mechanism in the first floor.

In the tall first story frames, greater distortions at the first floor were anticipated, but only the 4-story frames yielded in this manner. Table 3.1 shows that the mechanism in the tall first story frames generally occurred at 55% of the total frame height, although this number varies more than for the regular frames. Yielding tended to occur simultaneously for many members in the taller frames as seen in Figure 3.8.

The mechanism for the irregular stepped frames was anticipated to occur at the point of geometry change at mid-height of the frame, although this was only the case in the 4-story frames as shown in Figures 3.9 through 3.12. Excluding the 4-story frames,

the mechanism generally occurred at 90 to 100% of the total building height shown by Table 3.1. Except for the uniform load distribution, a "structural" mechanism occurred in the all of the irregular frames. A structural mechanism is defined as yielding of the columns at the base of the frame and all of the girders in the frame. Table 3.1 indicates the occurrence of structural mechanisms in the irregular frames. Generally, additional member hinging occurred at the first and second stories as seen in Figures 3.9 through 3.12.

As expected, the base shear strength of the frames increased with increasing height. The frames subjected to a uniform load pattern had the greatest base shear strength for any configuration or number of stories. The frames subjected to the other three load distributions had nearly the same base shear strength. This was confirmed by taking the average and standard deviation with and without using the base shear strength from the uniform load pattern, as shown in Table 3.2. The shorter the frame, the less the base shear strength using the uniform load pattern deviated from the average. Generally, the frames with regular geometry had the greatest base shear strengths, followed by the frames with irregular configuration and tall first story frames.

### 3.4.2 Distorted Shape of Frames and Story Drift

The second set of results observed in the static analysis included the distorted shapes of the frames at the time the controlling mechanism occurred. From these distorted shapes, the story drift ratios and mean drift ratios at that mechanism were calculated. Story drift ratio is defined as the total drift within a story as a percentage of the story height. Mean drift ratio is defined as the total frame drift as a percentage of the total frame height. The distorted shapes of the frames are shown in Figures 3.13 through 3.19. Figures 3.13 through 3.15 group the distorted shapes of the frames by configuration. These figures show drift as a percentage of the total height of frame with respect to both total frame height and number of stories. The drift values were normalized to the average roof drift. Figures 3.16 through 3.19 rearrange these distorted shapes and group them by number of stories. These figures show un-normalized drift as a percentage of the total height of frame with respect to both total frame height and number of stories. The story drift ratios, with the maximum within each frame highlighted, and mean drift ratios are summarized in Tables 3.3 through 3.5.

Figures 3.13 through 3.15 include the first mode shape of the frames shown along with the distorted shapes of the frames during static analysis. These figures show that the distorted shapes of the four loading distributions resembled each other and generally resembled the first mode shape for all number of stories and configurations. This is especially true of the irregular frames and even using the uniform load. The shapes indicate that the more demand on the bottom of the frame, the more distortion

to the bottom of the frame. Therefore, the uniform load distribution resulted in the maximum story drift ratio consistently occurring lower in the frame as shown in Tables 3.3 through 3.5.

Each load distribution resulted in approximately the same level of drift at the roof at the formation of a mechanism for the three frame geometries. The standard deviation, which is included in Tables 3.3 through 3.5, ranged from 0.04 to 0.11 for the regular frames, 0.05 to 0.25 for the tall first story frames, and 0.09 to 0.21 for the irregular frames. More variation is noted in the 16-story tall first story frames because of the large variation in column yielding. Columns at several stories yielded at the same load increment as seen in Figure 3.8.

In general, the taller the frame, the larger the mean drift ratio at the formation of a mechanism. This indicates that shorter buildings can withstand less distortion before yielding begins to occur and are less flexible than tall buildings. Although there is an exception to this rule; it is interesting to note that the 12-story frames for the regular and tall first story frames had a higher mean drift ratio at the controlling mechanism than the 16-story frames as shown in Table 3.3 and 3.4.

## 3.5 DYNAMIC ANALYSIS RESULTS

### 3.5.1 Base Shear, Member Yielding, and Column Ductility

The first set of results observed in the dynamic nonlinear analysis was the location and progression of member yielding, noting where and when the controlling mechanism was reached. Figures 3.20 through 3.31 show member yielding of the frames induced by the earthquake. Table 3.6 summarizes the location of maximum column ductility for each of the frames and indicates the percentage of the total height of the frame that is represented. Table 3.7 summarizes the total base shear in the frames induced by the earthquake.

Figures 3.20 through 3.31 show the location of member yielding in the frames. The scaling of the records did not induce any column yielding other than the base of the first story columns in more than half of the 12- and 16-story frames. On the other hand, if the records were not scaled, most of the columns and many of the girders would not yield. Therefore, scaling the records proved to be worthwhile. Over half of the 4-story frames had three or more levels of column yielding. The column yielding did not occur at the first level of the tall first story frames as anticipated. The column yielding in the regular and tall first story frames occurred in nearly the same manner; in general, the same girders and columns were yielded as a result of the ten earthquake loadings. Nearly all of the irregular frames exhibited column yielding at the mid-height of the frames where the change in geometry occurred.

Rather than noting the location of column yielding, Table 3.6 lists the location of maximum column ductility. These two values can be compared, because the location of maximum column ductility indicates the level at which column yielding began. The maximum column ductility usually occurred at the third level in the 4-story regular frames and the eighth level in the 8-story regular frames. The maximum column ductility in the 12-story regular frames occurred between 58 and 92% of the total frame height. The location of the maximum column ductility in the 16-story regular frames varied widely from 6% to 88%.

The maximum column ductility in the 4-story tall first story frames occurred most often at the first level. The maximum column ductility in the 8-, 12-, and 16-story tall first story frames varied widely and occurred between 63% and 100%, 58% and 92%, and 31% and 88% of the total frame height, respectively. Generally, the location of the maximum column ductility slightly lowered as the frames got taller.

Although the 4- and 8-story irregular frames had a high standard deviation, the maximum column ductility occurred at either the top level or at the mid-height of the frame with no exception. The maximum column ductility in the 12-story irregular frames occurred between 42 and 83% of the total frame height. The maximum column ductility in the irregular 16-story frames mostly occurred at the mid-height of the frames.

Table 3.7 summarizes the base shear of the frames induced by the earthquake. Sendai had the smallest base shear in over 90% frames, whereas Nahinni had the largest in 74% of the frames. The tall first story frames had the least average base shear for most of the frame heights. The 4-story tall first story frame had the least standard deviation of all frames.

### 3.5.2 Distorted Shape of Frames and Story Drift

The second set of results observed in the dynamic analysis included the distorted shapes of the frames induced by the earthquake at any time. From these distorted shapes, the mean drift ratios at that time were calculated. The story drift ratios were calculated and the maximum at any time was reported. The distorted shapes of the frames are shown in Figures 3.32 through 3.38. Figures 3.32 through 3.34 group the distorted shapes of the frames by configuration. These figures show drift as a percentage of the total height of frame with respect to both total frame height and number of stories. The drift values were normalized to the average roof drift. Figures 3.35 through 3.38 rearrange these distorted shapes and group them by number of stories. These figures show un-normalized drift as a percentage of the total height of frame with respect to the both total frame height and number of stories. The story drift ratios, with the maximum within each frame highlighted, and mean drift ratios are summarized in Tables 3.8 through 3.10.

Figures 3.32 through 3.34 show that the distorted shapes of the frames generally do not resemble the first mode shape of the frame. The 4-story regular and tall first story frames were the closest match to the first mode shape, where as the 4- and 16-story irregular frames were the farthest match. The more yielding in the irregular frames, the more they tended to exhibit a distortion at the mid-height of the frame where the change in geometry occurred. The two Valparaiso records appear to induce higher mode effects in the 16-story frames.

Tables 3.8 through 3.10 summarize the story and mean drift ratios in the frames. The largest story drift ratios of all the frames were calculated in the first story of the tall first story frames. The maximum story drift ratios in the 4-story regular frames occurred only in the bottom half of the frames, or in the first and second stories. All of the maximum story drift ratios in the 8-, 12-, and 16-story regular frames occurred in the middle portion of the frames, and many near or slightly above 50% of the total frame height. Table 3.9 shows that the maximum story drift ratios in the 4-story tall first story frames occurred in the first story for all earthquakes. A majority of the maximum story drift ratios in the 8-story tall first story frames occurred in the bottom two stories. Similar to the regular frames, the maximum story drift ratios for the 12- and 16-story tall first story frames occurred in the middle portion of the frames, but near or slightly lower than 50% of the total frame height. Table 3.10 shows that the maximum story drift ratio in the irregular frames occurred higher than the regular and tall first story frames. The maximum in the irregular frames occurred at the third

story in the 4-story frames and primarily the sixth story in the 8-story frames. The maximum occurred in the upper quarter of the most of the 16-story irregular frames.

The mean drift ratios of the frames varied for all number of stories and configurations as shown in Tables 3.8 through 3.10. The standard deviation of the mean story drift ratios ranged from 0.4 to 0.6 for all of the frames. Generally, the mean drift ratios in the irregular frames were largest, whereas the mean drift ratios in the regular and tall first story frames were approximately equal. Figures 3.35 through 3.38 show the range of mean drift ratios in the frames. The Loma Prieta record usually displayed the most roof drift. In the 8-story frames, Loma Prieta, Erzincan, and El Centro, in that order, always had the most roof drift, whereas in the 12- and 16-story frames, Loma Prieta and Erzincan always had the most roof drift.

## 3.6 CORRELATION BETWEEN DYNAMIC AND STATIC ANALYSES

### 3.6.1 Base Shear, Member Yielding, and Controlling Mechanism/Column Ductility

Figures 3.1 though 3.12, which show the locations of member yielding from static loading, were compared to Figures 3.20 through 3.31, which show the locations of member yielding from dynamic loading. In the 4- and 8-story regular frames, the column yielding patterns were similar in most cases. The 12- and 16-story regular

frames were dissimilar in that a first story mechanism was observed in the static analysis but did not occur in the dynamic analysis. In some of the frames that were pushed further by more demanding earthquakes, the columns in the first story showed some yielding. Generally, static analysis gives a good indication of where yielding in the members will occur in regular low-rise buildings, but does not give a sufficient indication in regular high-rise buildings.

In most cases of the tall first story frames, the member yielding from static loading resembled the member yielding from dynamic loading. The 12-story tall first story frames subjected to static loading showed yielding in the middle of the frames, whereas the frames subjected to dynamic loading were dominated by the formation of a structural mechanism. The yielding was more difficult to analyze and compare in the 16-story frames because many levels of column yielding occurred at the same load step. Static analysis gives a good indication of where yielding in the members will occur in tall first story low-rise buildings, but does not give a sufficient indication in tall first story high-rise buildings.

The members in the 4-story irregular frames yielded in a very similar pattern. In the 8- and 12-story irregular frames, column yielding at the mid-height and top of the frames occurred in the dynamic loading. In the static loading, column yielding occurred at the top but not at the mid-height of the frames. In the 16-story frames, column yielding at the mid-height of the frames occurred in the dynamic loading,

whereas in the static loading, column yielding occurred in only the bottom two stories of the frames. Static analysis gives a good indication of where yielding in the members will occur in irregular short-rise buildings, but does not give a sufficient indication in irregular high-rise buildings.

Table 3.11 shows the correlation between the static loading mechanism location and dynamic loading maximum column ductility location. The percentage differences reported in Table 3.11 are based on the following equation:

$$\%difference = \frac{static - dynamic}{dynamic} \tag{3.1}$$

The percentage differences of the base shear values of the averages of all number of stories for each configuration were near 20% for the regular and tall first story frames and 42% for the irregular frames. The percentage differences for individual frames varied widely from 0% to 98%. Overall, the static analysis using the four specified loading distributions did not predict the general location of the controlling mechanism of the frames analyzed in the study.

Table 3.12 shows the correlation between the base shears from static and dynamic analyses. The percentage differences of the base shear values, found using Equation 3.1, of the averages of all number of stories for each configuration ranged from 17% to 40%. The percentage differences for individual frames ranged from 1% to 55%.

The base shears from the dynamic analyses were always larger than the base shears from the static analyses because the frames were pushed further in the dynamic analyses in many cases. The uniform loading distribution best predicted the base shear of all of the frames analyzed in the study (within 41%). The loading distributions best predicted the base shears in the tall first-story frames followed by the regular frames.

### 3.6.2 Distorted Shape of Frames and Story Drift

The distorted shapes of the frames are shown in Figures 3.39 through 3.42. The shapes of the frames due to dynamic loading are shown with the shapes of the frames due to the four static loadings at 1% and 2% mean drift ratio. In general, the shorter the frame, the better the dynamic shape matched the static shape. All configurations of the 4- and 8-story frames matched well, but the 12- and 16-story frames showed more stiffness at the top of the frame in the static analysis. The regular and tall first story configurations matched especially well for the 4- and 8-story frames.

In order to correlate the results obtained from the static and dynamic analyses, a method for comparing the distorted shapes of the frames from the analyses was developed. For each earthquake analysis result, the load step for each load distribution that pushed the frame to within 5% of the calculated mean-drift ratio from the dynamic analysis was found. In the cases where several levels of column

yielding occurred at the same load step, the mean drift ratios could not be found to within 5%, and the load step with the closest mean drift ratio was used. The static distorted shape was then normalized to the dynamic distorted shape.

The first parameter compared between the static and dynamic analyses was the drift at each level. Using the normalized shapes, the percentage difference of the drift calculated in the static analyses from the drift calculated in the dynamic analyses was determined for each loading distribution at each story. The maximum percentage difference was calculated at each story. Table 3.13 shows the maximum, minimum, and average percentage differences, the associated earthquake, and the associated level. The minimum of each category is denoted in bold. Some of the average and maximum percentage differences are quite large because extremely small and sometimes negative values from dynamic analyses were compared to much larger positive values from static analyses. In some cases, these values were several orders of magnitude larger. This leads to the notion that the minimum percentages values hold a greater meaning than the average and maximum values.

Table 3.13 shows that the load distribution described in the FEMA provisions was the closest match between drift at each level from static and dynamic analyses for all number of stories and configurations, with the exception of the linear load distribution matching the irregular 4-story frames more closely. Furthermore, for every category in which the FEMA load distribution holds the minimum percentage

difference, the percentage difference associated with the linear load distribution is close in number. Therefore, the linear load distribution matched sufficiently well. Following the linear load pattern, the first-mode shaped load pattern was the next best match. The uniform load pattern had the largest percentage difference in most cases. As anticipated, the taller the frame, the greater the percentage difference between drift at each level from static and dynamic analyses.

Overall, the earthquakes that resulted in the minimum and maximum percentage differences between drift from static and dynamic analyses at each level are mostly dependent upon the height of the frame but also the configuration of the frame. However, the minimum and maximum values were not dependent upon the loading distribution. The results are shown in detail in Table 3.13. The earthquake that resulted in the minimum value for the 4-story frames varied, whereas Tarzana most often resulted in the maximum. Erzincan most often resulted in the minimum value for the 8-story frames, whereas the maximum was dependent upon the frame configuration. El Centro and Nahinni most often resulted in the minimum value for 12-story frames, whereas Sendai and the second Valparaiso record most often resulted in the maximum. Nahinni resulted in the minimum value for the regular and tall first story 16-story frames, whereas the first Valparaiso record resulted in the maximum. Turkey resulted in the minimum value for the irregular 16-story frames, whereas El Centro resulted in the maximum. The minimum percentage differences

between drift from the static and dynamic analyses were most often found at the first level of the frames.

The second parameter compared between the static and dynamic analyses using the normalized shapes of the frames was the story drift ratio at each level. Using the normalized results, the percentage difference of the story drift ratio calculated in the static analyses from the story drift ratio calculated in the dynamic analyses was determined for each loading distribution at each story. The maximum percentage difference was calculated at each story. Table 3.14 shows the maximum, minimum, and average percentage differences, the associated earthquake, and the associated level. The minimum of each category is denoted in bold. For reasons explained earlier, some of the percentage difference values are quite large.

Similar to the drift correlation, the load distribution described in the FEMA provisions was the closest match to story drift ratios from static and dynamic analyses, including the 4-story irregular frame results. The linear load distribution was the second closest match, followed by the first-mode shaped load distribution. The uniform load pattern was the worst match.

The earthquakes that resulted in the minimum and maximum percentage differences between story drift ratios from static and dynamic analyses at each level are mostly dependent upon the height of the frame but also the configuration of the frame.

However, the minimum and maximum values were not dependent upon the loading distribution. The results are shown in detail in Table 3.14. Sendai most often resulted in the minimum value for the 4-story frames, whereas Erzincan and Tarzana most often resulted in the maximum. Erzincan and Loma Prieta most often resulted in the minimum value for the 8-story frames, the second Valparaiso record most often resulted in the maximum. Erzincan and Tarzana most often resulted in the minimum value for 12-story frames, whereas Nahinni and the first Valparaiso record most often resulted in the maximum. El Centro and Loma Prieta most often resulted in the minimum value for the regular and tall first-story 16-story frames, whereas Llolleo resulted in the maximum. Tarzana resulted in the minimum value for the irregular 16-story frames, whereas Nahinni resulted in the maximum. The minimum percentage differences between story drift ratio from the static and dynamic analyses were most often found at the top level of the frames.

### 3.6.3 Shear and Rotation in Members

The maximum shear in both the columns and beams was estimated by adding the maximum calculated moments at each end of the member and dividing by the total length of the member. To correlate the shear in the members from the static and dynamic analyses, the percentage difference of the maximum member shear at the formation of a mechanism in the static analysis from the maximum member shear in the dynamic analysis was calculated. The maximum shear from the earthquakes that

resulted in the fifth largest and largest roof drifts are reported in Table 3.15 to represent average and maximum values. The uniform loading distribution most often resulted in the minimum percentage difference in the column shears for the regular and tall first story frames, although no correlation was found in the column shears for the irregular frames. The minimum percentage difference in the column shears ranged from 1% to 54%. The minimum percentage difference in the beam shears varied widely for all configurations of the frame, loading distributions, and number of stories; thus, no correlation was found. On the other hand, the minimum percentage difference resulted in much less of a range, from 0.4% to 22%

To correlate the rotation in the members from the static and dynamic analyses, the percentage difference of the maximum member rotation at the formation of a mechanism in the static analysis from the maximum member rotation in the dynamic analysis was calculated. The uniform loading distribution resulted in the minimum percentage difference in the column shears in half of the frames, although the minimum percentage difference varied widely from 1% to 85%. The minimum percentage difference in the beam rotations varied widely for all configurations of the frame, loading distributions, and number of stories; thus, no correlation was found. The minimum percentage difference ranged from 0.1% to 63%.

## 3.4 SUMMARY

Chapter 3 discussed the static and dynamic analysis procedures and summarized the results of the analyses. The analyses were conducted in order to correlate results from nonlinear static and dynamic analyses, optimize the lateral load distribution, and determine the simplest lateral load distribution that provides adequate results.

The static analysis procedure of the frames was first outlined. The twelve frames varying in configuration and number of stories were modeled in the static version of LARZ and subjected to four loading distributions: linear, uniform, first mode shape, and FEMA-based loading. The frames were pushed to the controlling mechanism, 1% and 2% of the deformation induced by the dynamic analysis, and the maximum roof drift as defined by the dynamic results.

Next, the dynamic analysis procedure of the frames was discussed. The same twelve frames were modeled in the dynamic version of LARZ and subjected to the ten selected earthquake loadings. The earthquake records were scaled in order to induce sufficient yielding in the members to provide adequate results.

The results from the static analyses were discussed. The pattern of member yielding and the location of the controlling mechanism were summarized. The base shear strength of each frame was recorded. The distorted shapes of the frames were shown, and the story and mean drift ratios were summarized.

The results from the dynamic analysis were discussed. The pattern of member yielding, the locations of mechanisms, if any, and the locations of the maximum column ductility were summarized. The base shear of each frame was recorded. The distorted shapes of the frames were shown, and the story and mean drift ratios were summarized.

The correlations among many key factors between the static and dynamic analyses were discussed. The distorted shapes of the frames resulting from static and dynamic analyses were compared. The location of the controlling mechanism from the static analysis was compared to the location of the maximum column ductility from the dynamic analysis. The percentage differences between the base shear values from the static and dynamic analyses were calculated. The drifts at each level and story drift ratios in the frames were correlated. The percentage differences between the maximum member shears and rotations from the static and dynamic analyses were calculated.

# CHAPTER 4

# SUMMARY AND CONCLUSIONS

The focus of the study was on determining the correlation between results from nonlinear static and dynamic analyses. From this correlation, the optimal and simplest lateral load distribution that provides adequate results was determined. Key factors, such as mechanism and maximum column ductility location, base shear capacity, drift, story drift ratio, member shear, and member rotation, were evaluated to determine their relative importance for analysis and design.

## 4.1 SUMMARY OF FRAME BEHAVIOR

### 4.1.1 Based on Static Loading Distribution

Twelve frames varying in configuration and number of stories were analyzed statically with four selected loading distributions: 1) a linear load, 2) a load based on the first fundamental mode shape of the frame, 3) a uniform load, and 4) a loading pattern as described in FEMA. Certain frame behaviors were characteristic to the loading distribution used in the analysis.

The selected shape of the loading distribution is critical for determining where yielding of members and a controlling mechanism will occur. The loading distribution based on the FEMA provisions caused yielding of members higher in the frames, whereas the uniform loading distribution caused yielding of members lower in the frames.

The loading distribution affected the base shear strength of the frames. The uniform loading pattern caused larger base shear strengths.

### 4.1.2 Based on Configuration

Three frame configurations varying from four to sixteen stories were analyzed both statically and dynamically in the study. These configurations included regular frames, tall first story frames, and irregular stepped frames. Certain behaviors were characteristic to the configuration of the frames.

The location of the controlling mechanism and member yielding was dependent upon the configuration of the frames. The controlling mechanism and member yielding occurred higher in irregular frames and lower in tall first story frames.

The base shear strength of a frame was dependent upon the configuration of the frame. The regular frames had a larger base shear strength, followed by the frames with irregular configuration and tall first story frames.

### 4.1.3 Based on Number of Stories

Four frames heights varying in configuration were analyzed both statically and dynamically in the study. The four heights included 4-, 8-, 12-, and 16-story frames. Certain behaviors were characteristic to the number of stories in the frames.

The value of the mean drift ratio, location of the maximum column ductility, and base shear of a frame was dependent upon the number of stories in the frames. The mean drift ratio of the frames increased with increasing number of stories. The location of the maximum column ductility in the frames lowered with increasing number of stories. The taller the frame, the larger its base shear strength. Also, some earthquakes caused a larger response in the taller frames, whereas others caused a larger response in the shorter frames.

## 4.2 CONCLUSIONS

The results of the study led to several observations on the correlation between frames analyzed statically and dynamically:

- Static analysis gave a good indication of where member yielding occurred in the 4- and 8-story frames but gave an inadequate indication in the 12- and 16-story frames.
- Static analysis did not predict the general location of the controlling mechanism of the frames, although the linear, first mode shaped, and FEMA-based loads did predict the general location in the 4-story frames.
- The uniform loading distribution best predicted the base shear of the frames.
- The distorted shape of the frames found by static analysis sufficiently matched the actual shape in the 4- and 8-story frames but did not match sufficiently in the 12- and 16-story frames.
- The FEMA-based loading distribution best matched the drift and story drift ratios at each level of the frames. The linear loading distribution was nearly as good as the FEMA-based loading distribution.
- The uniform loading distribution best matched the maximum shear and rotation in the columns, although the results varied as much as 72%.

Based on these observations, using the combination of a uniform and FEMA-based loading distribution will ensure the safest design of a frame. For the frames considered, using a uniform loading pattern ensures that the base shear strength of the frame and the maximum shear and rotation in the columns will not be underestimated in design and analysis. Using a FEMA-based loading pattern will ensure that the maximum drift and story drift ratio will not be underestimated in design and analysis.

Overall, precise results from static analysis can not be expected because the results from dynamic analysis vary widely.

## REFERENCES

Applied Technology Council. 1996. *Seismic Evaluation and Retrofit of Concrete Buildings*, ATC40, Redwood City, California.

Browning, J., Y. R. Li, A. Lynn, and J. P. Moehle. 1997. "Performance Assessment for a Reinforced Concrete Frame Building," *Proceedings of the International Workshop on Seismic Design Methodologies for the Next Generation of Codes*, Bled, Slovenia, June 24-27, pp. 265-276.

Eberhard, M. O. and M. A. Sozen. 1989. Experiments and Analyses to Study the Seismic Response of Reinforced Concrete Frame-Wall Structures with Yielding Columns," *Structural Research Series No. 548*, Civil Engineering Studies, University of Illinois, Urbana, Illinois.

Fajfar, P. and M. Fischinger. 1987. "Non-linear Seismic Analysis of RC Buildings: Implications of a Case Study", *European Earthquake Engineering*, vol. 1, pp. 31-43.

Fajfar, P. and M. Fischinger. 1988. "N2-A Method for Non-linear Seismic Analysis of Regular Buildings", *Proceedings*, 9th World Conference of Earthquake Engineering, Tokyo-Kyoto, Japan, pp. 39-44.

Federal Emergency Management Agency. 1997. *NEHRP Guidelines for the Seismic Rehabilitation of Buildings*, FEMA-273, Washington, D.C.

Federal Emergency Management Agency. 2000. *Prestandard and Commentary for the Seismic Rehabilitation of Buildings*, FEMA-356, Washington, D.C.

Kim, S. and E. D'Amore. 1999. "Push-over Analysis Procedure in Earthquake Engineering", *Earthquake Spectra*, vol. 15, pp. 417-434.

Krawinkler, H. and G. D. P. K. Seneviratna. 1998. "Pros and Cons of a Pushover Analysis of Seismic Performance Evaluation", *Engineering Structures*, vol. 20, pp. 452-464.

Kunnath, S. K. and B. Gupta. 1999. "Spectra-Compatible Pushover Analysis of Structures", *U.S.-Japan Workshop on Performance-Based Earthquake Engineering Methodology for Reinforced Concrete Building Structures*, Maui, Hawaii, Sept. 13, pp. 69-78.

LePage, A. 1997. "A Method for Drift Control in Earthquake-Resistant Design of Reinforced Concrete Building Structures," Thesis submitted in partial fulfillment

of the requirements for the degree of Ph.D. in Civil Engineering, University of Illinois at Urbana-Champaign.

Lew, H. S. and S. K. Kunnath. 2000. "Evaluation of Analysis Procedures for Performance-based Seismic Design of Buildings", *Proceedings*, 12th World Conference of Earthquake Engineering, pp. 1-8.

Lopez, R. R. 1988. "Numerical Model for Nonlinear Response of R/C Frame-Wall Structures," Ph.D. Thesis Submitted to the Graduate College of the University of Illinois, Urbana, Illinois.

Newmark, N. M. and W. J. Hall. 1982. "Earthquake Spectra and Design," *Monograph Series*, Earthquake Engineering Research Institute, Berkeley, California.

Otani, S. 1974. "SAKE: A Computer Program for Inelastic Response of R/C Frames to Earthquakes," *Structural Research Series No. 392*, Civil Engineering Studies, University of Illinois, Urbana, Illinois.

Saiidi, M. and M. A. Sozen. 1979a. "Simple and Complex Models for Nonlinear Seismic Response of Reinforced Concrete Structures," *Structural Research Series No. 465*, Civil Engineering Studies, University of Illinois, Urbana, Illinois.

Saiidi, M. and M. A. Sozen. 1979b. "User's Manual for the LARZ Family: Computer Programs for Nonlinear Seismic Analysis of Reinforced Concrete Planar Structures," *Structural Research Series No. 466*, Civil Engineering Studies, University of Illinois, Urbana, Illinois.

Takeda, T. M., M. A. Sozen, and N. N. Nielsen. 1970. "Reinforced Concrete Response to Simulated Earthquakes," *Journal of the Structural Division*, ASCE, vol. 96, no. ST12, pp. 2557-2573.

Yang, P. and Y. Wang. 2000. "A Study on Improvement of Pushover Analysis," *Proceedings*, 12th World Conference of Earthquake Engineering.

Yoshimura, M. 1997. "Nonlinear Analysis of a Reinforced Concrete Building with a Soft First Story Collapsed by the 1995 Hyogoken-Nanbu Earthquake," *Cement and Concrete Composites*, vol. 19, pp. 213-221.

# TABLES

Table 2.1: Member Characteristics

| Frame | Member | Dimension mm x mm | Effective Shear Area x $10^3$ $mm^2$ | Moment of Inertia x $10^6$ $mm^4$ | Cracking Moment kN-m | Maximum Yield Moment kN-m | Maximum Yield Curvature x $10^{-6}$ rad/m | Maximum Axial Load kN |
|---|---|---|---|---|---|---|---|---|
| 4-story | Girders | 305 x 510 | 130 | 5,350 | 379 | 1,601 | 60.5 | 0 |
| | Columns | 405 x 405 | 135 | 2,250 | 324 | 2,293 | 120 | 1,150 |
| 8-story | Girders | 305 x 510 | 130 | 5,350 | 379 | 1,601 | 60.5 | 0 |
| | Columns | 510 x 510 | 215 | 5,550 | 632 | 5,135 | 100 | 2,250 |
| 12-story | Girders | 305 x 510 | 130 | 5,350 | 379 | 1,601 | 60.5 | 0 |
| | Columns | 610 x 610 | 310 | 11,500 | 1,093 | 9,150 | 83.0 | 3,400 |
| 16-story | Girders | 305 x 510 | 130 | 5,350 | 379 | 1,601 | 60.5 | 0 |
| | Columns | 710 x 710 | 420 | 21,500 | 1,735 | 14,600 | 69.0 | 4,550 |

Table 2.2: Modal Characteristics of Four-Story Frames

| Level | First-Mode Shapes | | |
|---|---|---|---|
| | Regular Frame | Tall First-Story Frame | Irregular Stepped Frame |
| 4 | 1.00 | 1.00 | 1.00 |
| 3 | 0.86 | 0.93 | 0.81 |
| 2 | 0.60 | 0.79 | 0.51 |
| 1 | 0.27 | 0.59 | 0.23 |
| Periods of Vibration, sec: | | | |
| 1st | 0.62 | 0.88 | 0.52 |
| 2nd | 0.20 | 0.25 | 0.22 |
| 3rd | 0.11 | 0.13 | 0.11 |

Table 2.3: Modal Characteristics of Eight-Story Frames

| Level | First-Mode Shapes | | |
|---|---|---|---|
| | Regular Frame | Tall First-Story Frame | Irregular Stepped Frame |
| 8 | 1.00 | 1.00 | 1.00 |
| 7 | 0.95 | 0.97 | 0.93 |
| 6 | 0.88 | 0.91 | 0.82 |
| 5 | 0.77 | 0.83 | 0.68 |
| 4 | 0.63 | 0.72 | 0.52 |
| 3 | 0.47 | 0.60 | 0.39 |
| 2 | 0.29 | 0.46 | 0.25 |
| 1 | 0.12 | 0.30 | 0.10 |
| Periods of Vibration, sec: | | | |
| 1st | 1.02 | 1.19 | 0.84 |
| 2nd | 0.33 | 0.38 | 0.36 |
| 3rd | 0.19 | 0.21 | 0.18 |

Table 2.4: Modal Characteristics of Twelve-Story Frames

| Level | First-Mode Shapes | | |
|---|---|---|---|
| | Regular Frame | Tall First-Story Frame | Irregular Stepped Frame |
| 12 | 1.00 | 1.00 | 1.00 |
| 11 | 0.97 | 0.98 | 0.96 |
| 10 | 0.94 | 0.94 | 0.90 |
| 9 | 0.88 | 0.90 | 0.83 |
| 8 | 0.81 | 0.84 | 0.73 |
| 7 | 0.73 | 0.77 | 0.62 |
| 6 | 0.64 | 0.69 | 0.52 |
| 5 | 0.53 | 0.60 | 0.43 |
| 4 | 0.42 | 0.50 | 0.34 |
| 3 | 0.30 | 0.39 | 0.25 |
| 2 | 0.18 | 0.28 | 0.15 |
| 1 | 0.07 | 0.17 | 0.05 |
| Periods of Vibration, sec: | | | |
| 1st | 1.51 | 1.57 | 1.15 |
| 2nd | 0.49 | 0.51 | 0.49 |
| 3rd | 0.28 | 0.29 | 0.25 |

Table 2.5: Modal Characteristics of Sixteen-Story Frames

| Level | First-Mode Shapes | | |
|---|---|---|---|
| | Regular Frame | Tall First-Story Frame | Irregular Stepped Frame |
| 16 | 1.00 | 1.00 | 1.00 |
| 15 | 0.98 | 0.98 | 0.97 |
| 14 | 0.96 | 0.96 | 0.93 |
| 13 | 0.92 | 0.93 | 0.88 |
| 12 | 0.88 | 0.89 | 0.82 |
| 11 | 0.83 | 0.85 | 0.75 |
| 10 | 0.77 | 0.79 | 0.67 |
| 9 | 0.71 | 0.73 | 0.59 |
| 8 | 0.64 | 0.67 | 0.51 |
| 7 | 0.56 | 0.60 | 0.44 |
| 6 | 0.47 | 0.52 | 0.38 |
| 5 | 0.39 | 0.44 | 0.31 |
| 4 | 0.30 | 0.36 | 0.24 |
| 3 | 0.21 | 0.27 | 0.17 |
| 2 | 0.12 | 0.19 | 0.10 |
| 1 | 0.04 | 0.10 | 0.03 |
| Periods of Vibration, sec: | | | |
| 1st | 1.74 | 1.84 | 1.44 |
| 2nd | 0.56 | 0.60 | 0.61 |
| 3rd | 0.32 | 0.34 | 0.31 |

Table 2.6: Earthquake Record Properties

| Event | Date | Location | Peak Ground Acc. $cm/s^2$ | Epicentral Distance km | Duration of Event sec | Focal Depth km | Time Step sec | Com-ponent | Mag-nitude |
|---|---|---|---|---|---|---|---|---|---|
| El Centro (Elc) | 5/18/40 | Imperial Valley, California | 342 | 8 | 25 | 12 | 0.02 | NS | 7.0 |
| Kobe (Kob) | 1/17/95 | Hyogo-Ken-Nanbu, Japan | 818 | 1 | 7 | -- | 0.02 | NS | 6.9 |
| Llolleo (Llo) | 3/3/85 | Llolleo, Chile | 698 | 60 | 48 | 33 | 0.005 | NS | 7.8 |
| Loma Prieta (Lom) | 10/18/89 | Loma Prieta, California | 362 | 42 | 5 | 18 | 0.02 | NS | 6.9 |
| Nahinni (Nah) | 12/23/85 | Nahinni, Canada | 957 | 7 | 8 | 6 | 0.005 | NS | 6.8 |
| Sendai (Sen) | 6/12/78 | Miyagi-Ken-Oki, Japan | 258 | -- | 12 | 48 | 0.02 | NS | 6.7 |
| Tarzana (Tar) | 1/17/94 | Northridge, California | 971 | 18 | 20 | 4 | 0.02 | NS | 6.7 |
| Erzincan (Erz) | 3/13/92 | Erzincan, Turkey | 471 | 2 | 3 | -- | 0.005 | EW | 6.9 |
| Valparaiso (Val1) | 3/3/85 | Valparaiso, Chile | 345 | 90 | 8 | 33 | 0.005 | NS | 7.8 |
| Valparaiso (Val2) | 3/3/85 | Valparaiso, Chile | 465 | 90 | 11 | 33 | 0.005 | EW | 7.8 |

Table 2.7: Earthquake Record Scaling Details

| Event | Characteristic Period sec | Spectral Displacement cm | Scaling Factor, 80/3*T | Scaling Factor, 40*T | Peak Ground Acceleration, 80/3*T $cm/s^2$ | Peak Ground Acceleration, 40*T $cm/s^2$ |
|---|---|---|---|---|---|---|
| El Centro | 0.55 | 8.9 | 1.6 | 2.5 | 564 | 846 |
| Kobe | 0.70 | 38.1 | 0.5 | 0.7 | 401 | 601 |
| Llolleo | 0.55 | 17.8 | 0.8 | 1.2 | 576 | 864 |
| Loma Prieta | 0.55 | 14.0 | 1.0 | 1.6 | 380 | 570 |
| Nahinni | 0.35 | 7.6 | 1.2 | 1.8 | 1172 | 1758 |
| Sendai | 0.95 | 40.6 | 0.6 | 0.9 | 161 | 241 |
| Tarzana | 0.45 | 22.9 | 0.5 | 0.8 | 510 | 764 |
| Erzincan | 0.65 | 16.5 | 1.0 | 1.6 | 494 | 742 |
| Valparaiso (1) | 0.65 | 19.1 | 0.9 | 1.4 | 314 | 472 |
| Valparaiso (2) | 0.70 | 22.9 | 0.8 | 1.2 | 380 | 570 |

Table 2.8: Dominant Earthquake Frequencies Matching Frame Frequencies

| | | 1st Frequency | EQ | $2^{0.5}$ * 1st Frequency | EQ | 2nd Frequency | EQ | $2^{0.5}$ * 2nd Frequency | EQ | 3rd Frequency | EQ | $2^{0.5}$ * 3rd Frequency | EQ |
|---|---|---|---|---|---|---|---|---|---|---|---|---|---|
| Regular | 4 | 1.6 | EKV | 2.3 | Llo | 5.0 | - | 7.1 | - | 9.1 | - | 12.9 | - |
| | 8 | 1.0 | Lom | 1.4 | EKV | 3.0 | Nah | 4.3 | - | 5.3 | - | 7.4 | - |
| | 12 | 0.7 | Lom | 0.9 | Lom | 2.0 | Tar | 2.9 | Nah | 3.6 | - | 5.1 | - |
| | 16 | 0.6 | - | 0.8 | Lom | 1.8 | EKV | 2.5 | Llo | 3.1 | Nah | 4.4 | - |
| Tall | 4 | 1.1 | Sen | 1.6 | EKV | 4.0 | - | 5.7 | - | 7.7 | - | 10.9 | - |
| | 8 | 0.8 | Lom | 1.2 | Sen | 2.6 | Llo | 3.7 | - | 4.8 | - | 6.7 | - |
| | 12 | 0.6 | - | 0.9 | Lom | 2.0 | Tar | 2.8 | Nah | 3.4 | - | 4.9 | - |
| | 16 | 0.5 | - | 0.8 | Lom | 1.7 | EKV | 2.4 | Llo | 2.9 | Nah | 4.2 | - |
| Irregular | 4 | 1.9 | Tar | 2.7 | Nah | 4.5 | - | 6.4 | - | 9.1 | - | 12.9 | - |
| | 8 | 1.2 | Sen | 1.7 | EKV | 2.8 | Nah | 3.9 | - | 5.6 | - | 7.9 | - |
| | 12 | 0.9 | Lom | 1.2 | Sen | 2.0 | Tar | 2.9 | Nah | 4.0 | - | 5.7 | - |
| | 16 | 0.7 | Lom | 1.0 | Lom | 1.6 | EKV | 2.3 | Llo | 3.2 | Nah | 4.6 | - |

EKV : Elc, Kob, Erz, Val1, Val2

Table 3.1: Mechanism Locations, Static Analysis

| | | Level(s) of Column Yielding | | | | Average Percent Height of Frame | | | | |
|---|---|---|---|---|---|---|---|---|---|---|
| | | Linear | 1st Mode | Uniform | FEMA | Linear | 1st Mode | Uniform | FEMA | Average |
| Regular | 4 | 3 | 3 | 2 | 3 | 75 | 75 | 50 | 75 | 69 |
| | 8 | 6 | 5 | 4 | 6 | 75 | 63 | 50 | 75 | 66 |
| | 12 | 8 - 9 | 8 | 7 - 8 | 8 - 9 | 71 | 67 | 63 | 71 | 68 |
| | 16 | 10 - 11 | 10 - 12 | 9 - 11 | 11 - 13 | 66 | 69 | 63 | 75 | 68 |
| | | | | | Average | 72 | 68 | 56 | 74 | **68** |
| Tall | 4 | 1 | 1 | 1 | 2 | 35 | 35 | 35 | 50 | 39 |
| | 8 | 4 | 4 | 4 | 5 | 53 | 53 | 53 | 65 | 56 |
| | 12 | 8 | 7 | 5 - 7 | 7 - 8 | 68 | 60 | 52 | 64 | 61 |
| | 16 | 6 - 14 | 9 - 11 | 8 - 11 | 8 - 15 | 64 | 64 | 61 | 73 | 65 |
| | | | | | Average | 55 | 53 | 50 | 63 | **55** |
| Irregular | 4 | 2 - 4 s | 2 - 4 s | 2 | 2 - 4 s | 75 | 75 | 50 | 75 | 69 |
| | 8 | 7 - 8 s | 7 - 8 s | 6 - 7 | 7 - 8 s | 94 | 94 | 81 | 94 | 91 |
| | 12 | 10 - 12 s | 12 s | 9 - 10 | 12 s | 92 | 100 | 79 | 100 | 93 |
| | 16 | 16 s | 16 s | 16 s | 16 s | 100 | 100 | 100 | 100 | 100 |
| | | | | | Average | 90 | 92 | 78 | 92 | **88** |

* s: structural mechanism

Table 3.2: Base Shear at Mechanism, Static Analysis

| | | Base Shear Strength, kN | | | | | | | |
|---|---|---|---|---|---|---|---|---|---|
| | | Linear | 1st Mode | Uniform | FEMA | Average (all) | Standard Deviation (all) | Average (w/o uniform) | Standard Deviation (w/o uniform) |
| Regular | 4 | 697 | 721 | 775 | 691 | 721 | 38 | 703 | 16 |
| | 8 | 837 | 843 | 1004 | 817 | 875 | 87 | 832 | 14 |
| | 12 | 851 | 893 | 1101 | 845 | 923 | 121 | 863 | 26 |
| | 16 | 886 | 886 | 1104 | 842 | 930 | 118 | 871 | 25 |
| Tall | 4 | 483 | 486 | 495 | 478 | 485 | 7 | 482 | 4 |
| | 8 | 700 | 715 | 780 | 684 | 720 | 42 | 700 | 16 |
| | 12 | 773 | 804 | 901 | 729 | 802 | 73 | 769 | 38 |
| | 16 | 806 | 832 | 961 | 748 | 837 | 90 | 795 | 43 |
| Irregular | 4 | 565 | 561 | 672 | 578 | 594 | 53 | 568 | 9 |
| | 8 | 736 | 746 | 929 | 735 | 787 | 95 | 739 | 6 |
| | 12 | 787 | 764 | 1022 | 746 | 830 | 129 | 765 | 20 |
| | 16 | 800 | 789 | 1058 | 769 | 854 | 137 | 786 | 16 |

Table 3.3: Story and Mean Drift Ratios at Mechanism, Static Analysis of Regular Frames

| | | Story Drift Ratio, % | | | | | |
|---|---|---|---|---|---|---|---|
| | | Linear | 1st mode | Uniform | FEMA | Average | Standard Deviation |
| 4-story | 4 | 0.39 | 0.39 | 0.24 | 0.40 | 0.36 | 0.08 |
| | 3 | 0.85 | 0.96 | 0.60 | 0.85 | 0.81 | 0.15 |
| | 2 | **1.20** | **1.48** | 1.09 | **1.20** | 1.24 | 0.16 |
| | 1 | 1.11 | 1.44 | **1.25** | 1.10 | 1.22 | 0.16 |
| | Mean Drift Ratio | 0.89 | 1.07 | 0.79 | 0.89 | 0.91 | 0.11 |
| 8-story | 8 | 0.26 | 0.23 | 0.14 | 0.30 | 0.23 | 0.07 |
| | 7 | 0.57 | 0.51 | 0.34 | 0.65 | 0.52 | 0.13 |
| | 6 | 1.08 | 1.00 | 0.74 | 1.19 | 1.00 | 0.19 |
| | 5 | 1.66 | 1.60 | 1.33 | 1.77 | 1.59 | 0.19 |
| | 4 | 2.14 | 2.12 | 1.98 | 2.22 | 2.11 | 0.10 |
| | 3 | **2.38** | **2.39** | 2.46 | **2.42** | 2.41 | 0.04 |
| | 2 | 2.22 | 2.25 | **2.58** | 2.22 | 2.32 | 0.17 |
| | 1 | 1.58 | 1.62 | 2.10 | 1.56 | 1.72 | 0.26 |
| | Mean Drift Ratio | 1.49 | 1.46 | 1.46 | 1.54 | 1.49 | 0.04 |

Table 3.3: --Continued

| | | Story Drift Ratio, % | | | | | |
|---|---|---|---|---|---|---|---|
| | | Linear | 1st mode | Uniform | FEMA | Average | Standard Deviation |
| 12-story | 12 | 0.23 | 0.21 | 0.14 | 0.31 | 0.22 | 0.07 |
| | 11 | 0.41 | 0.39 | 0.27 | 0.56 | 0.41 | 0.12 |
| | 10 | 0.75 | 0.73 | 0.51 | 0.97 | 0.74 | 0.19 |
| | 9 | 1.24 | 1.25 | 0.93 | 1.51 | 1.23 | 0.24 |
| | 8 | 1.79 | 1.84 | 1.49 | 2.08 | 1.80 | 0.24 |
| | 7 | 2.31 | 2.42 | 2.13 | 2.60 | 2.37 | 0.20 |
| | 6 | 2.74 | 2.90 | 2.75 | 2.99 | 2.85 | 0.12 |
| | 5 | 3.02 | 3.23 | 3.25 | 3.23 | 3.18 | 0.11 |
| | 4 | **3.10** | **3.35** | 3.55 | **3.26** | 3.31 | 0.19 |
| | 3 | 2.92 | 3.19 | **3.58** | 3.03 | 3.18 | 0.29 |
| | 2 | 2.43 | 2.70 | 3.24 | 2.49 | 2.72 | 0.37 |
| | 1 | 1.55 | 1.80 | 2.39 | 1.59 | 1.83 | 0.39 |
| | Mean Drift Ratio | 1.88 | 2.00 | 2.02 | 2.05 | 1.99 | 0.08 |

Table 3.3: --Continued

| | | Story Drift Ratio, % | | | | | |
|---|---|---|---|---|---|---|---|
| | | Linear | 1st mode | Uniform | FEMA | Average | Standard Deviation |
| 16-story | 16 | 0.22 | 0.22 | 0.11 | 0.28 | 0.21 | 0.07 |
| | 15 | 0.33 | 0.33 | 0.17 | 0.41 | 0.31 | 0.10 |
| | 14 | 0.53 | 0.52 | 0.29 | 0.65 | 0.50 | 0.15 |
| | 13 | 0.83 | 0.83 | 0.47 | 1.01 | 0.78 | 0.23 |
| | 12 | 1.22 | 1.22 | 0.75 | 1.43 | 1.15 | 0.29 |
| | 11 | 1.65 | 1.65 | 1.13 | 1.87 | 1.58 | 0.32 |
| | 10 | 2.08 | 2.08 | 1.56 | 2.29 | 2.01 | 0.31 |
| | 9 | 2.48 | 2.48 | 2.01 | 2.66 | 2.41 | 0.28 |
| | 8 | 2.81 | 2.81 | 2.44 | 2.94 | 2.75 | 0.21 |
| | 7 | 3.03 | 3.03 | 2.79 | 3.11 | 2.99 | 0.14 |
| | 6 | **3.15** | **3.14** | 3.04 | **3.17** | 3.12 | 0.06 |
| | 5 | 3.13 | 3.12 | **3.14** | 3.10 | 3.12 | 0.02 |
| | 4 | 2.94 | 2.94 | 3.10 | 2.87 | 2.96 | 0.10 |
| | 3 | 2.55 | 2.55 | 2.84 | 2.43 | 2.59 | 0.17 |
| | 2 | 1.94 | 1.94 | 2.31 | 1.80 | 2.00 | 0.22 |
| | 1 | 1.08 | 1.08 | 1.46 | 0.92 | 1.14 | 0.23 |
| | Mean Drift Ratio | 1.87 | 1.87 | 1.73 | 1.93 | 1.85 | 0.09 |

Table 3.4: Story and Mean Drift Ratios at Mechanism, Static Analysis of Tall First Story Frames

| | | Story Drift Ratio, % | | | | | |
|---|---|---|---|---|---|---|---|
| | | Linear | 1st mode | Uniform | FEMA | Average | Standard Deviation |
| 4-story | 4 | 0.19 | 0.14 | 0.11 | 0.20 | 0.16 | 0.04 |
| | 3 | 0.44 | 0.38 | 0.32 | 0.45 | 0.39 | 0.06 |
| | 2 | 0.81 | 0.75 | 0.68 | 0.81 | 0.76 | 0.06 |
| | 1 | **1.58** | **1.53** | **1.48** | **1.55** | 1.53 | 0.04 |
| | Mean Drift Ratio | 0.86 | 0.81 | 0.76 | 0.85 | 0.82 | 0.05 |
| 8-story | 8 | 0.16 | 0.13 | 0.07 | 0.19 | 0.14 | 0.05 |
| | 7 | 0.37 | 0.31 | 0.20 | 0.42 | 0.32 | 0.09 |
| | 6 | 0.75 | 0.65 | 0.42 | 0.83 | 0.66 | 0.18 |
| | 5 | 1.32 | 1.18 | 0.85 | 1.42 | 1.19 | 0.25 |
| | 4 | 1.95 | 1.82 | 1.47 | 2.04 | 1.82 | 0.25 |
| | 3 | 2.52 | 2.43 | 2.15 | 2.59 | 2.42 | 0.19 |
| | 2 | 2.92 | 2.87 | 2.71 | 2.95 | 2.86 | 0.11 |
| | 1 | **2.96** | **2.95** | **2.93** | **2.95** | 2.95 | 0.01 |
| | Mean Drift Ratio | 1.71 | 1.64 | 1.46 | 1.76 | 1.64 | 0.13 |

Table 3.4: --Continued

| | | Story Drift Ratio, % | | | | | |
|---|---|---|---|---|---|---|---|
| | | Linear | 1st mode | Uniform | FEMA | Average | Standard Deviation |
| 12-story | 12 | 0.14 | 0.11 | 0.08 | 0.23 | 0.14 | 0.07 |
| | 11 | 0.25 | 0.20 | 0.16 | 0.40 | 0.25 | 0.11 |
| | 10 | 0.45 | 0.37 | 0.31 | 0.71 | 0.46 | 0.18 |
| | 9 | 0.78 | 0.64 | 0.57 | 1.16 | 0.79 | 0.26 |
| | 8 | 1.24 | 1.05 | 0.98 | 1.68 | 1.24 | 0.31 |
| | 7 | 1.75 | 1.57 | 1.54 | 2.19 | 1.76 | 0.30 |
| | 6 | 2.25 | 2.10 | 2.17 | 2.65 | 2.29 | 0.25 |
| | 5 | 2.65 | 2.55 | 2.79 | 3.00 | 2.75 | 0.20 |
| | 4 | 2.94 | 2.89 | 3.30 | 3.22 | 3.09 | 0.20 |
| | 3 | **3.05** | **3.05** | 3.64 | **3.25** | 3.25 | 0.28 |
| | 2 | 2.93 | 2.99 | **3.73** | 3.06 | 3.18 | 0.37 |
| | 1 | 2.38 | 2.49 | 3.32 | 2.43 | 2.65 | 0.44 |
| | Mean Drift Ratio | 1.76 | 1.71 | 1.95 | 2.02 | 1.86 | 0.15 |

Table 3.4: --Continued

| | | Story Drift Ratio, % | | | | | |
|---|---|---|---|---|---|---|---|
| | | Linear | 1st mode | Uniform | FEMA | Average | Standard Deviation |
| 16-story | 16 | 0.13 | 0.09 | 0.07 | 0.21 | 0.13 | 0.06 |
| | 15 | 0.19 | 0.14 | 0.11 | 0.31 | 0.19 | 0.09 |
| | 14 | 0.29 | 0.22 | 0.19 | 0.47 | 0.29 | 0.13 |
| | 13 | 0.43 | 0.33 | 0.31 | 0.72 | 0.45 | 0.19 |
| | 12 | 0.64 | 0.49 | 0.48 | 1.02 | 0.66 | 0.25 |
| | 11 | 0.92 | 0.71 | 0.75 | 1.36 | 0.94 | 0.30 |
| | 10 | 1.22 | 0.97 | 1.12 | 1.70 | 1.25 | 0.31 |
| | 9 | 1.53 | 1.26 | 1.56 | 2.01 | 1.59 | 0.31 |
| | 8 | 1.80 | 1.53 | 2.01 | 2.25 | 1.90 | 0.31 |
| | 7 | 2.02 | 1.76 | 2.43 | 2.42 | 2.16 | 0.33 |
| | 6 | 2.17 | 1.92 | 2.77 | **2.51** | 2.34 | 0.37 |
| | 5 | **2.22** | **2.00** | 3.01 | 2.50 | 2.43 | 0.44 |
| | 4 | 2.16 | 1.98 | **3.11** | 2.38 | 2.41 | 0.50 |
| | 3 | 1.97 | 1.83 | 3.08 | 2.11 | 2.25 | 0.56 |
| | 2 | 1.62 | 1.52 | 2.85 | 1.70 | 1.92 | 0.62 |
| | 1 | 0.88 | 0.84 | 2.15 | 0.90 | 1.19 | 0.64 |
| | Mean Drift Ratio | 1.25 | 1.09 | 1.64 | 1.51 | 1.37 | 0.25 |

Table 3.5: Story and Mean Drift Ratios at Mechanism, Static Analysis of Irregular Frames

| | | Story Drift Ratio, % | | | | | |
|---|---|---|---|---|---|---|---|
| | | Linear | 1st mode | Uniform | FEMA | Average | Standard Deviation |
| 4-story | 4 | 1.25 | 1.18 | 0.60 | 0.94 | 0.99 | 0.29 |
| | 3 | **1.77** | **1.71** | 1.06 | **1.39** | 1.49 | 0.33 |
| | 2 | 1.00 | 0.97 | 1.15 | 0.96 | 1.02 | 0.09 |
| | 1 | 0.69 | 0.66 | **1.16** | 0.69 | 0.80 | 0.24 |
| | Mean Drift Ratio | 1.18 | 1.13 | 0.99 | 1.00 | 1.08 | 0.09 |
| 8-story | 8 | 0.82 | 0.77 | 0.43 | 0.77 | 0.70 | 0.18 |
| | 7 | 1.63 | 1.76 | 0.87 | 1.64 | 1.48 | 0.41 |
| | 6 | 2.16 | 2.36 | 1.45 | 2.18 | 2.04 | 0.40 |
| | 5 | **2.27** | **2.48** | 1.80 | **2.28** | 2.21 | 0.29 |
| | 4 | 1.92 | 2.12 | 1.84 | 1.91 | 1.95 | 0.12 |
| | 3 | 1.72 | 1.92 | **1.97** | 1.71 | 1.83 | 0.13 |
| | 2 | 1.36 | 1.52 | 1.86 | 1.35 | 1.52 | 0.24 |
| | 1 | 0.68 | 0.78 | 1.32 | 0.68 | 0.87 | 0.31 |
| | Mean Drift Ratio | 1.57 | 1.72 | 1.44 | 1.56 | 1.57 | 0.11 |

Table 3.5: --Continued

| | | Story Drift Ratio, % | | | | | |
|---|---|---|---|---|---|---|---|
| | | Linear | 1st mode | Uniform | FEMA | Average | Standard Deviation |
| 12-story | 12 | 1.26 | 0.95 | 0.54 | 1.19 | 0.99 | 0.33 |
| | 11 | 1.67 | 1.34 | 0.90 | 1.58 | 1.37 | 0.35 |
| | 10 | 2.20 | 1.86 | 1.44 | 2.06 | 1.89 | 0.33 |
| | 9 | 2.67 | 2.31 | 2.01 | 2.47 | 2.36 | 0.28 |
| | 8 | 2.94 | 2.58 | 2.48 | **2.69** | 2.67 | 0.20 |
| | 7 | **2.96** | **2.60** | 2.74 | 2.67 | 2.74 | 0.16 |
| | 6 | 2.72 | 2.37 | 2.81 | 2.39 | 2.57 | 0.23 |
| | 5 | 2.59 | 2.24 | 2.94 | 2.24 | 2.50 | 0.33 |
| | 4 | 2.39 | 2.05 | **2.98** | 2.03 | 2.36 | 0.45 |
| | 3 | 2.07 | 1.74 | 2.87 | 1.70 | 2.10 | 0.54 |
| | 2 | 1.57 | 1.27 | 2.51 | 1.23 | 1.64 | 0.60 |
| | 1 | 0.82 | 0.58 | 1.76 | 0.56 | 0.93 | 0.56 |
| | Mean Drift Ratio | 2.16 | 1.82 | 2.17 | 1.90 | 2.01 | 0.17 |

Table 3.5: --Continued

| | | Story Drift Ratio, % | | | | | |
|---|---|---|---|---|---|---|---|
| | | Linear | 1st mode | Uniform | FEMA | Average | Standard Deviation |
| 16-story | 16 | 1.37 | 1.35 | 0.51 | 1.89 | 1.28 | 0.57 |
| | 15 | 1.61 | 1.58 | 0.72 | 2.14 | 1.51 | 0.59 |
| | 14 | 1.96 | 1.94 | 1.07 | 2.51 | 1.87 | 0.60 |
| | 13 | 2.34 | 2.33 | 1.48 | 2.89 | 2.26 | 0.58 |
| | 12 | 2.69 | 2.69 | 1.92 | 3.23 | 2.63 | 0.54 |
| | 11 | 2.94 | 2.95 | 2.30 | 3.45 | 2.91 | 0.47 |
| | 10 | **3.06** | **3.07** | 2.59 | **3.52** | 3.06 | 0.38 |
| | 9 | 3.03 | 3.04 | 2.73 | 3.44 | 3.06 | 0.29 |
| | 8 | 2.85 | 2.85 | 2.76 | 3.18 | 2.91 | 0.18 |
| | 7 | 2.75 | 2.75 | 2.82 | 3.04 | 2.84 | 0.13 |
| | 6 | 2.62 | 2.61 | **2.85** | 2.86 | 2.74 | 0.14 |
| | 5 | 2.42 | 2.41 | 2.82 | 2.61 | 2.57 | 0.19 |
| | 4 | 2.14 | 2.12 | 2.69 | 2.27 | 2.31 | 0.27 |
| | 3 | 1.73 | 1.71 | 2.42 | 1.83 | 1.92 | 0.33 |
| | 2 | 1.20 | 1.18 | 1.93 | 1.26 | 1.39 | 0.36 |
| | 1 | 0.51 | 0.50 | 1.19 | 0.54 | 0.69 | 0.33 |
| | Mean Drift Ratio | 2.20 | 2.19 | 2.05 | 2.54 | 2.25 | 0.21 |

Table 3.6: Maximum Column Ductility Locations, Dynamic Analysis

| | | Percent Height of Frame at Level of Maximum Column Ductility | | | | | | | | | | | |
|---|---|---|---|---|---|---|---|---|---|---|---|---|---|
| | | Elc | Kob | Llo | Lom | Nah | Sen | Tar | Erz | Val1 | Val2 | Average | Standard Deviation |
| Regular | 4 | 75 | 75 | 100 | 50 | 75 | 75 | 100 | 75 | 75 | 75 | 78 | 14 |
| | 8 | 100 | 100 | 100 | 75 | 100 | 63 | 100 | 75 | 88 | 100 | 90 | 14 |
| | 12 | 58 | 92 | 92 | 83 | 83 | 83 | 58 | 67 | 83 | 92 | 79 | 13 |
| | 16 | 6 | 50 | 69 | 81 | 88 | 6 | 69 | 75 | 44 | 6 | 49 | 32 |
| | Average | 60 | 79 | 90 | 72 | 86 | 57 | 82 | 73 | 72 | 68 | **74** | 11 |
| Tall | 4 | 25 | 25 | 25 | 25 | 50 | 50 | 25 | 25 | 25 | 25 | 30 | 11 |
| | 8 | 75 | 88 | 75 | 63 | 100 | 88 | 75 | 63 | 88 | 88 | 80 | 12 |
| | 12 | 58 | 92 | 58 | 75 | 83 | 83 | 58 | 58 | 92 | 92 | 75 | 15 |
| | 16 | 56 | 50 | 63 | 81 | 88 | 75 | 69 | 81 | 44 | 31 | 64 | 18 |
| | Average | 54 | 64 | 55 | 61 | 80 | 74 | 57 | 57 | 62 | 59 | **62** | 9 |
| Irregular | 4 | 50 | 100 | 50 | 100 | 50 | 100 | 100 | 50 | 50 | 100 | 75 | 26 |
| | 8 | 50 | 100 | 100 | 100 | 50 | 50 | 100 | 50 | 100 | 100 | 80 | 26 |
| | 12 | 67 | 50 | 83 | 75 | 50 | 50 | 42 | 75 | 50 | 67 | 61 | 14 |
| | 16 | 50 | 50 | 50 | 81 | 50 | 50 | 81 | 50 | 50 | 6 | 52 | 21 |
| | Average | 56 | 83 | 78 | 92 | 50 | 67 | 81 | 58 | 67 | 89 | **72** | 15 |

Table 3.7: Base Shear Induced by Earthquakes, Dynamic Analysis

| | | Base Shear Strength, kN | | | | | | | | | | | |
|---|---|---|---|---|---|---|---|---|---|---|---|---|---|
| | | Elc | Kob | Llo | Lom | Nah | Sen | Tar | Erz | Val1 | Val2 | Average | Standard Deviation |
| Regular | 4 | 801 | 807 | 789 | 895 | **999** | **742** | 823 | 826 | 802 | 791 | 828 | 71 |
| | 8 | 1264 | 939 | 1048 | 1217 | **1368** | **702** | 1148 | 1264 | 973 | 1041 | 1096 | 197 |
| | 12 | 1699 | 1627 | 1338 | 1592 | **2027** | **994** | 1549 | 1646 | 1291 | 1230 | 1499 | 291 |
| | 16 | 2272 | 1626 | 1936 | 1710 | **2872** | **1023** | 1920 | 2039 | 1709 | 1586 | 1869 | 484 |
| Tall | 4 | 533 | 508 | 515 | 526 | 507 | 510 | 506 | 547 | 493 | **488** | 513 | 18 |
| | 8 | 825 | 729 | 765 | **957** | 790 | **515** | 869 | 919 | 675 | 814 | 786 | 127 |
| | 12 | 1346 | 1228 | 1120 | 1278 | **1664** | **959** | 1189 | 1326 | 1173 | 1302 | 1258 | 183 |
| | 16 | 1875 | 1420 | 1273 | 1414 | **2182** | **978** | 1660 | 1736 | 1413 | 1259 | 1521 | 347 |
| Irregular | 4 | 857 | 733 | 760 | 783 | **962** | **647** | 716 | 774 | 768 | 782 | 778 | 84 |
| | 8 | **1225** | 957 | 1086 | 1212 | 1223 | **827** | 1101 | 1086 | 993 | 1030 | 1074 | 129 |
| | 12 | 1767 | 1323 | 1521 | 1571 | **2170** | **1045** | 1505 | 1602 | 1433 | 1481 | 1542 | 291 |
| | 16 | 1204 | 1928 | 1687 | 1274 | **1989** | **1169** | 1909 | 1605 | 1406 | 1432 | 1560 | 309 |

Table 3.8: Story and Mean Drift Ratios, Dynamic Analysis of Regular Frames

| | | Story Drift Ratio, % | | | | | | | | | | | |
|---|---|---|---|---|---|---|---|---|---|---|---|---|---|
| | | Elc | Kob | Llo | Lom | Nah | Sen | Tar | Erz | Val1 | Val2 | Average | Standard Deviation |
| 4-story | 4 | 1.03 | 0.88 | 0.99 | 0.71 | 1.00 | 0.49 | 0.95 | 0.58 | 0.75 | 0.74 | 0.81 | 0.19 |
| | 3 | 1.97 | 1.89 | 1.15 | 1.60 | 1.73 | 0.94 | 0.99 | 1.34 | 1.57 | 1.13 | 1.43 | 0.37 |
| | 2 | **2.73** | **2.14** | 1.65 | 2.97 | **1.84** | **1.44** | 0.82 | **1.69** | **1.96** | 1.27 | 1.85 | 0.65 |
| | 1 | 2.50 | 1.52 | **1.71** | **3.14** | 1.56 | 1.38 | **1.02** | 1.59 | 1.90 | **1.33** | 1.77 | 0.62 |
| Mean Drift Ratio | | 1.90 | 1.54 | 1.16 | 2.01 | 1.42 | 1.03 | 0.77 | 1.20 | 1.38 | 0.94 | 1.33 | 0.40 |
| 8-story | 8 | 1.14 | 0.65 | 0.57 | 0.62 | 1.05 | 0.21 | 0.77 | 0.60 | 0.56 | 0.82 | 0.70 | 0.26 |
| | 7 | 1.69 | 0.86 | 0.79 | 1.11 | 1.09 | 0.36 | 1.04 | 0.91 | 0.93 | **1.14** | 0.99 | 0.33 |
| | 6 | 1.89 | 0.88 | 0.95 | 1.92 | **1.12** | 0.54 | 1.08 | 1.44 | **1.20** | 1.13 | 1.22 | 0.43 |
| | 5 | 1.78 | 1.10 | 0.95 | 2.60 | 0.98 | 0.69 | 1.01 | 2.08 | 1.18 | 0.89 | 1.32 | 0.62 |
| | 4 | **1.93** | 0.99 | 0.99 | **2.96** | 0.96 | 0.99 | 1.34 | 2.62 | 1.02 | 0.74 | 1.45 | 0.78 |
| | 3 | 1.87 | 1.13 | **1.14** | 2.91 | 0.98 | **1.10** | **1.54** | **2.90** | 1.01 | 0.71 | 1.53 | 0.79 |
| | 2 | 1.57 | **1.23** | 1.13 | 2.35 | 0.85 | 0.90 | 1.19 | 2.69 | 1.02 | 0.89 | 1.38 | 0.64 |
| | 1 | 1.02 | 0.85 | 0.83 | 0.98 | 0.68 | 0.45 | 0.61 | 1.94 | 0.62 | 0.66 | 0.86 | 0.42 |
| Mean Drift Ratio | | 1.20 | 0.66 | 0.68 | 1.86 | 0.65 | 0.61 | 0.76 | 1.82 | 0.78 | 0.54 | 0.96 | 0.50 |

Table 3.8: --Continued

| | | Story Drift Ratio, % | | | | | | | | | | | |
|---|---|---|---|---|---|---|---|---|---|---|---|---|---|
| | | Elc | Kob | Llo | Lom | Nah | Sen | Tar | Erz | Val1 | Val2 | Average | Standard Deviation |
| 12-story | 12 | 1.36 | 1.33 | 0.99 | 2.04 | 1.47 | 0.51 | 0.91 | 1.24 | 0.82 | 0.69 | 1.14 | 0.44 |
| | 11 | 1.59 | 1.44 | 1.04 | 2.40 | 1.54 | 0.74 | 1.03 | 1.44 | 1.12 | 0.97 | 1.33 | 0.47 |
| | 10 | 1.74 | **1.47** | 1.09 | 2.87 | 1.96 | 1.01 | 1.12 | 1.65 | 1.37 | 1.22 | 1.55 | 0.56 |
| | 9 | 1.75 | 1.46 | 1.07 | 3.38 | 2.23 | 1.28 | 1.25 | 1.94 | 1.50 | **1.23** | 1.71 | 0.69 |
| | 8 | 1.59 | 1.24 | 1.15 | 3.73 | **2.37** | **1.38** | 1.32 | 2.31 | **1.57** | 1.07 | 1.77 | 0.82 |
| | 7 | 1.59 | 1.26 | 1.40 | **3.80** | 2.22 | 1.34 | 1.58 | 2.79 | 1.47 | 0.90 | 1.84 | 0.87 |
| | 6 | 1.77 | 1.18 | **1.41** | 3.55 | 2.26 | 1.20 | **1.91** | 3.17 | 1.17 | 0.95 | 1.86 | 0.89 |
| | 5 | 2.03 | 0.99 | 1.33 | 3.27 | 2.36 | 0.96 | 1.80 | **3.24** | 0.88 | 1.04 | 1.79 | 0.92 |
| | 4 | **2.16** | 1.09 | 1.19 | 3.04 | 2.30 | 0.99 | 1.52 | 2.94 | 0.94 | 1.00 | 1.72 | 0.83 |
| | 3 | 2.06 | 1.20 | 1.19 | 2.93 | 2.17 | 1.01 | 1.45 | 2.36 | 0.99 | 1.01 | 1.64 | 0.69 |
| | 2 | 1.63 | 1.10 | 1.15 | 2.78 | 1.81 | 0.86 | 1.19 | 2.00 | 0.80 | 0.91 | 1.42 | 0.63 |
| | 1 | 1.08 | 0.61 | 0.69 | 2.16 | 1.10 | 0.43 | 0.57 | 1.30 | 0.44 | 0.61 | 0.90 | 0.53 |
| Mean Drift Ratio | | 1.07 | 0.68 | 0.75 | 2.45 | 1.35 | 0.69 | 0.99 | 1.61 | 0.87 | 0.51 | 1.10 | 0.58 |

Table 3.8: --Continued

| | | Story Drift Ratio, % | | | | | | | | | | | |
|---|---|---|---|---|---|---|---|---|---|---|---|---|---|
| | | Elc | Kob | Llo | Lom | Nah | Sen | Tar | Erz | Val1 | Val2 | Average | Standard Deviation |
| 16-story | 16 | 1.35 | 0.96 | 0.90 | 1.75 | 1.61 | 0.46 | 0.96 | 1.30 | 1.04 | 1.29 | 1.16 | 0.38 |
| | 15 | 1.42 | 1.06 | 0.95 | 1.86 | 1.59 | 0.59 | 1.05 | 1.41 | 1.15 | 1.43 | 1.25 | 0.36 |
| | 14 | 1.35 | 1.09 | 0.98 | 1.87 | 1.60 | 0.74 | 1.04 | 1.49 | 1.19 | **1.49** | 1.28 | 0.34 |
| | 13 | 1.39 | 1.06 | 0.85 | 2.12 | 1.83 | 0.85 | 1.05 | 1.55 | 1.21 | 1.38 | 1.33 | 0.42 |
| | 12 | 1.40 | 1.01 | 0.91 | 2.33 | **1.92** | 0.88 | 1.18 | 1.62 | **1.27** | 1.21 | 1.37 | 0.46 |
| | 11 | 1.42 | 1.18 | 1.08 | 2.48 | 1.64 | 0.85 | 1.23 | 2.10 | 1.25 | 1.14 | 1.44 | 0.50 |
| | 10 | 1.66 | **1.30** | 1.15 | 2.63 | 1.46 | 0.86 | 1.50 | 2.44 | 1.18 | 1.12 | 1.53 | 0.58 |
| | 9 | 1.80 | **1.30** | 1.24 | **2.69** | 1.66 | 0.81 | **1.75** | **2.62** | 1.14 | 1.09 | 1.61 | 0.63 |
| | 8 | 1.99 | 1.14 | 1.20 | 2.62 | 1.72 | 0.75 | 1.73 | **2.62** | 0.97 | 0.99 | 1.57 | 0.68 |
| | 7 | **2.24** | 0.86 | 1.03 | 2.53 | 1.72 | 0.74 | 1.54 | 2.50 | 0.97 | 1.03 | 1.52 | 0.70 |
| | 6 | 2.27 | 1.03 | 1.22 | 2.57 | 1.61 | 0.95 | 1.61 | 2.30 | 0.97 | 0.96 | 1.55 | 0.63 |
| | 5 | 2.10 | 1.08 | **1.26** | 2.66 | 1.45 | **1.07** | 1.56 | 2.06 | 1.00 | 0.87 | 1.51 | 0.59 |
| | 4 | 1.93 | 0.99 | 1.10 | 2.62 | 1.40 | **1.07** | 1.55 | 1.98 | 1.02 | 1.11 | 1.48 | 0.54 |
| | 3 | 1.70 | 0.96 | 0.89 | 2.40 | 1.31 | 0.95 | 1.40 | 1.71 | 1.02 | 1.19 | 1.35 | 0.48 |
| | 2 | 1.39 | 0.90 | 0.75 | 1.94 | 1.06 | 0.67 | 1.12 | 1.20 | 0.92 | 0.99 | 1.09 | 0.36 |
| | 1 | 0.83 | 0.48 | 0.38 | 1.15 | 0.59 | 0.30 | 0.56 | 0.62 | 0.51 | 0.49 | 0.59 | 0.24 |
| Mean Drift Ratio | | 1.15 | 0.57 | 0.50 | 1.86 | 0.89 | 0.46 | 1.00 | 1.29 | 0.52 | 0.56 | 0.88 | 0.46 |

Table 3.9: Story and Mean Drift Ratios, Dynamic Analysis of Tall First Story Frames

| | | Story Drift Ratio, % | | | | | | | | | | | |
|---|---|---|---|---|---|---|---|---|---|---|---|---|---|
| | | Elc | Kob | Llo | Lom | Nah | Sen | Tar | Erz | Val1 | Val2 | Average | Standard Deviation |
| 4-story | 4 | 0.40 | 0.47 | 0.35 | 0.38 | 0.56 | 0.23 | 0.55 | 0.25 | 0.47 | 0.40 | 0.41 | 0.11 |
| | 3 | 0.71 | 0.76 | 0.61 | 0.71 | 0.90 | 0.56 | 0.76 | 0.59 | 0.79 | 0.66 | 0.71 | 0.10 |
| | 2 | 1.33 | 1.12 | 0.95 | 1.18 | 1.43 | 1.07 | 0.94 | 1.46 | 1.12 | 0.84 | 1.14 | 0.21 |
| | 1 | **4.54** | **2.63** | **2.33** | **5.55** | **2.53** | **2.33** | **1.90** | **6.24** | **2.31** | **2.08** | 3.25 | 1.58 |
| Mean Drift Ratio | | 1.71 | 1.12 | 1.00 | 1.98 | 1.28 | 1.08 | 0.88 | 2.27 | 1.09 | 0.91 | 1.33 | 0.49 |
| 8-story | 8 | 0.61 | 0.41 | 0.43 | 0.49 | 0.69 | 0.22 | 0.51 | 0.40 | 0.36 | 0.47 | 0.46 | 0.13 |
| | 7 | 0.88 | 0.67 | 0.58 | 0.89 | 0.89 | 0.38 | 0.79 | 0.65 | 0.61 | 0.73 | 0.71 | 0.17 |
| | 6 | 1.13 | 0.85 | 0.74 | 1.64 | 0.79 | 0.52 | 1.02 | 1.01 | 0.78 | 0.86 | 0.94 | 0.30 |
| | 5 | 1.34 | 1.01 | 0.87 | 2.59 | 0.84 | 0.58 | **1.13** | 1.66 | 0.80 | 0.73 | 1.15 | 0.60 |
| | 4 | 1.48 | 0.99 | 0.87 | 3.13 | 0.76 | 0.56 | 0.96 | 2.27 | 0.82 | 0.63 | 1.25 | 0.83 |
| | 3 | 1.88 | 1.10 | 0.82 | **3.23** | 0.98 | 0.60 | 0.97 | 2.75 | 0.77 | 0.57 | 1.37 | 0.94 |
| | 2 | **2.09** | **1.18** | 0.90 | 2.88 | 1.09 | **0.62** | 0.96 | **3.01** | **0.99** | 0.70 | 1.44 | 0.89 |
| | 1 | 1.95 | 0.93 | **0.92** | 2.08 | **1.18** | 0.56 | 1.09 | 2.98 | 0.93 | **0.88** | 1.35 | 0.75 |
| Mean Drift Ratio | | 1.16 | 0.74 | 0.65 | 2.02 | 0.60 | 0.41 | 0.65 | 1.88 | 0.58 | 0.44 | 0.91 | 0.59 |

Table 3.9: --Continued

| | | Story Drift Ratio, % | | | | | | | | | | | |
|---|---|---|---|---|---|---|---|---|---|---|---|---|---|
| | | Elc | Kob | Llo | Lom | Nah | Sen | Tar | Erz | Val1 | Val2 | Average | Standard Deviation |
| 12-story | 12 | 1.14 | 0.93 | 0.59 | 1.46 | 1.11 | 0.66 | 0.64 | 0.95 | 1.06 | 0.77 | 0.93 | 0.27 |
| | 11 | 1.42 | 1.09 | 0.66 | 1.77 | 1.26 | 0.93 | 0.83 | 1.21 | 1.31 | 1.01 | 1.15 | 0.32 |
| | 10 | 1.57 | 1.25 | 0.73 | 2.18 | 1.69 | 1.23 | 0.90 | 1.42 | 1.43 | 1.15 | 1.36 | 0.41 |
| | 9 | 1.49 | 1.30 | 0.82 | 2.56 | 2.05 | 1.47 | 0.97 | 1.57 | **1.40** | **1.17** | 1.48 | 0.51 |
| | 8 | 1.44 | 1.22 | 1.00 | 2.92 | **2.21** | **1.52** | 1.09 | 1.76 | 1.37 | 1.09 | 1.56 | 0.60 |
| | 7 | 1.44 | **1.32** | 1.18 | 3.16 | 2.05 | 1.37 | 1.31 | 2.39 | 1.22 | 1.08 | 1.65 | 0.67 |
| | 6 | 1.50 | 1.29 | **1.28** | 3.14 | 1.98 | 1.16 | 1.69 | 2.88 | 0.97 | 1.05 | 1.69 | 0.76 |
| | 5 | 1.92 | 1.12 | 1.24 | 2.94 | 2.10 | 0.96 | **1.79** | 3.03 | 0.78 | 1.06 | 1.69 | 0.81 |
| | 4 | **2.27** | 0.92 | 1.11 | 2.99 | 2.08 | 1.27 | 1.60 | **2.91** | 0.78 | 1.04 | 1.70 | 0.82 |
| | 3 | 2.30 | 1.10 | 1.13 | 3.05 | 1.95 | 1.46 | 1.58 | 2.54 | 0.87 | 1.03 | 1.70 | 0.73 |
| | 2 | 2.03 | 1.18 | 1.16 | **3.17** | 1.77 | 1.41 | 1.43 | 2.36 | 0.87 | 0.97 | 1.63 | 0.72 |
| | 1 | 1.52 | 0.89 | 0.97 | 2.95 | 1.18 | 0.90 | 0.88 | 1.90 | 0.70 | 0.91 | 1.28 | 0.69 |
| Mean Drift Ratio | | 1.07 | 0.71 | 0.63 | 2.31 | 1.24 | 0.77 | 0.96 | 1.53 | 0.77 | 0.58 | 1.06 | 0.53 |

Table 3.9: --Continued

| | | Story Drift Ratio, % | | | | | | | | | | | |
|---|---|---|---|---|---|---|---|---|---|---|---|---|---|
| | | Elc | Kob | Llo | Lom | Nah | Sen | Tar | Erz | Val1 | Val2 | Average | Standard Deviation |
| 16-story | 16 | 1.21 | 0.89 | 0.72 | 1.55 | 1.33 | 0.55 | 0.80 | 1.17 | 0.91 | 1.03 | 1.02 | 0.30 |
| | 15 | 1.29 | 0.99 | 0.81 | 1.64 | 1.37 | 0.68 | 0.86 | 1.23 | 1.04 | 1.17 | 1.11 | 0.29 |
| | 14 | 1.27 | 1.02 | 0.83 | 1.66 | 1.39 | 0.80 | 0.85 | 1.31 | 1.09 | **1.27** | 1.15 | 0.28 |
| | 13 | 1.28 | 1.00 | 0.82 | 1.80 | 1.61 | 0.88 | 0.84 | 1.41 | 1.11 | 1.25 | 1.20 | 0.33 |
| | 12 | 1.30 | 0.87 | 0.81 | 2.07 | 1.61 | 0.88 | 1.09 | 1.49 | 1.17 | 1.11 | 1.24 | 0.39 |
| | 11 | 1.41 | 1.06 | 1.00 | 2.27 | 1.43 | 0.86 | 1.29 | 1.91 | **1.20** | 0.92 | 1.33 | 0.45 |
| | 10 | 1.67 | 1.20 | 1.09 | 2.42 | 1.39 | 0.92 | 1.36 | 2.22 | 1.16 | 0.80 | 1.42 | 0.53 |
| | 9 | 1.81 | **1.24** | 1.06 | 2.54 | 1.63 | 0.90 | 1.51 | 2.39 | 1.17 | 0.72 | 1.50 | 0.61 |
| | 8 | 1.84 | 1.15 | 1.09 | 2.55 | 1.73 | 0.82 | 1.47 | **2.46** | 1.05 | 0.71 | 1.49 | 0.65 |
| | 7 | 2.12 | 0.92 | 0.96 | 2.44 | **1.74** | 0.70 | 1.46 | 2.40 | 0.97 | 0.78 | 1.45 | 0.68 |
| | 6 | **2.25** | 0.88 | 1.16 | 2.41 | 1.68 | 0.68 | 1.47 | 2.25 | 0.96 | 0.76 | 1.45 | 0.66 |
| | 5 | 2.15 | 1.05 | **1.22** | 2.50 | 1.55 | 0.85 | 1.50 | 2.07 | 0.97 | 0.75 | 1.46 | 0.60 |
| | 4 | 2.00 | 1.09 | 1.12 | **2.53** | 1.41 | **0.93** | **1.54** | 2.03 | 1.05 | 1.03 | 1.47 | 0.54 |
| | 3 | 1.89 | 1.04 | 0.91 | 2.51 | 1.40 | 0.89 | 1.48 | 1.86 | 1.13 | 1.21 | 1.43 | 0.52 |
| | 2 | 1.68 | 1.07 | 0.89 | 2.29 | 1.28 | 0.74 | 1.26 | 1.48 | 1.06 | 1.20 | 1.29 | 0.44 |
| | 1 | 1.14 | 0.73 | 0.60 | 1.61 | 0.78 | 0.48 | 0.77 | 0.93 | 0.75 | 0.78 | 0.86 | 0.32 |
| Mean Drift Ratio | | 1.19 | 0.52 | 0.45 | 1.75 | 0.86 | 0.48 | 0.95 | 1.28 | 0.47 | 0.49 | 0.84 | 0.45 |

Table 3.10: Story and Mean Drift Ratios, Dynamic Analysis of Irregular Frames

| | | Story Drift Ratio, % | | | | | | | | | | | |
|---|---|---|---|---|---|---|---|---|---|---|---|---|---|
| | | Elc | Kob | Llo | Lom | Nah | Sen | Tar | Erz | Val1 | Val2 | Average | Standard Deviation |
| 4-story | 4 | 2.12 | 2.14 | 1.57 | 3.07 | 1.45 | 1.06 | 1.72 | 1.46 | 1.42 | 2.36 | 1.84 | 0.59 |
| | 3 | **3.09** | **2.78** | **1.93** | **3.80** | **1.99** | **1.49** | **1.84** | **2.25** | **2.24** | **2.76** | 2.42 | 0.69 |
| | 2 | 1.48 | 1.69 | 1.08 | 2.17 | 1.53 | 0.97 | 0.73 | 1.94 | 2.16 | 1.36 | 1.51 | 0.49 |
| | 1 | 1.65 | 1.56 | 1.06 | 1.73 | 1.43 | 0.83 | 0.72 | 1.33 | 2.07 | 1.37 | 1.38 | 0.41 |
| Mean Drift Ratio | | 1.90 | 1.53 | 1.22 | 2.38 | 1.25 | 1.04 | 0.92 | 1.64 | 1.67 | 1.48 | 1.50 | 0.43 |
| 8-story | 8 | 2.17 | 1.25 | 1.21 | 1.43 | 1.66 | 0.68 | 1.57 | 1.20 | 1.23 | 1.00 | 1.34 | 0.40 |
| | 7 | 2.49 | 1.56 | 1.60 | 2.39 | 1.86 | 1.01 | **1.64** | 1.76 | 1.55 | 1.25 | 1.71 | 0.45 |
| | 6 | **2.73** | **1.64** | **1.81** | **2.87** | **2.02** | **1.16** | 1.39 | **2.29** | **1.63** | **1.35** | 1.89 | 0.58 |
| | 5 | 2.42 | 1.52 | 1.55 | 2.78 | 1.83 | 1.09 | 1.12 | 2.26 | 1.28 | 1.16 | 1.70 | 0.60 |
| | 4 | 1.56 | 0.84 | 1.17 | 2.03 | 1.07 | 1.04 | 1.03 | 1.60 | 0.90 | 0.74 | 1.20 | 0.41 |
| | 3 | 1.59 | 0.76 | 1.06 | 1.70 | 1.20 | 1.06 | 1.03 | 1.65 | 0.89 | 0.87 | 1.18 | 0.34 |
| | 2 | 1.51 | 0.83 | 0.94 | 1.60 | 0.80 | 0.88 | 1.07 | 1.71 | 0.82 | 0.94 | 1.11 | 0.35 |
| | 1 | 1.08 | 0.53 | 0.59 | 1.34 | 0.53 | 0.48 | 0.66 | 1.27 | 0.51 | 0.59 | 0.76 | 0.34 |
| Mean Drift Ratio | | 1.42 | 0.88 | 0.94 | 1.78 | 1.09 | 0.75 | 0.85 | 1.49 | 0.81 | 0.69 | 1.07 | 0.37 |

Table 3.10: --Continued

| | | Story Drift Ratio, % | | | | | | | | | | | |
|---|---|---|---|---|---|---|---|---|---|---|---|---|---|
| | | Elc | Kob | Llo | Lom | Nah | Sen | Tar | Erz | Val1 | Val2 | Average | Standard Deviation |
| 12-story | 12 | 3.07 | 2.18 | **2.13** | 2.90 | 1.48 | 1.79 | **1.95** | 2.40 | 2.06 | 2.26 | 2.22 | 0.48 |
| | 11 | 3.17 | 2.20 | 2.01 | 3.08 | 1.71 | 1.95 | 1.93 | 2.54 | 2.26 | **2.40** | 2.32 | 0.49 |
| | 10 | **2.97** | **1.97** | 1.82 | 3.27 | 2.17 | **2.04** | 1.85 | 2.73 | **2.33** | 2.32 | 2.35 | 0.49 |
| | 9 | 2.71 | 1.94 | 1.82 | 4.05 | **2.38** | 1.99 | 1.76 | 3.13 | 2.18 | 1.90 | 2.39 | 0.73 |
| | 8 | 2.43 | 1.90 | 1.68 | **4.24** | 2.23 | 1.73 | 1.66 | 3.35 | 1.85 | 1.34 | 2.24 | 0.90 |
| | 7 | 2.07 | 1.56 | 1.76 | 4.06 | 1.62 | 1.31 | 1.85 | **3.44** | 1.34 | 0.95 | 2.00 | 0.99 |
| | 6 | 1.72 | 1.08 | 1.42 | 3.46 | 1.47 | 0.95 | 1.56 | 3.17 | 0.76 | 0.80 | 1.64 | 0.94 |
| | 5 | 1.72 | 1.08 | 1.33 | 3.40 | 1.62 | 1.01 | 1.24 | 2.92 | 1.05 | 1.02 | 1.64 | 0.85 |
| | 4 | 1.60 | 1.31 | 1.27 | 3.56 | 1.80 | 1.18 | 1.20 | 2.60 | 1.24 | 1.06 | 1.68 | 0.80 |
| | 3 | 1.55 | 1.25 | 1.21 | 3.82 | 1.84 | 1.25 | 1.11 | 2.40 | 1.36 | 1.04 | 1.68 | 0.86 |
| | 2 | 1.55 | 1.06 | 1.08 | 3.69 | 1.51 | 1.05 | 0.82 | 2.03 | 1.25 | 1.04 | 1.51 | 0.84 |
| | 1 | 1.16 | 0.58 | 0.70 | 2.90 | 1.06 | 0.53 | 0.50 | 1.44 | 0.74 | 0.73 | 1.03 | 0.72 |
| Mean Drift Ratio | | 1.72 | 1.07 | 0.95 | 2.55 | 0.98 | 0.91 | 1.00 | 2.09 | 1.08 | 0.84 | 1.32 | 0.59 |

Table 3.10: --Continued

| | | Story Drift Ratio, % | | | | | | | | | | | |
|---|---|---|---|---|---|---|---|---|---|---|---|---|---|
| | | Elc | Kob | Llo | Lom | Nah | Sen | Tar | Erz | Val1 | Val2 | Average | Standard Deviation |
| 16-story | 16 | 0.98 | 2.05 | **1.12** | 1.91 | 0.73 | 1.93 | **2.26** | 0.80 | 1.03 | 1.49 | 1.43 | 0.57 |
| | 15 | 1.11 | 2.17 | **1.12** | 2.01 | 0.84 | 2.05 | 2.24 | 0.94 | 1.18 | **1.54** | 1.52 | 0.55 |
| | 14 | 1.24 | **2.22** | 0.96 | **2.03** | 0.93 | **2.13** | 2.01 | 1.11 | 1.33 | 1.47 | 1.54 | 0.51 |
| | 13 | **1.30** | 2.06 | 0.73 | 2.01 | 0.98 | 2.09 | 1.56 | 1.25 | **1.40** | 1.24 | 1.46 | 0.47 |
| | 12 | 1.28 | 1.45 | 0.58 | 1.97 | 1.03 | 1.91 | 1.36 | 1.38 | 1.36 | 0.95 | 1.33 | 0.42 |
| | 11 | 1.18 | 0.97 | 0.54 | 1.89 | 1.08 | 1.62 | 1.34 | 1.50 | 1.18 | 0.65 | 1.19 | 0.42 |
| | 10 | 1.02 | 0.56 | 0.60 | 1.78 | **1.09** | 1.28 | 1.44 | **1.58** | 0.92 | 0.39 | 1.07 | 0.46 |
| | 9 | 0.78 | 0.22 | 0.66 | 1.60 | 0.95 | 0.94 | 1.57 | **1.58** | 0.66 | 0.19 | 0.91 | 0.53 |
| | 8 | 0.49 | 0.10 | 0.68 | 1.35 | 0.66 | 0.64 | 1.58 | 1.52 | 0.44 | 0.02 | 0.75 | 0.56 |
| | 7 | 0.37 | 0.02 | 0.72 | 1.21 | 0.50 | 0.55 | 1.57 | 1.51 | 0.40 | 0.08 | 0.69 | 0.56 |
| | 6 | 0.28 | 0.20 | 0.79 | 1.10 | 0.36 | 0.46 | 1.44 | 1.47 | 0.36 | 0.15 | 0.66 | 0.51 |
| | 5 | 0.19 | 0.36 | 0.86 | 0.99 | 0.22 | 0.36 | 1.17 | 1.37 | 0.23 | 0.16 | 0.59 | 0.46 |
| | 4 | 0.10 | 0.42 | 0.88 | 0.86 | 0.09 | 0.25 | 0.82 | 1.19 | 0.01 | 0.12 | 0.47 | 0.43 |
| | 3 | 0.03 | 0.37 | 0.78 | 0.69 | 0.03 | 0.14 | 0.51 | 0.91 | 0.24 | 0.04 | 0.37 | 0.33 |
| | 2 | 0.01 | 0.25 | 0.54 | 0.49 | 0.11 | 0.06 | 0.31 | 0.56 | 0.36 | 0.03 | 0.27 | 0.21 |
| | 1 | 0.02 | 0.12 | 0.22 | 0.32 | 0.09 | 0.01 | 0.23 | 0.18 | 0.25 | 0.04 | 0.15 | 0.11 |
| Mean Drift Ratio | | 0.64 | 0.83 | 0.74 | 1.39 | 0.58 | 1.03 | 1.34 | 1.18 | 0.60 | 0.47 | 0.88 | 0.33 |

Table 3.11: Location of Mechanism and Maximum Column Ductility Correlation

| | | | | | | | | Percentage Difference | | | | |
|---|---|---|---|---|---|---|---|---|---|---|---|---|
| | | Linear | 1st Mode | Uniform | FEMA | Average, All Static | Average, Dynamic | Linear | 1st Mode | Uniform | FEMA | All Static |
| Regular | 4 | 75 | 75 | 50 | 75 | 69 | 78 | 3 | 3 | 35 | 3 | 11 |
| | 8 | 75 | 63 | 50 | 75 | 66 | 90 | 17 | 31 | 44 | 17 | 27 |
| | 12 | 71 | 67 | 63 | 71 | 68 | 79 | 11 | 16 | 21 | 11 | 14 |
| | 16 | 66 | 69 | 63 | 75 | 68 | 49 | 33 | 39 | 27 | 52 | 38 |
| | average | | | | | | | **16** | **22** | **32** | **21** | **23** |
| Tall | 4 | 35 | 35 | 35 | 50 | 39 | 30 | 16 | 16 | 16 | 67 | 29 |
| | 8 | 53 | 53 | 53 | 65 | 56 | 80 | 33 | 33 | 33 | 19 | 30 |
| | 12 | 68 | 60 | 52 | 64 | 61 | 75 | 9 | 20 | 30 | 14 | 18 |
| | 16 | 64 | 64 | 61 | 73 | 65 | 64 | 0 | 0 | 5 | 14 | 3 |
| | average | | | | | | | **15** | **17** | **21** | **28** | **20** |
| Irregular | 4 | 75 | 75 | 50 | 75 | 69 | 75 | 0 | 0 | 33 | 0 | 8 |
| | 8 | 94 | 94 | 81 | 94 | 91 | 80 | 17 | 17 | 2 | 17 | 13 |
| | 12 | 92 | 100 | 79 | 100 | 93 | 61 | 51 | 64 | 30 | 64 | 52 |
| | 16 | 100 | 100 | 100 | 100 | 100 | 52 | 93 | 93 | 93 | 93 | 93 |
| | average | | | | | | | **40** | **44** | **39** | **44** | **42** |

Table 3.12: Base Shear Correlation

| | | | | | | | | Percentage Difference | | | | |
|---|---|---|---|---|---|---|---|---|---|---|---|---|
| | | Linear | 1st Mode | Uniform | FEMA | Average, All Static | Average, Dynamic | Linear | 1st Mode | Uniform | FEMA | All Static |
| Regular | 4 | 697 | 721 | 775 | 691 | 721 | 828 | 16 | 13 | 6 | 16 | 13 |
| | 8 | 837 | 843 | 1004 | 817 | 875 | 1096 | 24 | 23 | 8 | 26 | 20 |
| | 12 | 851 | 893 | 1101 | 845 | 923 | 1499 | 43 | 40 | 27 | 44 | 38 |
| | 16 | 886 | 886 | 1104 | 842 | 930 | 1869 | 53 | 53 | 41 | 55 | 50 |
| | average | | | | | | | **34** | **32** | **21** | **35** | **30** |
| Tall | 4 | 483 | 486 | 495 | 478 | 485 | 513 | 6 | 5 | 4 | 7 | 5 |
| | 8 | 700 | 715 | 780 | 684 | 720 | 786 | 11 | 9 | 1 | 13 | 8 |
| | 12 | 773 | 804 | 901 | 729 | 802 | 1258 | 39 | 36 | 28 | 42 | 36 |
| | 16 | 806 | 832 | 961 | 748 | 837 | 1521 | 47 | 45 | 37 | 51 | 45 |
| | average | | | | | | | **26** | **24** | **17** | **28** | **24** |
| Irregular | 4 | 565 | 561 | 672 | 578 | 594 | 778 | 27 | 28 | 14 | 26 | 24 |
| | 8 | 736 | 746 | 929 | 735 | 787 | 1074 | 31 | 31 | 14 | 32 | 27 |
| | 12 | 787 | 764 | 1022 | 746 | 830 | 1542 | 49 | 50 | 34 | 52 | 46 |
| | 16 | 800 | 789 | 1058 | 769 | 854 | 1560 | 49 | 49 | 32 | 51 | 45 |
| | average | | | | | | | **39** | **40** | **23** | **40** | **35** |

Table 3.13: Correlation of Drift at Each Level, Percentage Difference

| | | Linear | | | 1st mode | | | Uniform | | | FEMA | | | |
|---|---|---|---|---|---|---|---|---|---|---|---|---|---|---|
| | | EQ | Difference | Level | EQ | Difference | Level | EQ | Difference | Level | EQ | Difference | Level | |
| Regular | 4 | | 16.4 | | | 17.7 | | | 30.4 | | | **16.1** | | average |
| | | Erz | 2.3 | 1 | Sen | **0.8** | 1 | Lom | 4.4 | 1 | Erz | 2.5 | 1 | minimum |
| | | Tar | 42.8 | 1 | Tar | 46.2 | 1 | Tar | 69.1 | 1 | Tar | **41.1** | 1 | maximum |
| | 8 | | 51.2 | | | 53.9 | | | 76.9 | | | **47.8** | | |
| | | Erz | 1.4 | 1 | Sen | 3.7 | 1 | Kob | 3.6 | 1 | Erz | **1.0** | 3 | |
| | | Nah | 169 | 1 | Nah | 176 | 1 | Nah | 232 | 1 | Nah | **161** | 1 | |
| | 12 | | 120 | | | 126 | | | 165 | | | **109** | | |
| | | Elc | **5.9** | 1 | Elc | 6.6 | 1 | Elc | 23.1 | 1 | Elc | 7.0 | 1 | |
| | | Sen | 673 | 2 | Sen | 695 | 2 | Sen | 846 | 1 | Sen | **624** | 2 | |
| | 16 | | 164 | | | 207 | | | 168 | | | **148** | | |
| | | Nah | 18.5 | 1 | Nah | 35.1 | 1 | Nah | 20.7 | 1 | Nah | **13.1** | 1 | |
| | | Val1 | 616 | 5 | Val1 | 732 | 5 | Val1 | 629 | 5 | Val1 | **570** | 5 | |

Table 3.13: --Continued

| | | Linear | | | 1st mode | | | Uniform | | | FEMA | | | |
|---|---|---|---|---|---|---|---|---|---|---|---|---|---|---|
| | | EQ | Difference | Level | EQ | Difference | Level | EQ | Difference | Level | EQ | Difference | Level | |
| Tall | 4 | | 7.4 | | | 8.0 | | | 9.0 | | | **7.4** | | average |
| | | Val2 | **0.6** | 1 | Llo | 0.9 | 2 | Llo | 1.8 | 1 | Val2 | 0.9 | 1 | minimum |
| | | Tar | 16.0 | 1 | Tar | 19.0 | 1 | Tar | 22.0 | 1 | Tar | **15.3** | 1 | maximum |
| | 8 | | 34.3 | | | 38.3 | | | 48.9 | | | **31.3** | | |
| | | Elc | **0.6** | 1 | Erz | 6.9 | 1 | Nah | 6.0 | 1 | Elc | 2.3 | 1 | |
| | | Tar | 135 | 1 | Tar | 146 | 1 | Tar | 177 | 1 | Tar | **128** | 1 | |
| | 12 | | 238 | | | 260 | | | 309 | | | **210** | | |
| | | Elc | 3.6 | 1 | Elc | **1.8** | 2 | Elc | 13.1 | 1 | Elc | 8.4 | 1 | |
| | | Val1 | 1815 | 1 | Val1 | 1974 | 1 | Val1 | 2328 | 1 | Val1 | **1626** | 1 | |
| | 16 | | 2219 | | | 2346 | | | 2664 | | | **1933** | | |
| | | Nah | 19.1 | 1 | Nah | 23.2 | 1 | Nah | 32.5 | 1 | Nah | **10.2** | 1 | |
| | | Val1 | 21604 | 4 | Val1 | 22814 | 4 | Val1 | 25846 | 4 | Val1 | **18863** | 4 | |

Table 3.13: --Continued

| | | Linear | | | 1st mode | | | Uniform | | | FEMA | | | |
|---|---|---|---|---|---|---|---|---|---|---|---|---|---|---|
| | | EQ | Difference | Level | EQ | Difference | Level | EQ | Difference | Level | EQ | Difference | Level | |
| Irregular | 4 | | 116 | | | **115** | | | 240 | | | 134 | | average |
| | | Sen | **1.7** | 2 | Sen | 2.5 | 1 | Vall | 37.4 | 1 | Vall | 2.3 | 2 | minimum |
| | | Tar | **694** | 2 | Tar | 703 | 2 | Tar | 1125 | 1 | Tar | 763 | 1 | maximum |
| | 8 | | 56.5 | | | 58.1 | | | 110 | | | **56.0** | | |
| | | Erz | 8.7 | 4 | Erz | 9.7 | 4 | Sen | 8.8 | 1 | Erz | **8.1** | 4 | |
| | | Elc | 141 | 1 | Elc | 143 | 1 | Elc | 276 | 1 | Elc | **139** | 1 | |
| | 12 | | 1123 | | | 1128 | | | 1628 | | | **1066** | | |
| | | Nah | 5.4 | 6 | Nah | **5.1** | 6 | Nah | 19.6 | 1 | Nah | 8.1 | 5 | |
| | | Sen | 10387 | 3 | Sen | 10421 | 3 | Sen | 14909 | 3 | Sen | **9844** | 3 | |
| | 16 | | 422 | | | 420 | | | 586 | | | **386** | | |
| | | Llo | 12.6 | 12 | Erz | 12.6 | 1 | Llo | 26.6 | 1 | Erz | **7.1** | 1 | |
| | | Elc | 1472 | 3 | Elc | 1475 | 3 | Elc | 2123 | 2 | Elc | **1335** | 3 | |

Table 3.14: Story Drift Ratio Correlation, Percentage Difference

| | | Linear | | | 1st mode | | | Uniform | | | FEMA | | | |
|---|---|---|---|---|---|---|---|---|---|---|---|---|---|---|
| | | EQ | Difference | Story | EQ | Difference | Story | EQ | Difference | Story | EQ | Difference | Story | |
| Regular | 4 | | **18.5** | | | 20.0 | | | 32.9 | | | 18.7 | | average |
| | | Sen | 6.6 | 4 | Sen | 8.0 | 4 | Sen | 17.9 | 4 | Sen | **5.2** | 4 | minimum |
| | | Tar | 30.6 | 3 | Tar | 31.5 | 4 | Tar | 45.5 | 1 | Tar | **30.2** | 4 | maximum |
| | 8 | | 30.1 | | | 32.0 | | | 42.3 | | | **28.6** | | |
| | | Erz | 11.4 | 8 | Sen | 14.5 | 8 | Sen | 29.8 | 8 | Erz | **9.4** | 8 | |
| | | Val2 | 41.8 | 8 | Val2 | 42.8 | 8 | Lom | 57.8 | 8 | Val2 | **41.5** | 8 | |
| | 12 | | 39.2 | | | 61.9 | | | 69.9 | | | **38.0** | | |
| | | Tar | 31.3 | 12 | Llo | 42.8 | 12 | Llo | 44.8 | 12 | Tar | **29.7** | 12 | |
| | | Val1 | 50.1 | 12 | Val1 | 108 | 5 | Val1 | 131 | 1 | Val2 | **47.5** | 12 | |
| | 16 | | 40.6 | | | 44.7 | | | 41.0 | | | **40.0** | | |
| | | Lom | 31.4 | 16 | Elc | 37.6 | 16 | Lom | 33.0 | 16 | Tar | **30.9** | 16 | |
| | | Llo | 50.1 | 16 | Llo | **49.1** | 16 | Llo | 50.1 | 16 | Llo | 50.3 | 16 | |

Table 3.14: --Continued

| | | Linear | | | 1st mode | | | Uniform | | | FEMA | | | |
|---|---|---|---|---|---|---|---|---|---|---|---|---|---|---|
| | | EQ | Difference | Story | EQ | Difference | Story | EQ | Difference | Story | EQ | Difference | Story | |
| Tall | 4 | | 28.5 | | | 29.7 | | | 31.0 | | | **28.5** | | average |
| | | Sen | 7.7 | 1 | Sen | 13.0 | 4 | Sen | 19.7 | 4 | Sen | **7.2** | 1 | minimum |
| | | Erz | 62.9 | 4 | Erz | 51.1 | 4 | Tar | **39.3** | 4 | Erz | 66.8 | 4 | maximum |
| | 8 | | 34.5 | | | 37.7 | | | 45.6 | | | **31.9** | | |
| | | Erz | 18.7 | 8 | Erz | 23.4 | 8 | Erz | 34.9 | 8 | Erz | **13.9** | 8 | |
| | | Val2 | 40.8 | 8 | Lom | 44.6 | 1 | Lom | 54.4 | 8 | Val2 | **39.8** | 8 | |
| | 12 | | 41.9 | | | 44.9 | | | 50.9 | | | **38.4** | | |
| | | Tar | 32.7 | 12 | Tar | 37.8 | 12 | Elc | 44.1 | 12 | Tar | **27.2** | 12 | |
| | | Val1 | 55.6 | 12 | Val1 | 59.2 | 12 | Val1 | 66.6 | 12 | Val1 | **50.0** | 12 | |
| | 16 | | 42.4 | | | 43.8 | | | 47.9 | | | **40.5** | | |
| | | Elc | 32.9 | 16 | Elc | 34.7 | 16 | Elc | 40.8 | 16 | Lom | **31.1** | 16 | |
| | | Llo | 53.9 | 16 | Llo | 54.0 | 16 | Llo | 54.1 | 16 | Val1 | **53.8** | 16 | |

Table 3.14: --Continued

| | | Linear | | | 1st mode | | | Uniform | | | FEMA | | | |
|---|---|---|---|---|---|---|---|---|---|---|---|---|---|---|
| | | EQ | Difference | Story | EQ | Difference | Story | EQ | Difference | Story | EQ | Difference | Story | |
| Irregular | 4 | | 20.6 | | | 20.6 | | | 36.2 | | | **18.3** | | average |
| | | Tar | 7.9 | 1 | Tar | 8.7 | 1 | Val1 | 20.0 | 4 | Sen | **6.5** | 1 | minimum |
| | | Val2 | 28.2 | 1 | Erz | 28.1 | 4 | Tar | 51.0 | 4 | Kob | **24.8** | 4 | maximum |
| | 8 | | 24.8 | | | 25.2 | | | 34.1 | | | **24.8** | | |
| | | Lom | **18.0** | 1 | Lom | 19.4 | 8 | Sen | 23.4 | 8 | Lom | 18.2 | 1 | |
| | | Val2 | 30.9 | 8 | Val2 | 30.9 | 8 | Nah | 49.3 | 8 | Val2 | **30.8** | 8 | |
| | 12 | | 33.9 | | | 34.1 | | | 36.5 | | | **33.9** | | |
| | | Erz | **23.8** | 12 | Erz | 24.3 | 1 | Lom | 29.1 | 12 | Erz | 24.5 | 1 | |
| | | Nah | 44.1 | 12 | Nah | 44.1 | 12 | Val1 | **43.1** | 12 | Nah | 44.3 | 12 | |
| | 16 | | **41.0** | | | 41.3 | | | 41.8 | | | 41.7 | | |
| | | Tar | **22.9** | 16 | Tar | 23.7 | 16 | Tar | 20.4 | 16 | Kob | 24.8 | 16 | |
| | | Nah | 61.9 | 16 | Nah | 62.0 | 16 | Elc | **61.7** | 16 | Nah | 62.3 | 16 | |

Table 3.15: Maximum Member Shear Correlation, Percentage Difference

| | | | Column Shear | | | | Beam Shear | | | | |
|---|---|---|---|---|---|---|---|---|---|---|---|
| | | | Linear | 1st Mode | Uniform | FEMA | Linear | 1st Mode | Uniform | FEMA | |
| Regular | 4 | Turk | 10.9 | 9.9 | 25.4 | **9.0** | 11.3 | **8.6** | 12.2 | 9.0 | 5th EQ |
| | | Lom | **10.5** | 11.6 | 26.3 | 10.9 | 7.1 | **6.9** | 10.0 | 7.0 | largest EQ |
| | 8 | Llo | 25.5 | 24.2 | **9.6** | 27.2 | 13.0 | 12.9 | 14.1 | **12.5** | |
| | | Lom | 18.0 | 15.3 | **1.0** | 18.9 | **9.0** | 11.0 | 15.5 | 9.3 | |
| | 12 | Vall | 24.4 | 24.3 | **7.9** | 28.9 | 14.5 | 13.2 | 16.7 | **11.7** | |
| | | Lom | 43.2 | 43.9 | **33.2** | 44.3 | 14.0 | **10.1** | 19.3 | 14.1 | |
| | 16 | Kob | 59.6 | 59.5 | **53.7** | 61.0 | **11.4** | 15.4 | 11.6 | 12.3 | |
| | | Lom | 54.8 | **33.5** | 44.4 | 46.8 | **21.7** | 96.2 | 25.8 | 42.7 | |

Table 3.15: --Continued

| | | | Column Shear | | | | Beam Shear | | | | |
|---|---|---|---|---|---|---|---|---|---|---|---|
| | | | Linear | 1st Mode | Uniform | FEMA | Linear | 1st Mode | Uniform | FEMA | |
| Tall | 4 | Vall | 9.0 | **8.6** | 10.1 | 9.1 | 12.9 | 11.2 | **11.2** | 12.7 | 5th EQ |
| | | Turk | 9.9 | 10.2 | **9.0** | 9.8 | **1.0** | 2.5 | 2.6 | 1.2 | largest EQ |
| | 8 | Tar | 14.1 | 14.1 | **5.4** | 15.6 | 12.3 | 11.3 | 16.9 | **10.4** | |
| | | Lom | 22.3 | 20.8 | **15.5** | 22.2 | **10.8** | 11.5 | 13.3 | 11.8 | |
| | 12 | Vall | 30.0 | 27.6 | **23.6** | 34.2 | 13.4 | 16.8 | 15.5 | **12.0** | |
| | | Lom | 36.7 | 36.3 | **35.0** | 44.6 | 24.0 | 24.5 | 20.9 | **14.1** | |
| | 16 | Kob | 56.8 | 55.0 | **50.4** | 60.3 | 11.3 | 12.0 | 15.3 | **9.5** | |
| | | Lom | 57.1 | 57.0 | **47.2** | 56.9 | 11.5 | **8.7** | 24.9 | 14.6 | |

Table 3.15: --Continued

| | | | Column Shear | | | | Beam Shear | | | | |
|---|---|---|---|---|---|---|---|---|---|---|---|
| | | | Linear | 1st Mode | Uniform | FEMA | Linear | 1st Mode | Uniform | FEMA | |
| Irregular | 4 | Val2 | 3.0 | 4.0 | 15.6 | **0.7** | 0.9 | 0.8 | **0.4** | 1.4 | 5th EQ |
| | | Lom | 14.1 | 14.8 | 32.2 | **12.0** | 1.5 | 1.0 | 3.1 | **0.7** | largest EQ |
| | 8 | Kob | **8.5** | 9.6 | 9.2 | 8.6 | **7.7** | 8.1 | 9.0 | 8.1 | |
| | | Lom | **4.7** | 4.5 | **4.0** | 6.0 | **5.8** | 6.8 | 7.0 | 8.5 | |
| | 12 | Tar | 38.2 | **21.7** | 32.9 | 37.5 | **7.9** | 33.7 | 10.8 | 7.9 | |
| | | Lom | 43.5 | 54.7 | **38.7** | 42.1 | 5.3 | 14.0 | 7.8 | **4.5** | |
| | 16 | Llo | 45.2 | 44.1 | 51.2 | **44.1** | 8.1 | 8.7 | 11.0 | **7.9** | |
| | | Lom | 48.4 | 47.4 | **35.6** | 46.2 | **8.7** | 10.5 | 11.8 | 9.3 | |

Table 3.16: Maximum Member Rotation Correlation, Percentage Difference

| | | | Column Shear | | | | Beam Shear | | | | |
|---|---|---|---|---|---|---|---|---|---|---|---|
| | | | Linear | 1st Mode | Uniform | FEMA | Linear | 1st Mode | Uniform | FEMA | |
| Regular | 4 | Turk | **4.1** | 54.0 | 21.5 | 5.5 | 8.1 | **0.1** | 17.0 | 2.1 | 5th EQ |
| | | Lom | 9.7 | 49.9 | **5.8** | 8.5 | 6.0 | **4.2** | 5.1 | 4.9 | largest EQ |
| | 8 | Llo | 45.4 | 43.9 | **12.4** | 48.5 | 5.0 | 5.0 | 14.6 | **2.1** | |
| | | Lom | 91.6 | 114 | 182 | **84.9** | 6.4 | **0.6** | 13.0 | 6.4 | |
| | 12 | Vall | **3.6** | **3.6** | 90.9 | 9.1 | **1.5** | **1.5** | 9.9 | 5.5 | |
| | | Lom | **6.4** | 8.8 | 38.8 | 8.2 | **1.4** | 5.6 | 13.5 | 4.2 | |
| | 16 | Kob | 50.0 | 50.0 | **36.7** | 55.0 | 61.6 | 65.2 | 71.0 | **57.3** | |
| | | Lom | **7.2** | 215 | 59.7 | 88.4 | **29.2** | 76.3 | 41.6 | 44.5 | |

Table 3.16: --Continued

| | | | Column Shear | | | | Beam Shear | | | | |
|---|---|---|---|---|---|---|---|---|---|---|---|
| | | | Linear | 1st Mode | Uniform | FEMA | Linear | 1st Mode | Uniform | FEMA | |
| Tall | 4 | Vall | 8.5 | 11.6 | 12.0 | **6.4** | **15.8** | 20.8 | 24.9 | 12.4 | 5th EQ |
| | | Turk | 67.0 | 68.1 | 68.3 | **66.2** | 44.4 | 47.7 | 50.5 | **42.2** | largest EQ |
| | 8 | Tar | 22.8 | 21.0 | **15.4** | 29.9 | 1.4 | **0.5** | 24.4 | 6.2 | |
| | | Lom | **72.2** | 76.1 | 86.8 | 73.6 | **3.3** | 4.3 | 5.2 | 4.9 | |
| | 12 | Vall | **1.0** | 21.6 | 28.4 | 7.5 | 4.0 | 3.7 | **3.3** | 7.6 | |
| | | Lom | 14.9 | 17.5 | **11.1** | 22.3 | 28.9 | 28.6 | 18.1 | **3.2** | |
| | 16 | Kob | 45.4 | 42.0 | **30.0** | 53.9 | 67.7 | 70.7 | 74.6 | **63.0** | |
| | | Lom | 55.4 | 57.4 | **38.3** | 54.8 | 58.0 | 67.2 | 63.1 | **39.6** | |

Table 3.16: --Continued

| | | | Column Shear | | | | Beam Shear | | | | |
|---|---|---|---|---|---|---|---|---|---|---|---|
| | | | Linear | 1st Mode | Uniform | FEMA | Linear | 1st Mode | Uniform | FEMA | |
| Irregular | 4 | Val2 | 35.5 | 37.4 | **23.9** | 42.7 | **24.8** | 26.1 | 31.2 | 32.5 | 5th EQ |
| | | Lom | 28.6 | 31.6 | **7.6** | 28.0 | 18.7 | 21.0 | **13.7** | 24.7 | largest EQ |
| | 8 | Kob | 16.6 | 15.2 | **4.2** | 18.0 | 17.4 | 18.6 | 26.9 | 16.1 | |
| | | Lom | 15.3 | 13.2 | 23.9 | **9.5** | 14.4 | 13.0 | 19.4 | **6.9** | |
| | 12 | Tar | 45.7 | 110.3 | **9.1** | 48.4 | **19.3** | 74.0 | 26.4 | 22.8 | |
| | | Lom | 65.7 | 92.5 | **31.6** | 73.2 | **15.8** | 62.1 | 16.9 | 19.3 | |
| | 16 | Llo | 45.4 | 45.4 | **19.2** | 52.0 | 31.5 | **28.5** | 34.4 | 30.9 | |
| | | Lom | 76.2 | 74.9 | **52.9** | 78.0 | 21.1 | **15.8** | 22.6 | 18.5 | |

# FIGURES

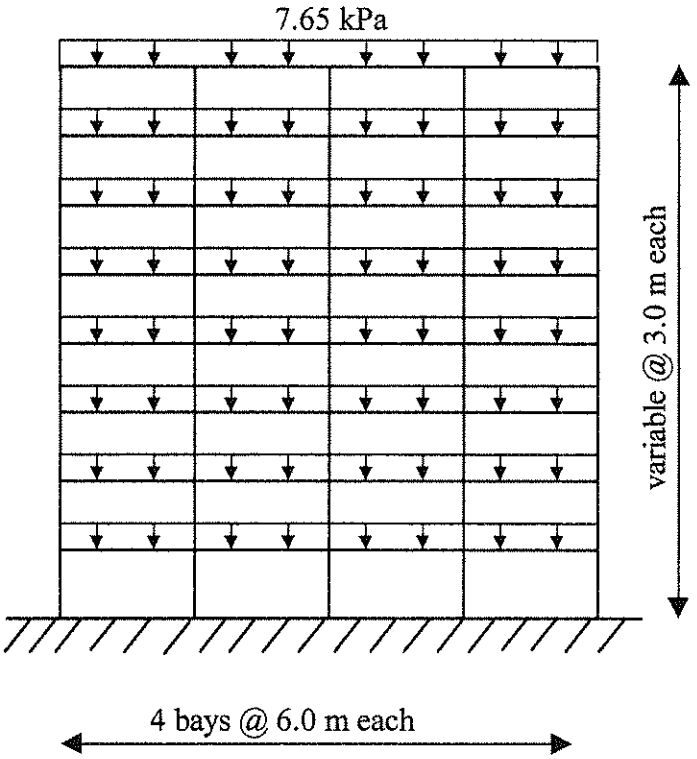


Figure 2.1: Representative Frame

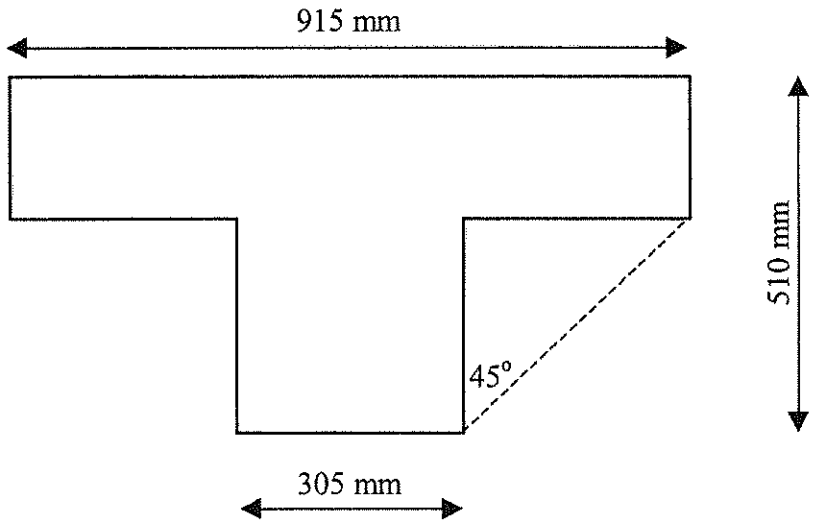


Figure 2.2: Representative Girder

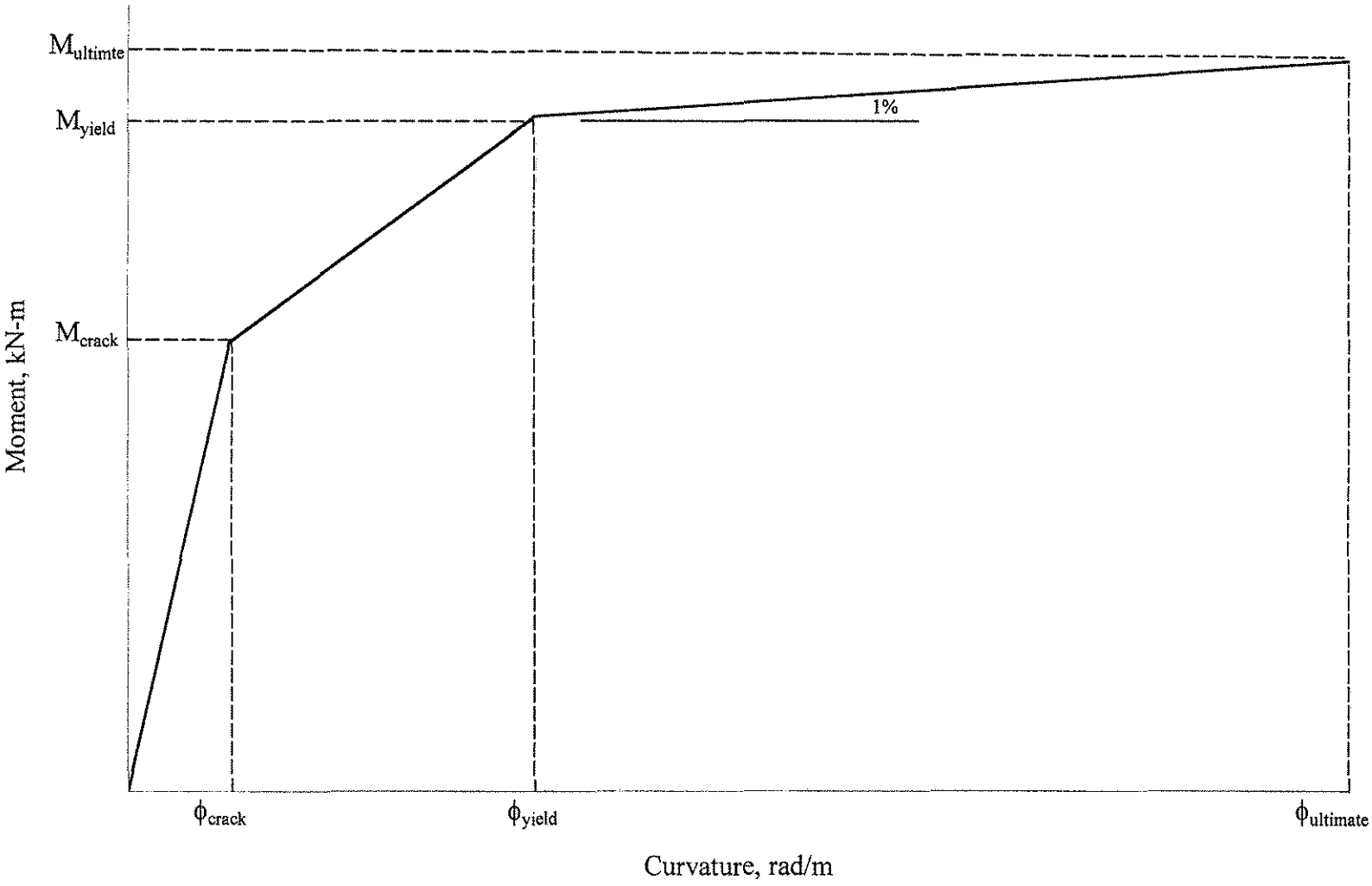


Figure 2.3: Sample of Tri-linear Representation of Members

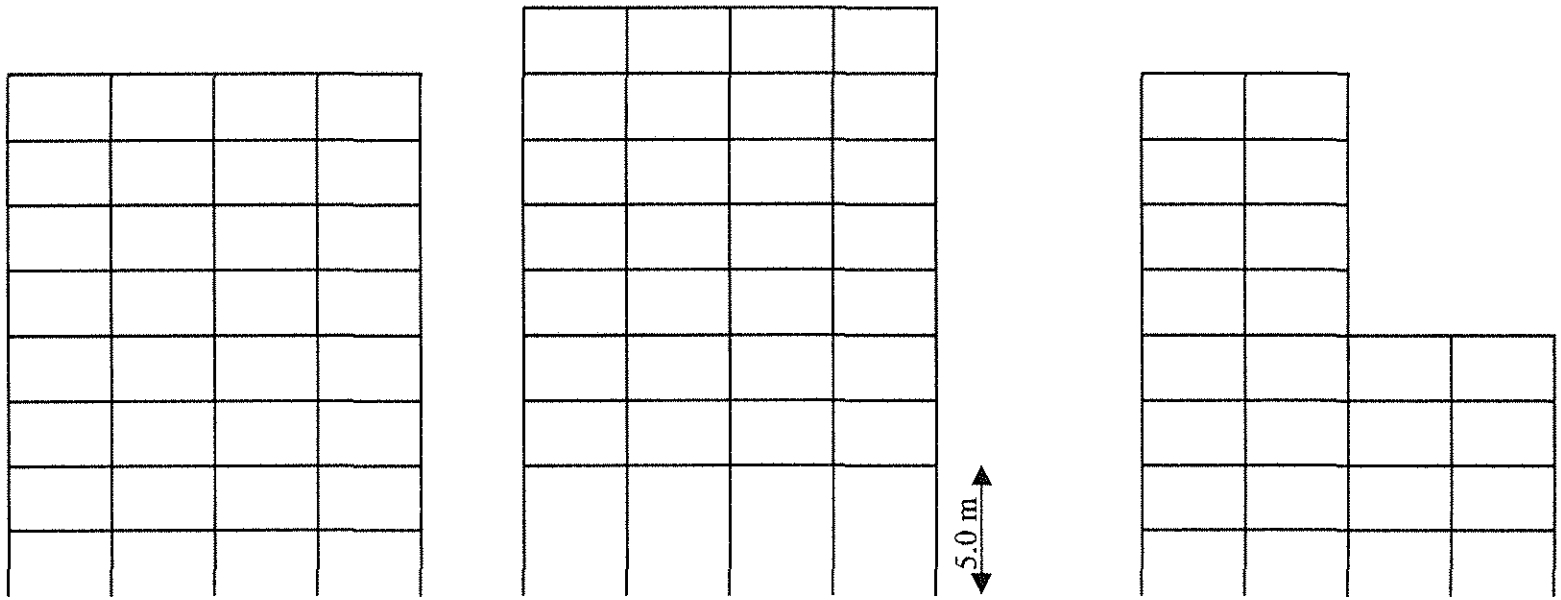


(a) Regular Frame (b) Tall First Story Frame (c) Irregular Stepped Frame

Figure 2.4: Frame Geometries

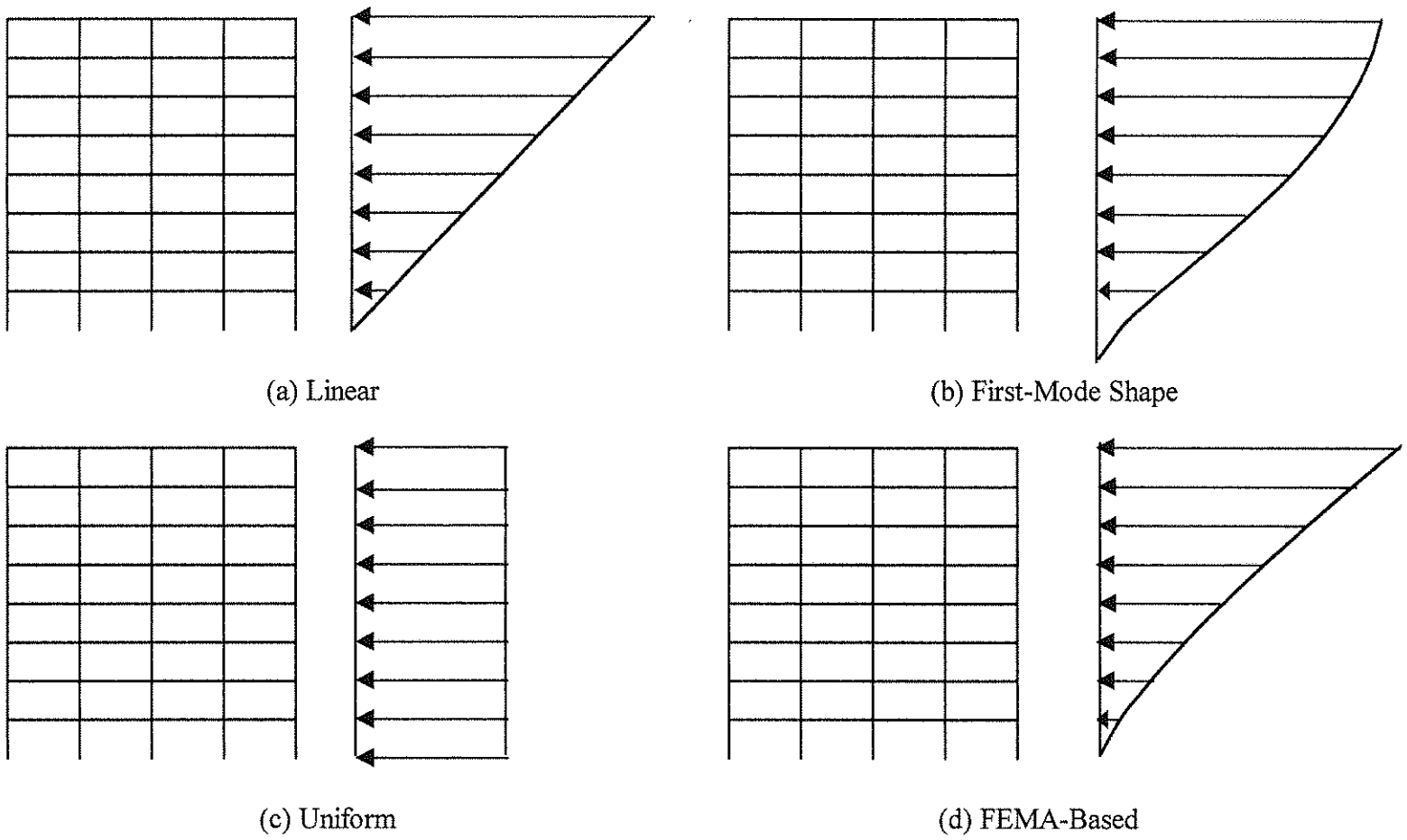


Figure 2.5: Loading Distributions

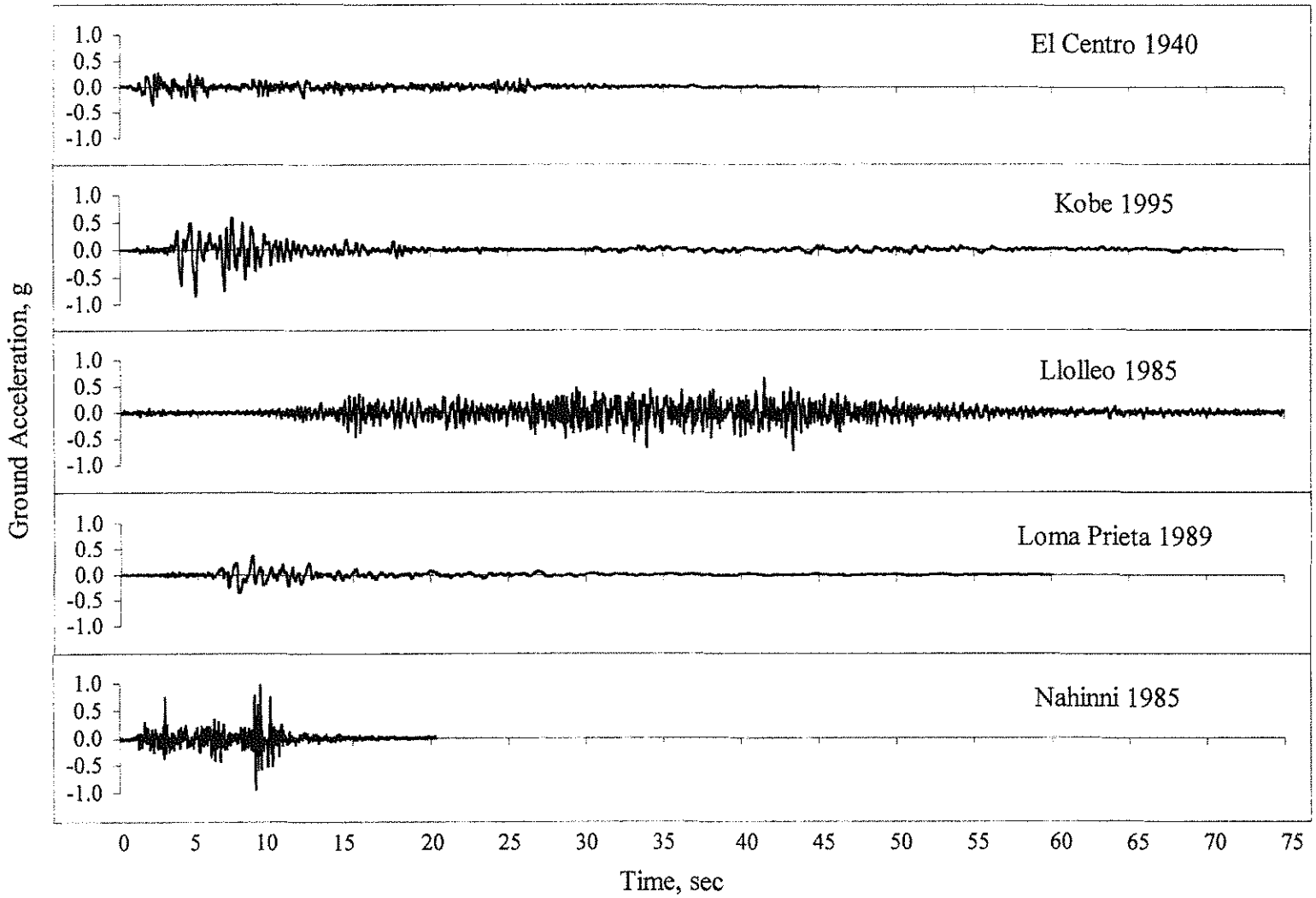


Figure 2.6: Acceleration Records

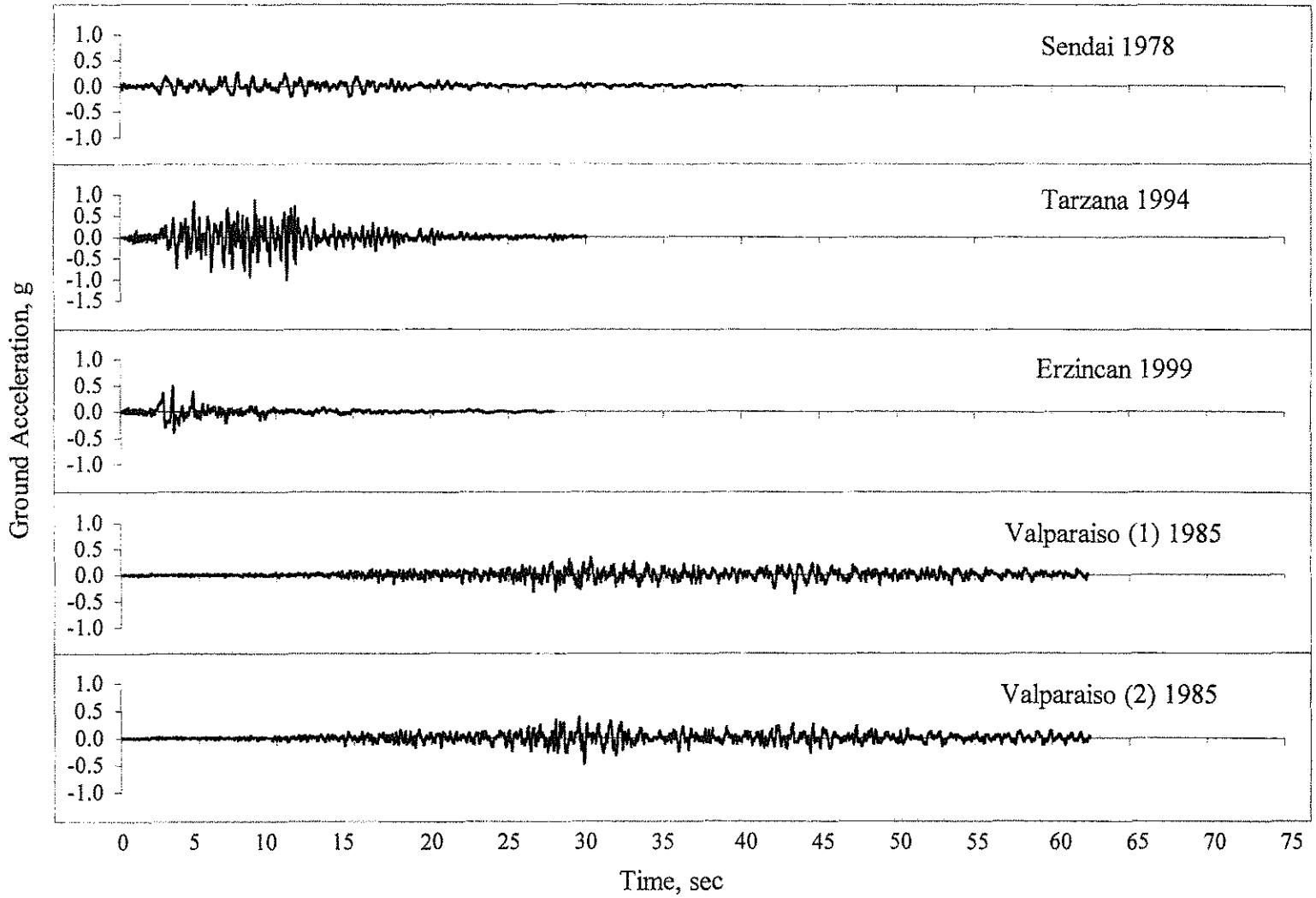


Figure 2.6: --Continued

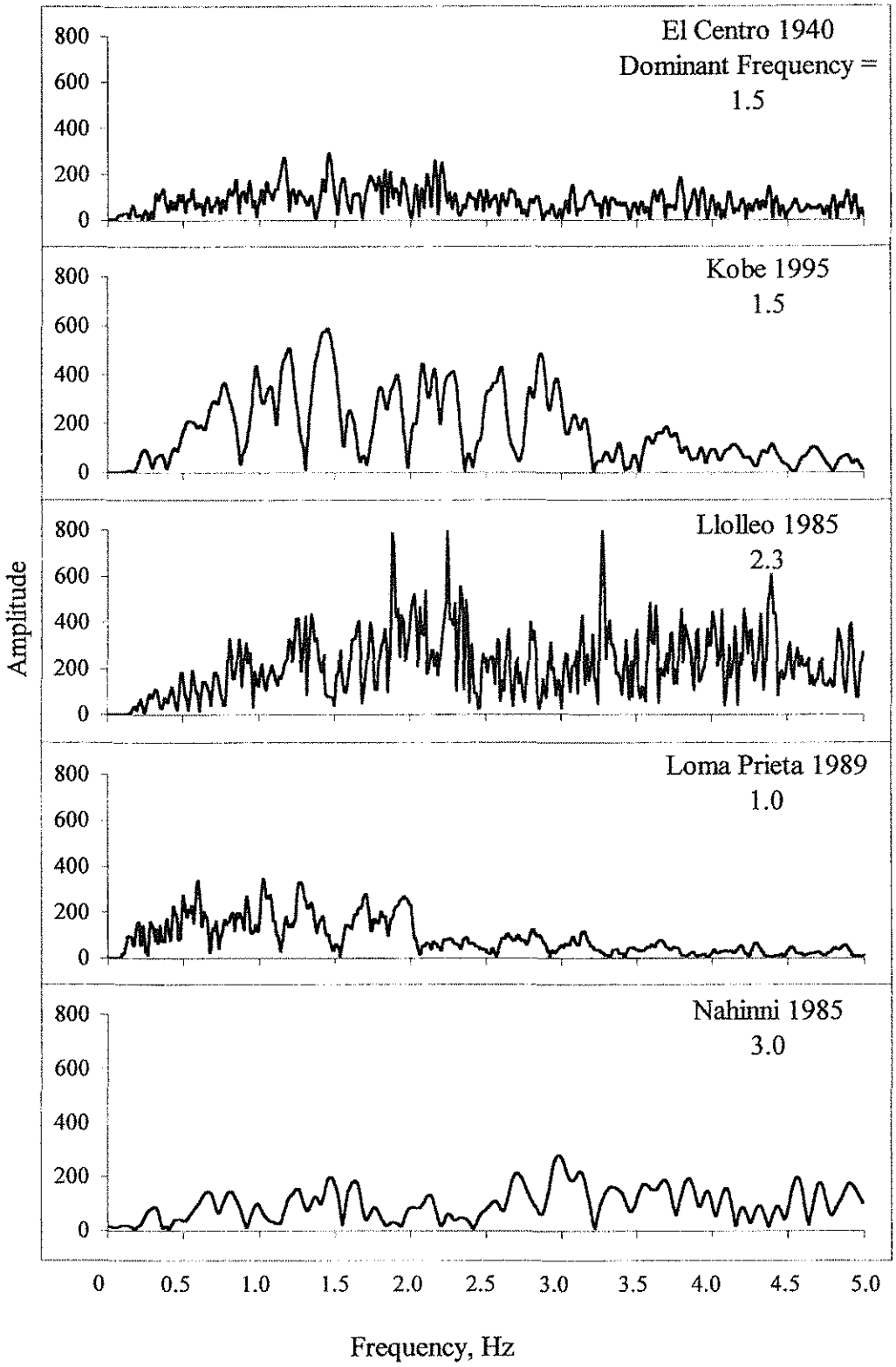


Figure 2.7: Fourier Amplitude Spectra for Acceleration Records

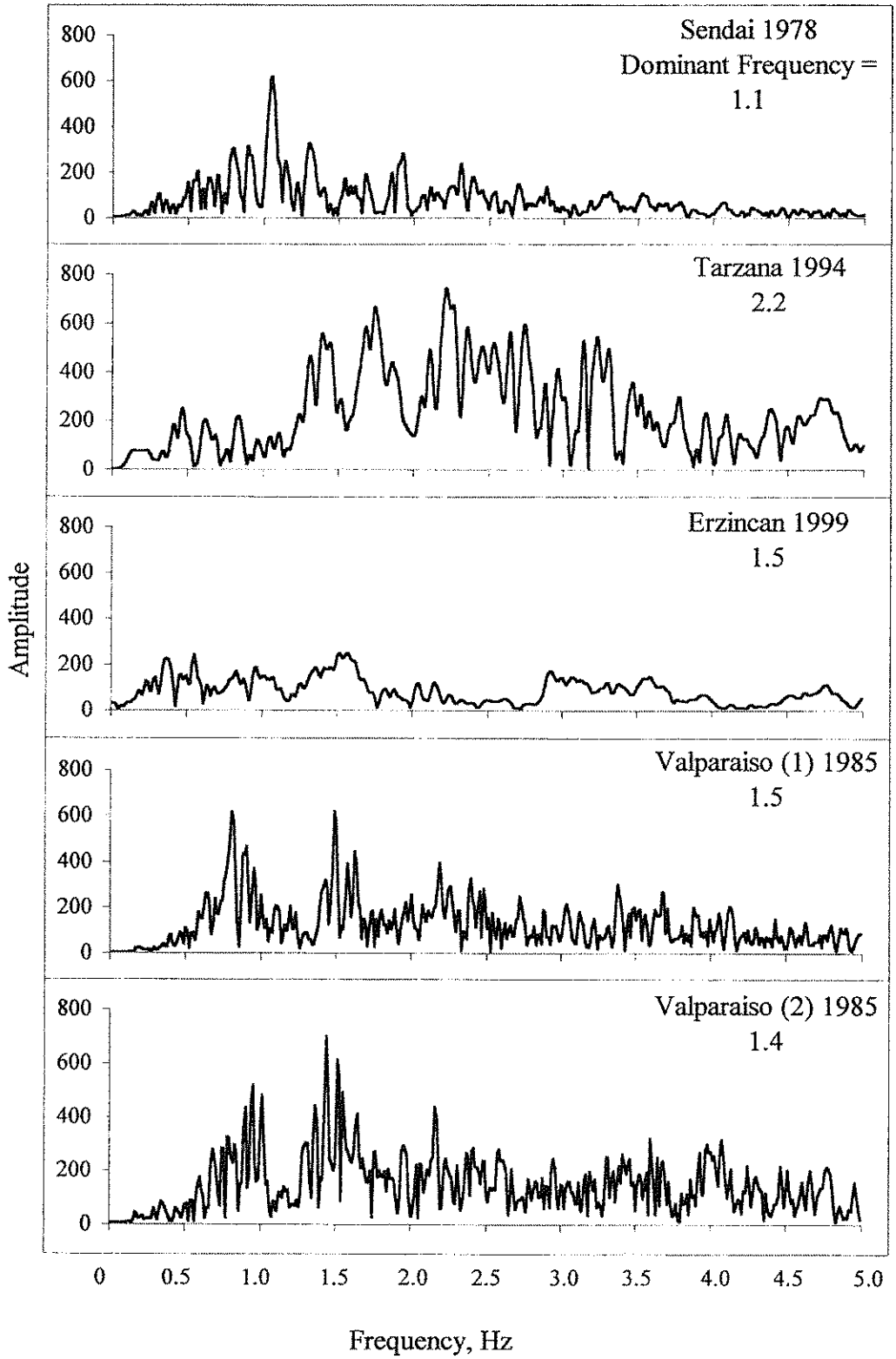


Figure 2.7: --Continued

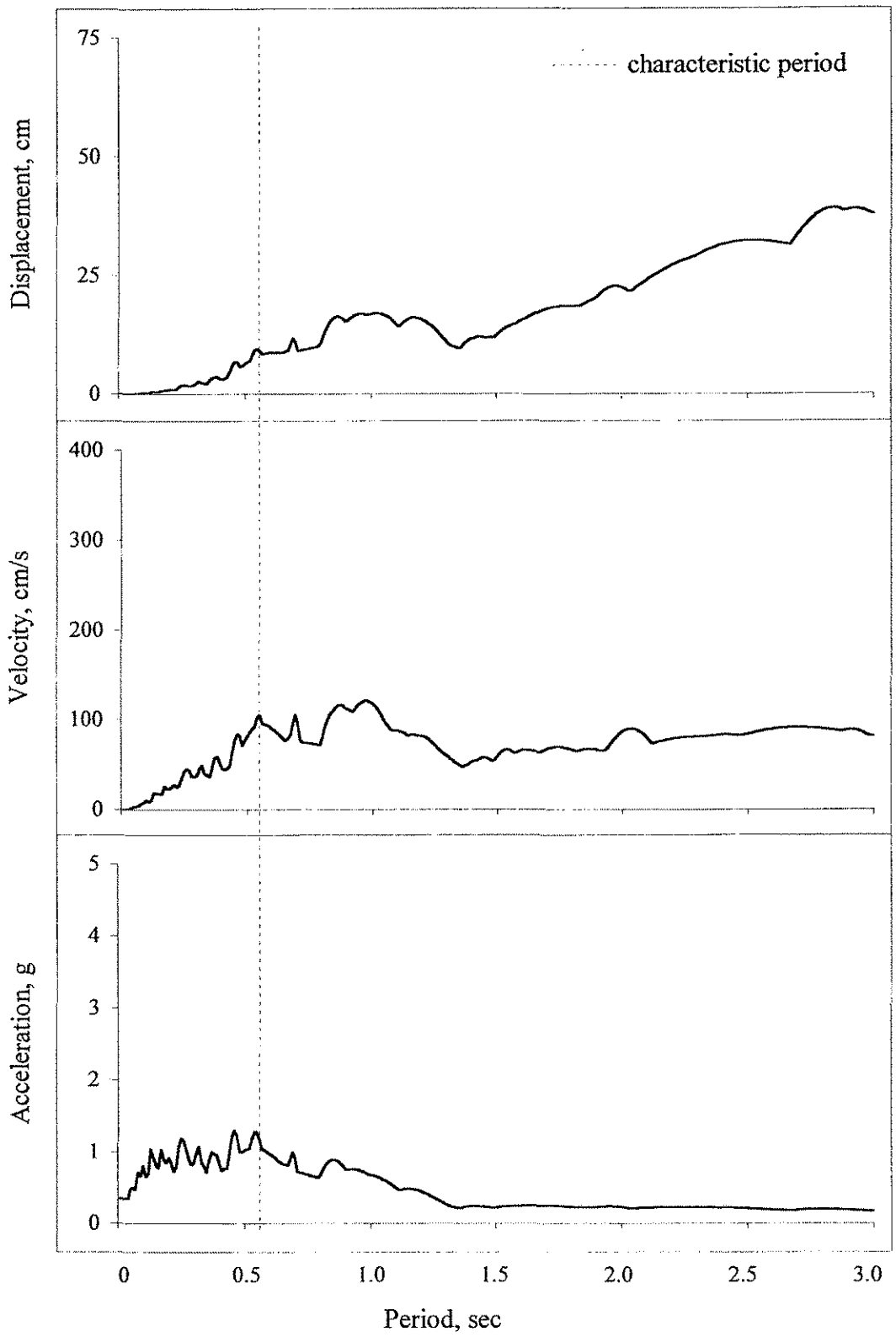


Figure 2.8: Response Spectra for El Centro, 2% damping

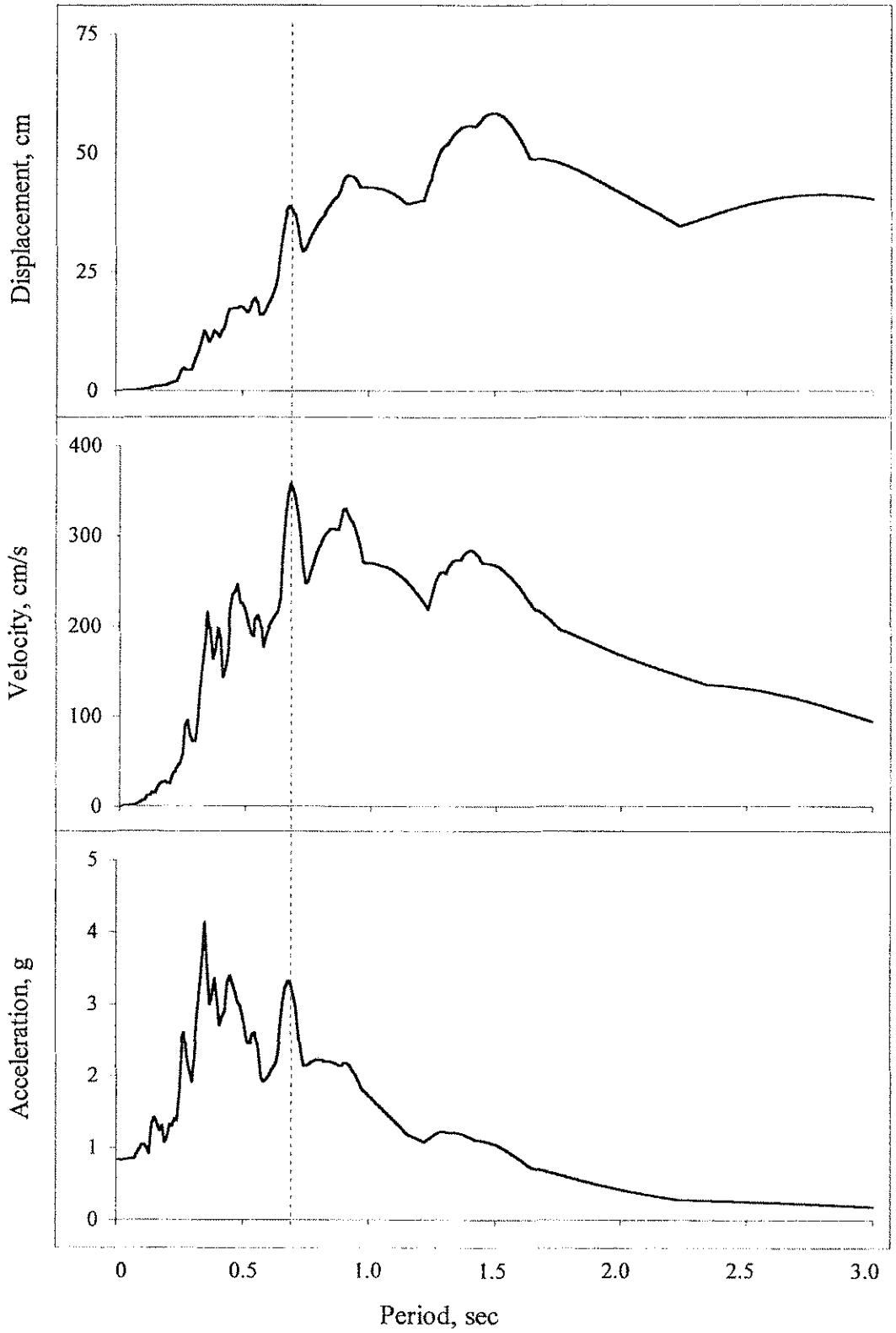


Figure 2.9: Response Spectra for Kobe, 2% damping

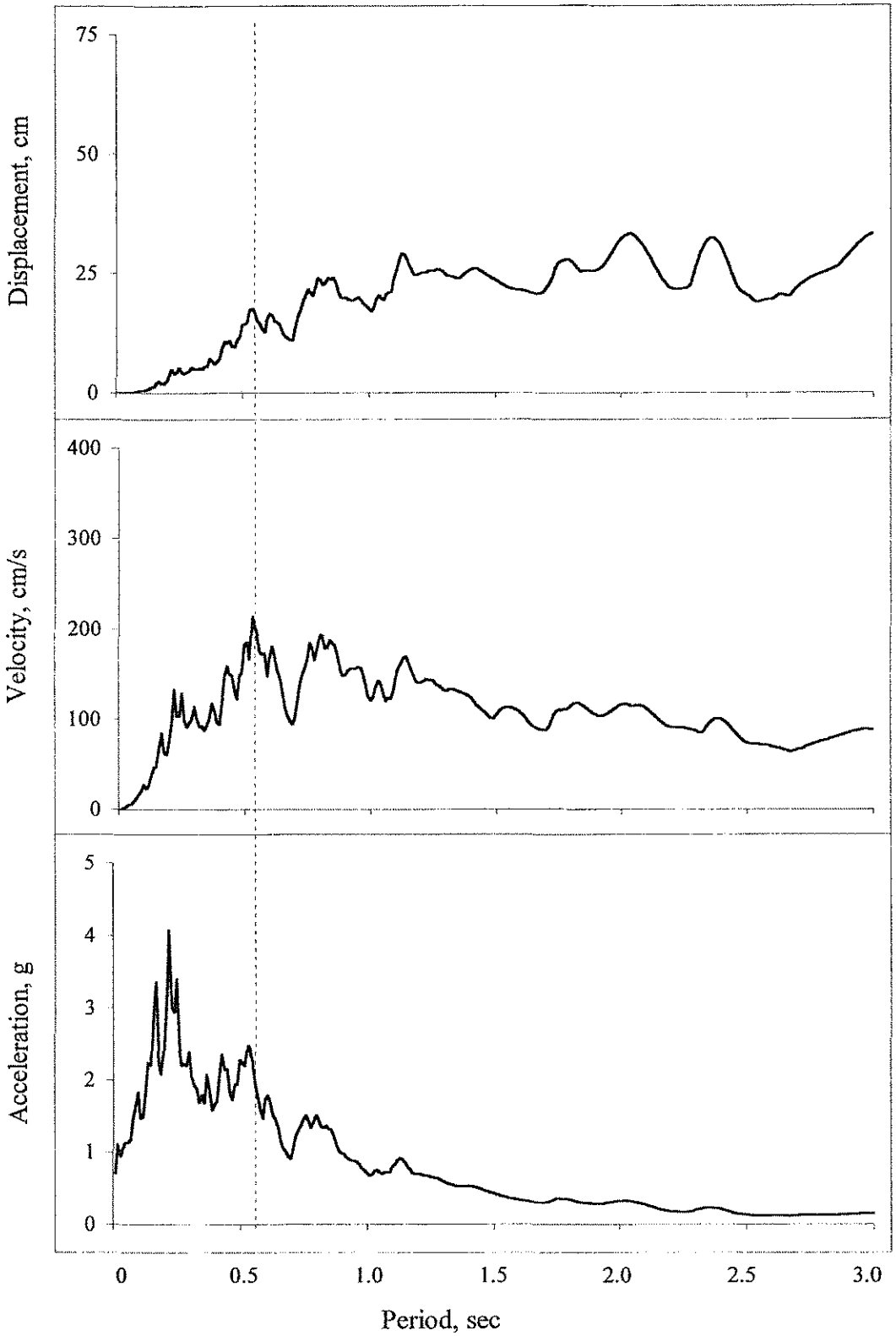


Figure 2.10: Response Spectra for Llolleo, 2% damping

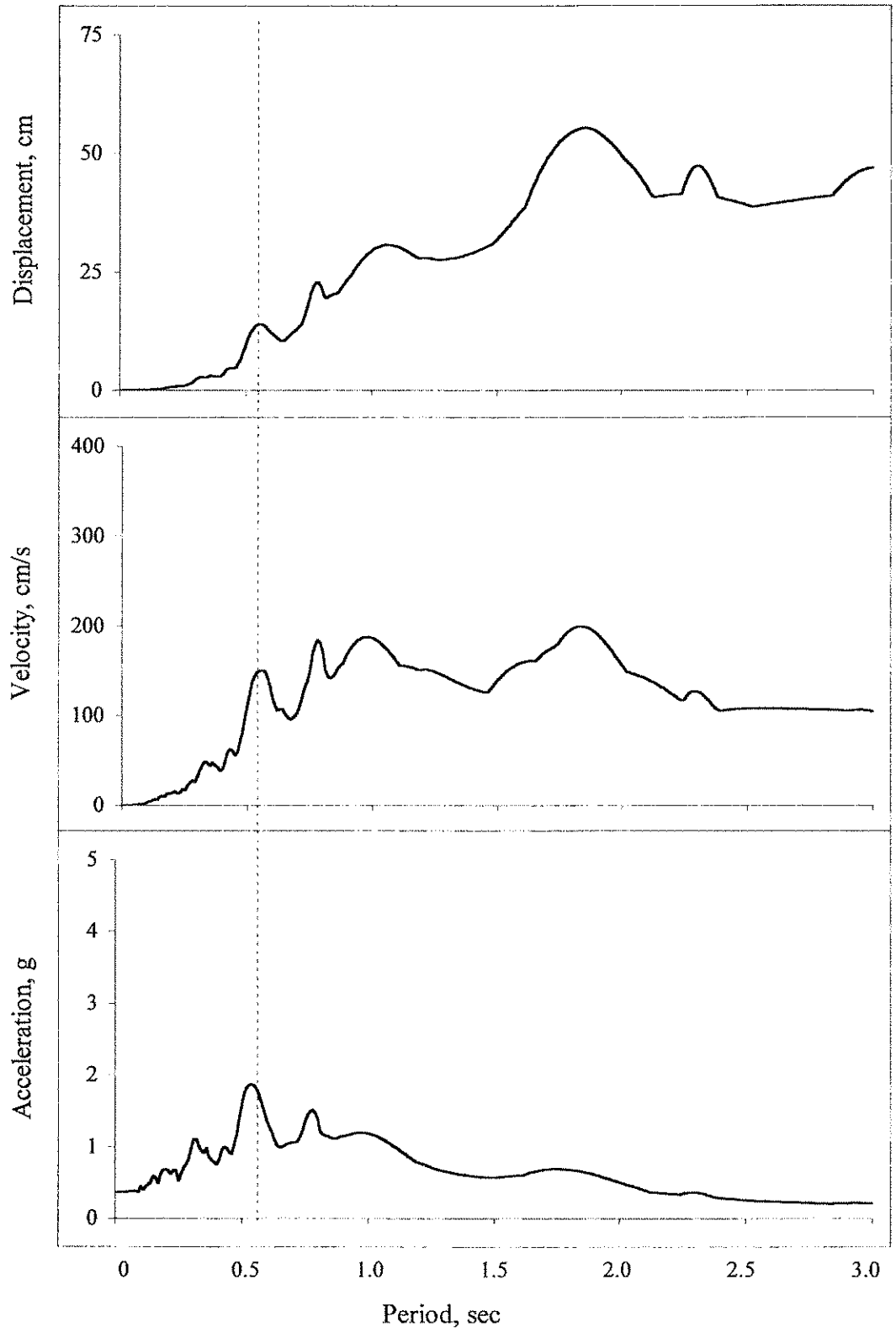


Figure 2.11: Response Spectra for Loma Prieta, 2% damping

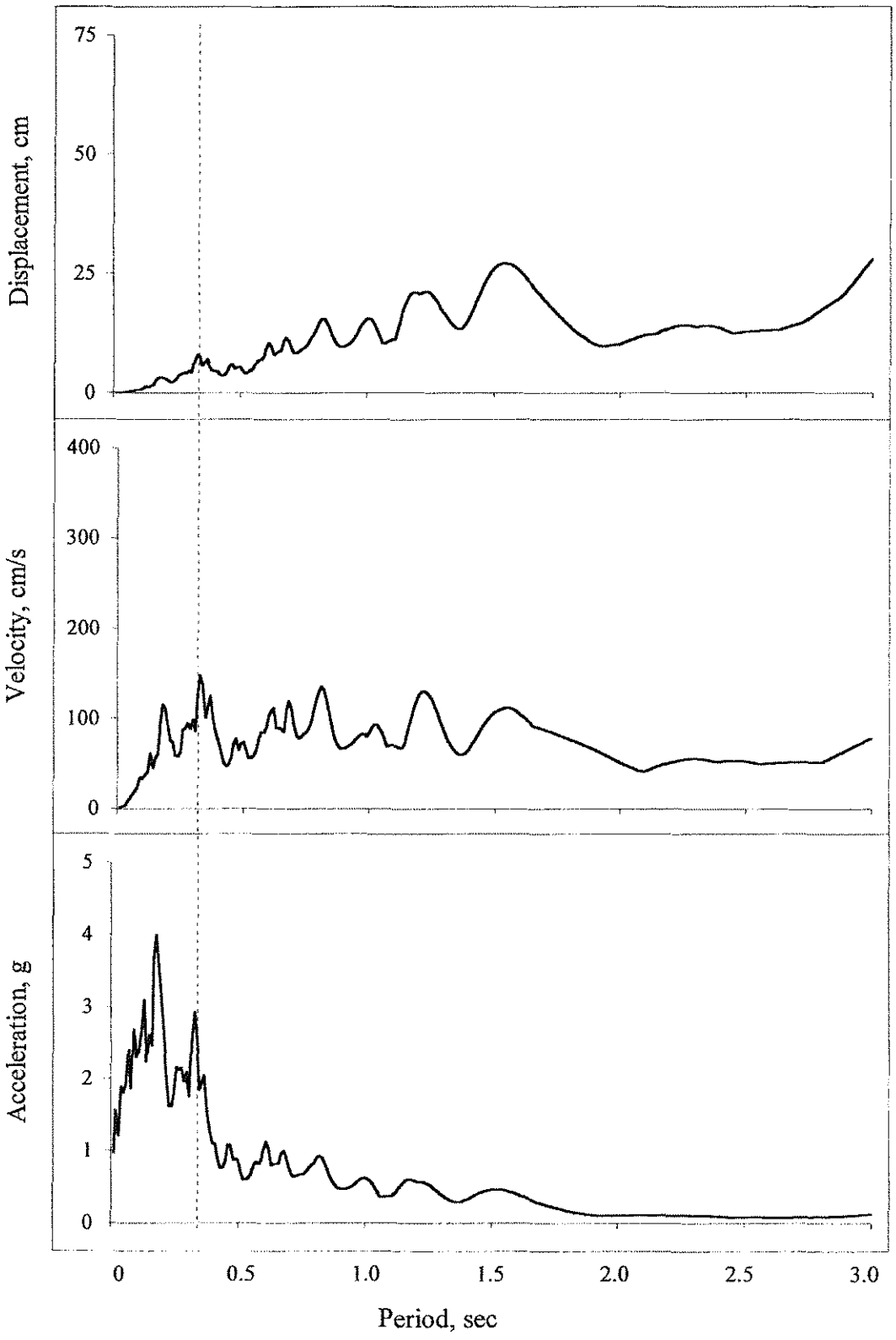


Figure 2.12: Response Spectra for Nahinni, 2% damping

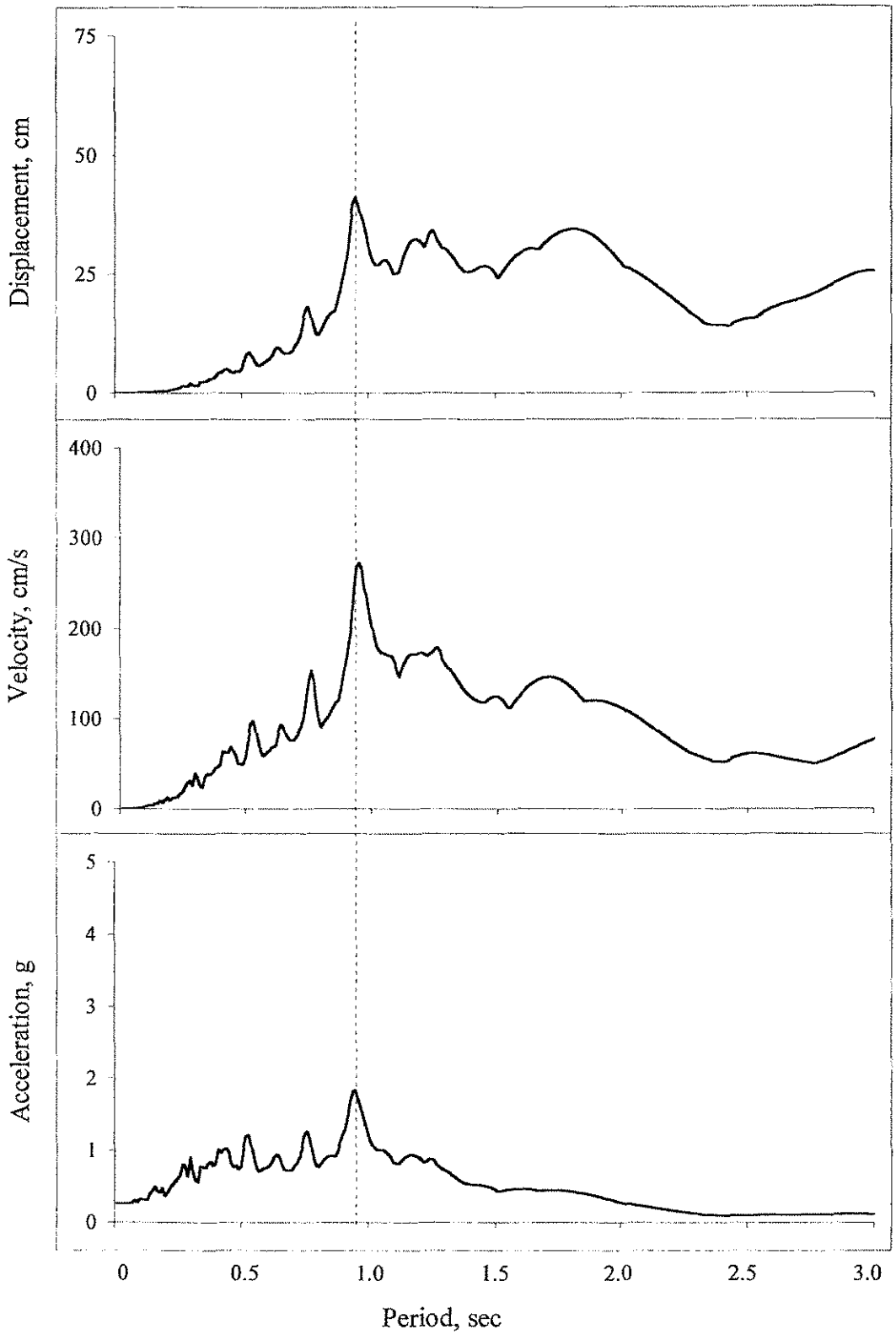


Figure 2.13: Response Spectra for Sendai, 2% damping

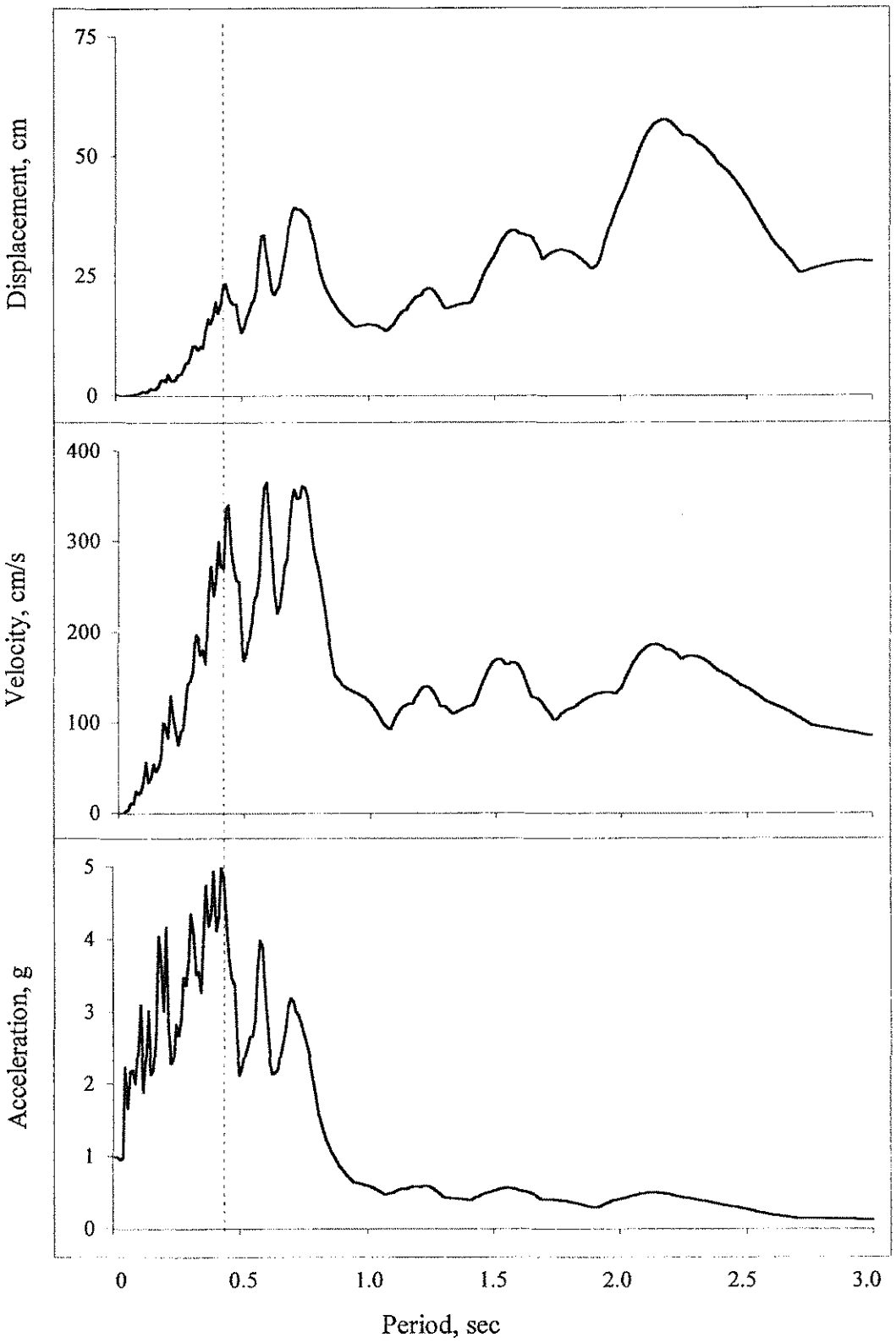


Figure 2.14: Response Spectra for Tarzana, 2% damping

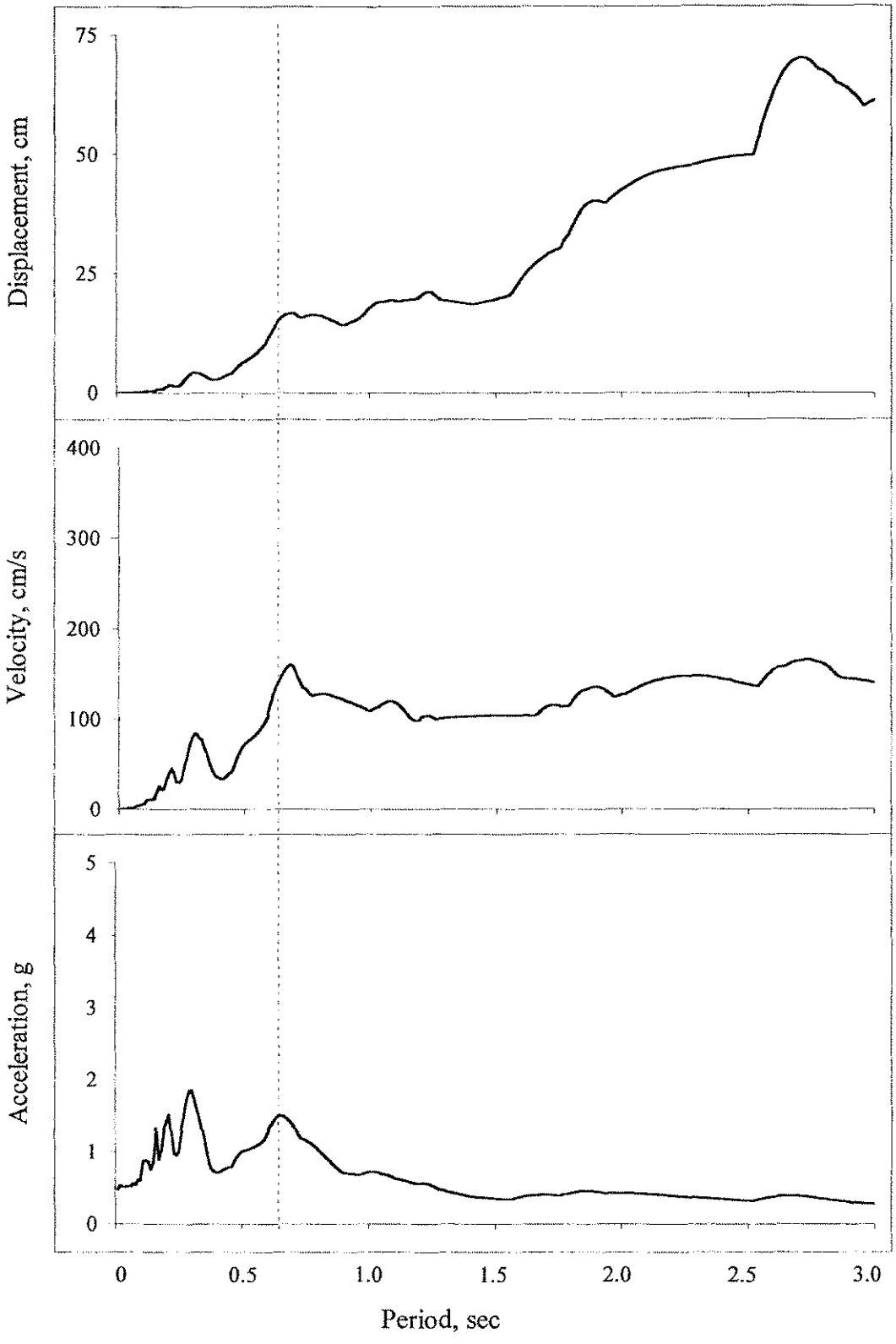


Figure 2.15: Response Spectra for Erzincan, 2% damping

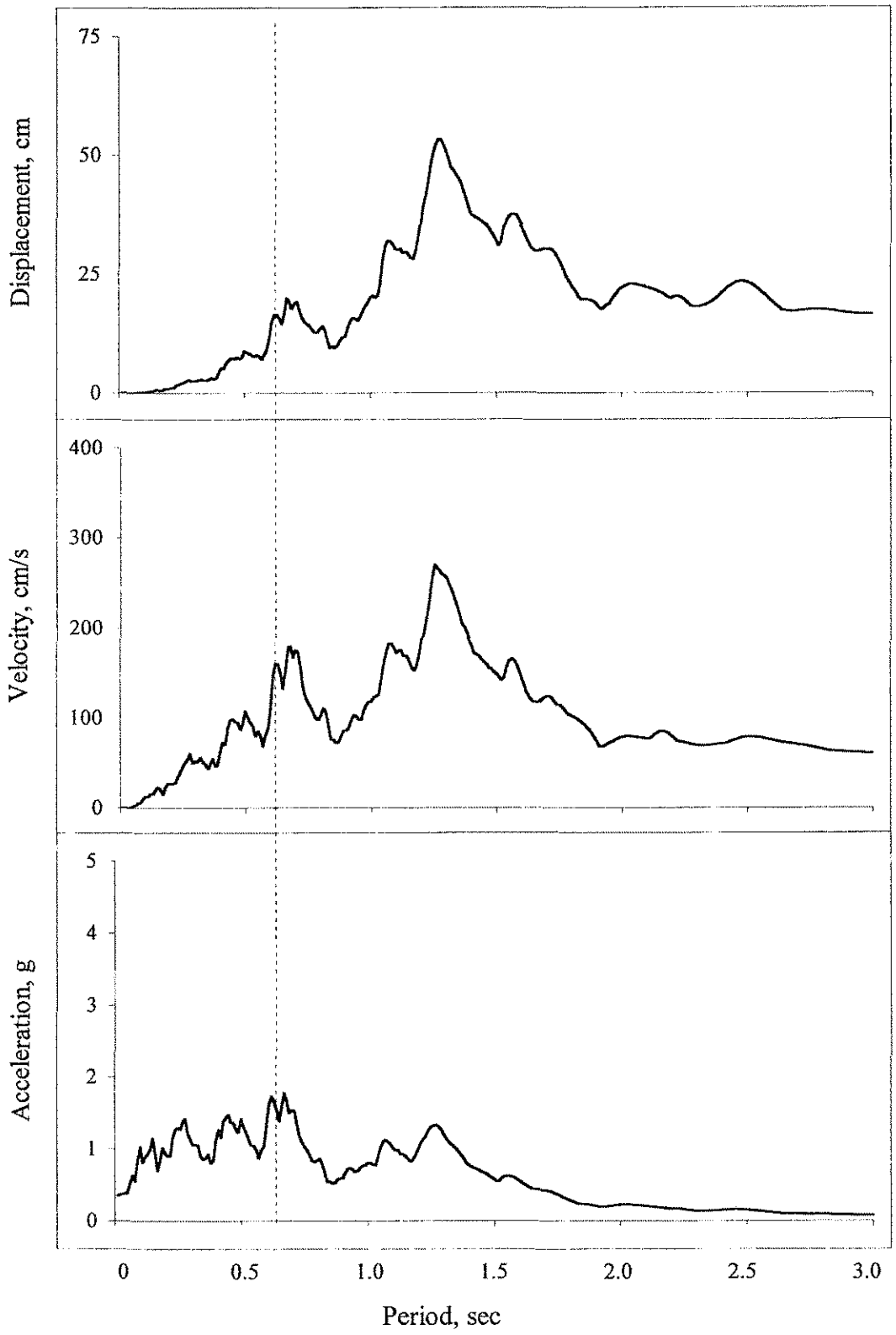


Figure 2.16: Response Spectra for Valparaiso (1), 2% damping

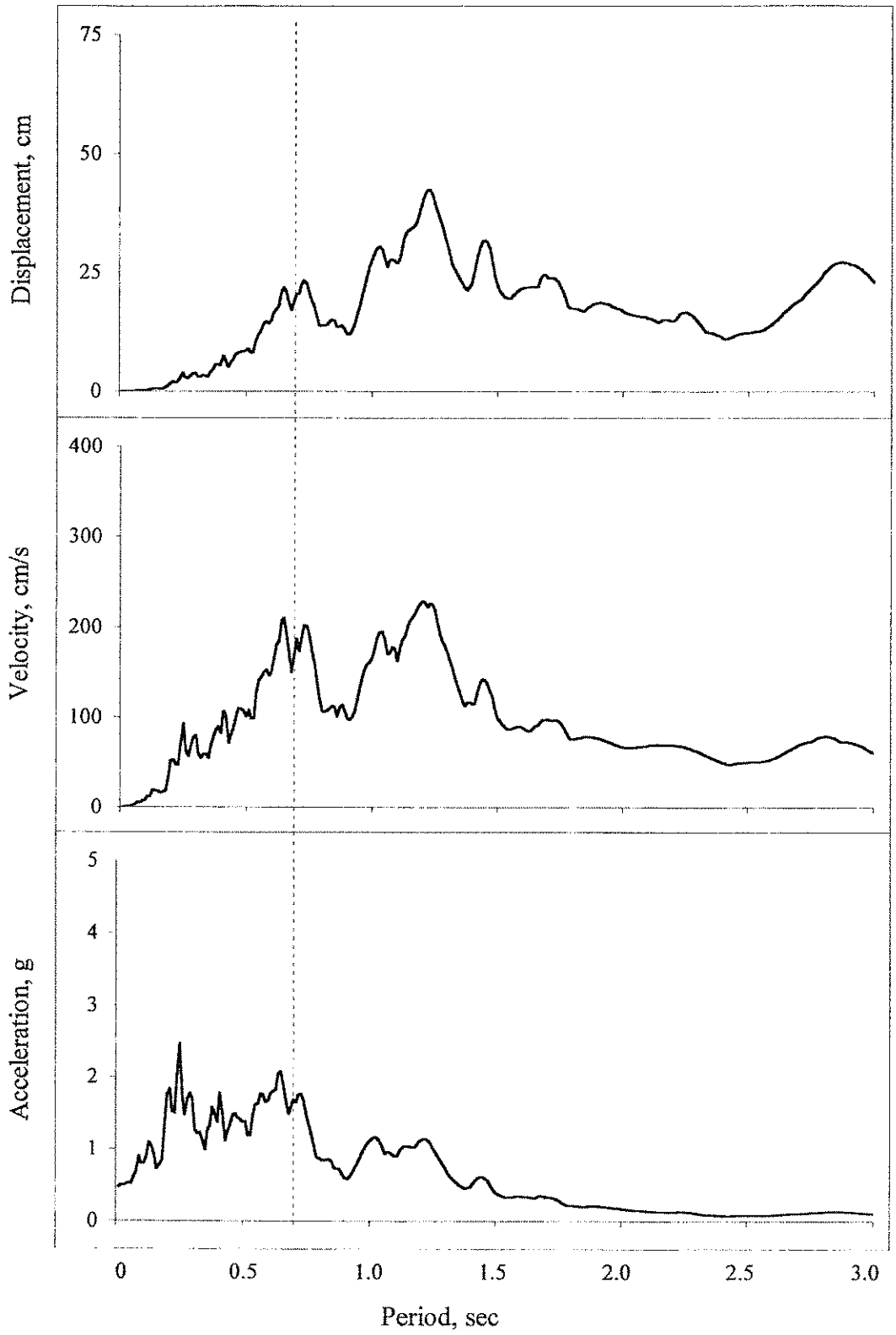


Figure 2.17: Response Spectra for Valparaiso (2), 2% damping

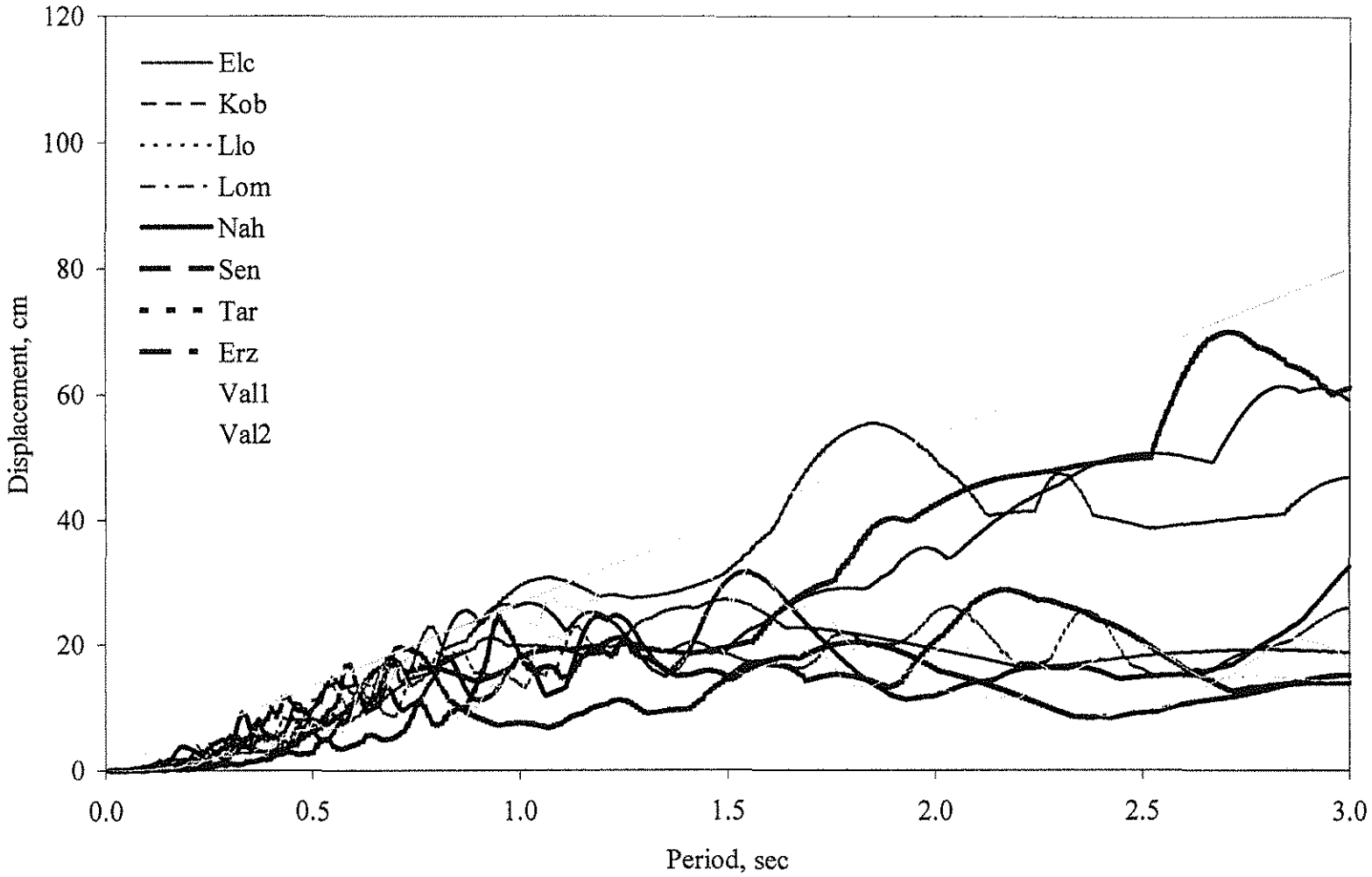


Figure 2.18: Displacement Response Spectra Scaled to 80/3*$T$

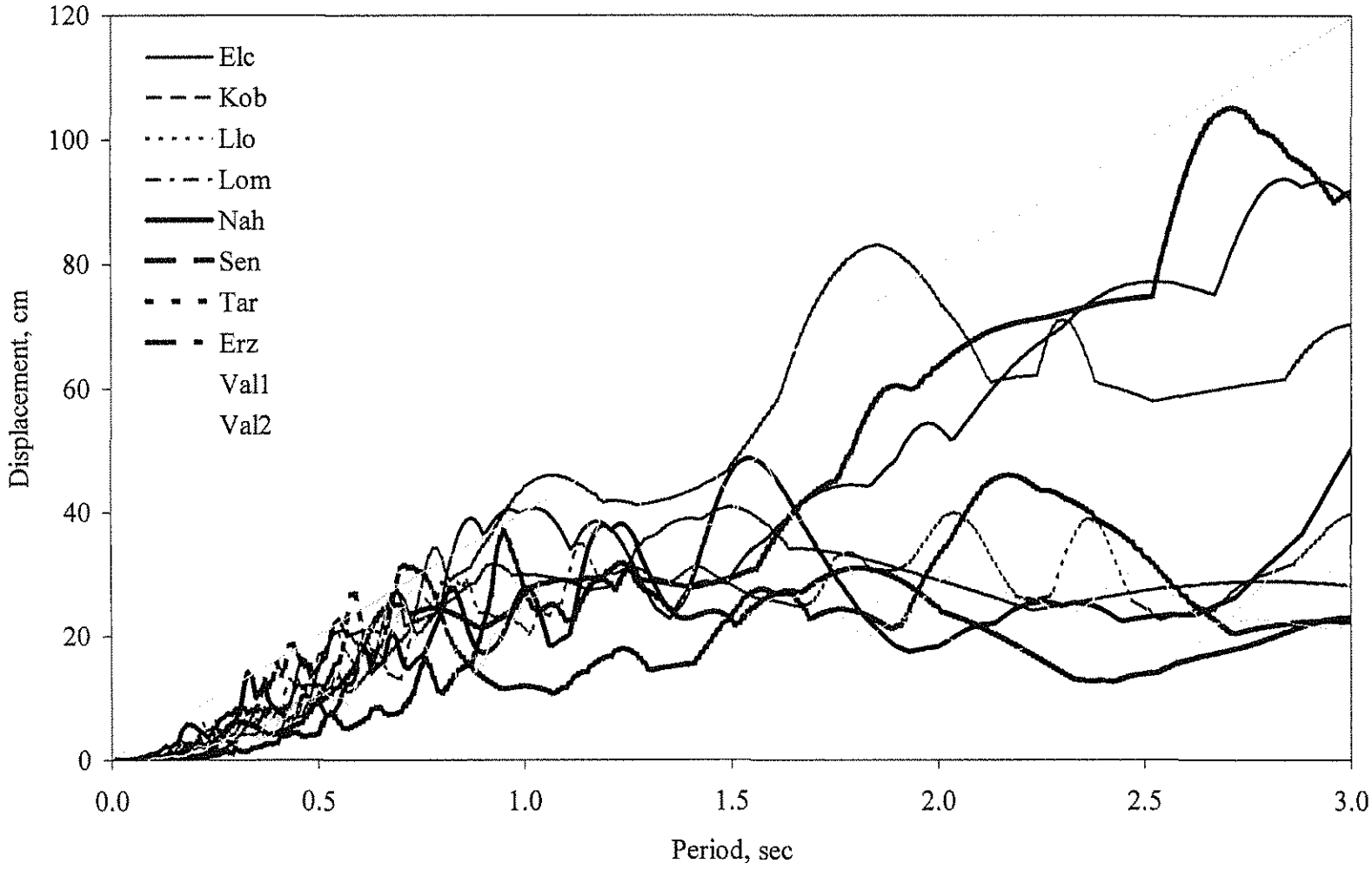


Figure 2.19: Displacement Response Spectra Scaled to 40*$T$

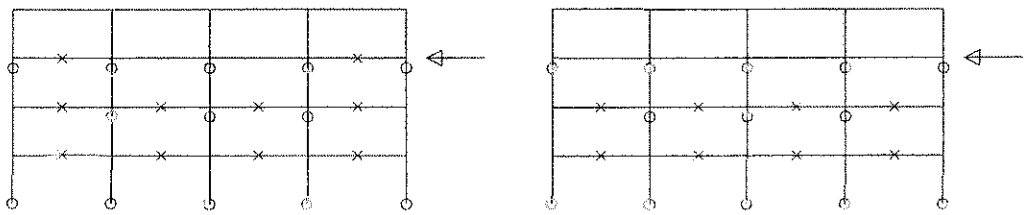

a) Linear

b) 1st Mode

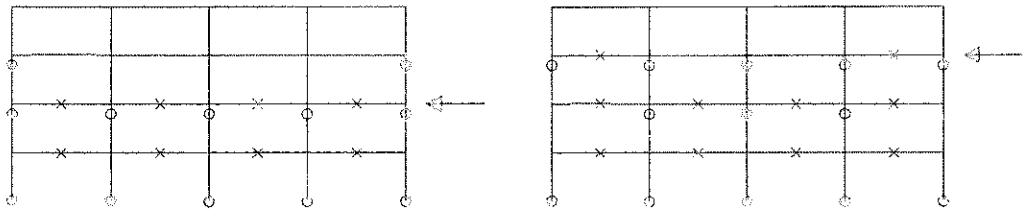

c) Uniform

d) FEMA

Figure 3.1: Member Yielding in Regular 4-Story Frames at Mechanism, Static Analysis

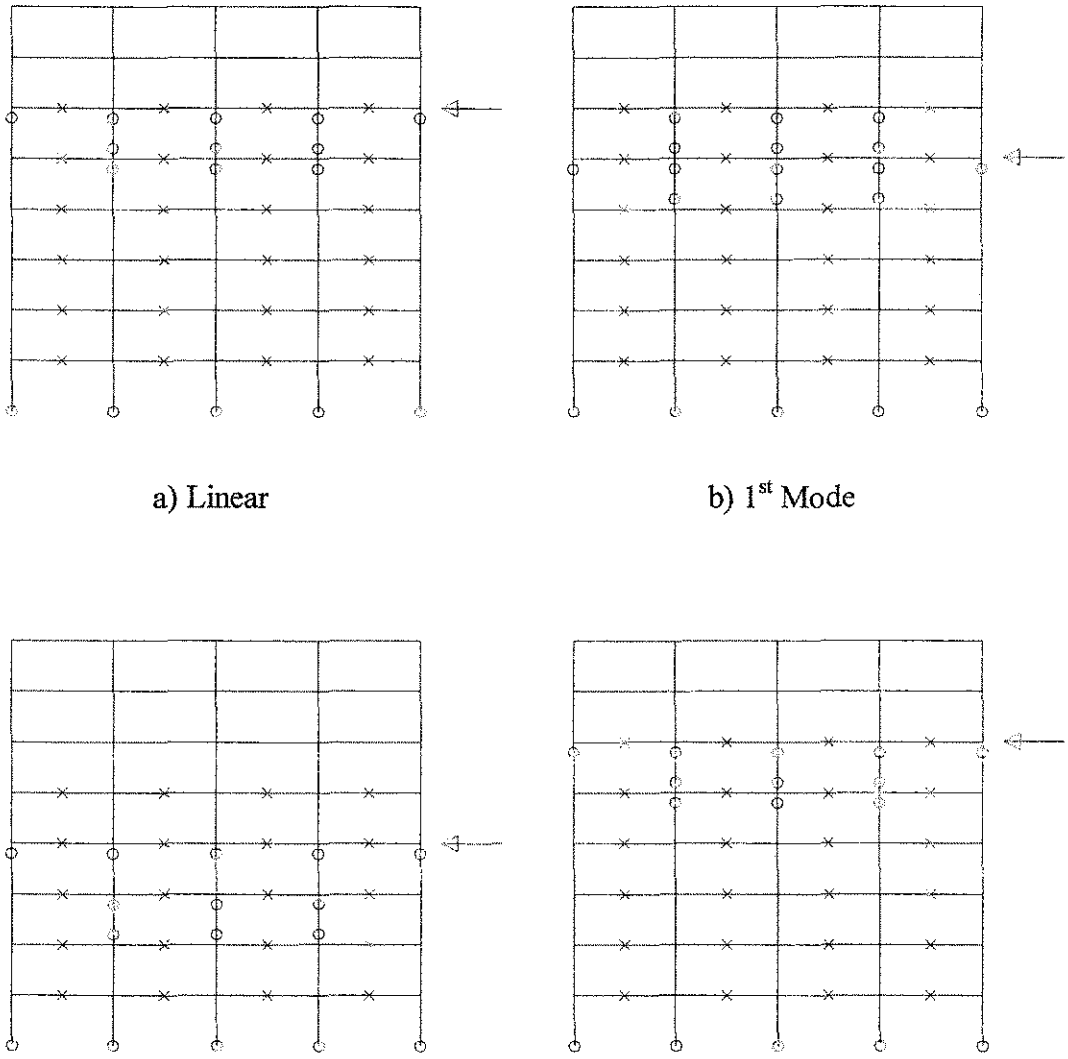

a) Linear

b) 1st Mode

c) Uniform

d) FEMA

Figure 3.2: Member Yielding in Regular 8-Story Frames at Mechanism, Static Analysis

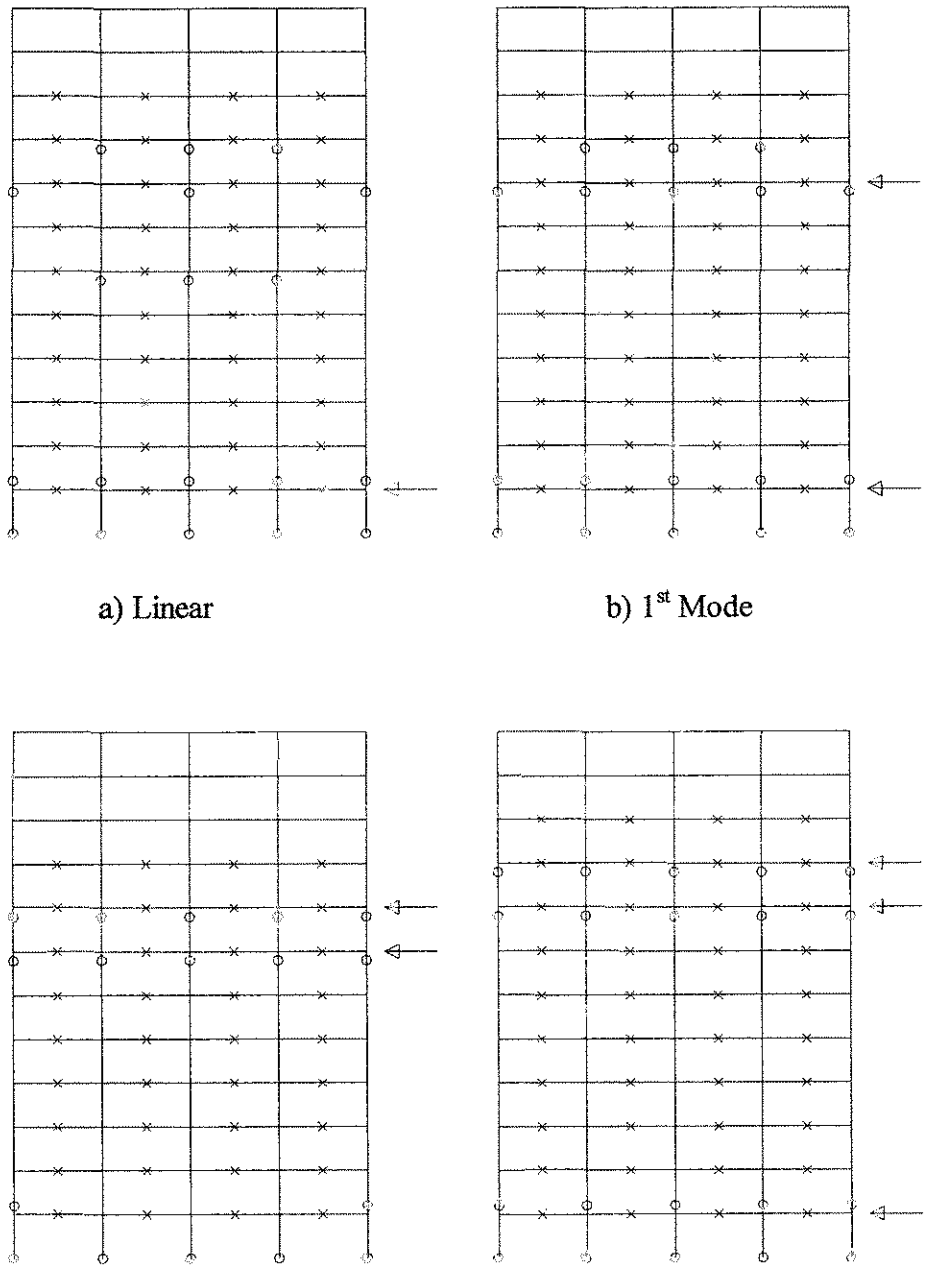

a) Linear

b) 1st Mode

c) Uniform

d) FEMA

Figure 3.3: Member Yielding in Regular 12-Story Frames at Mechanism, Static Analysis

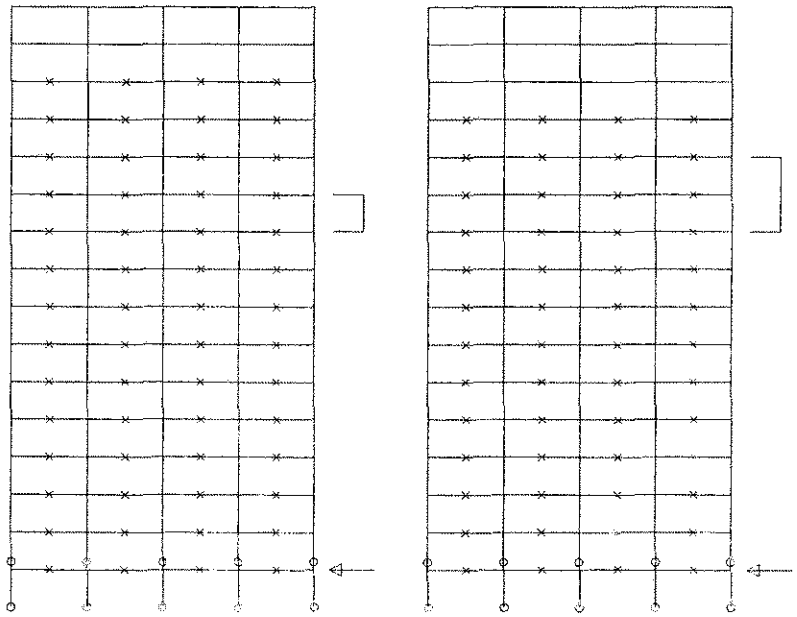

a) Linear b) 1st Mode

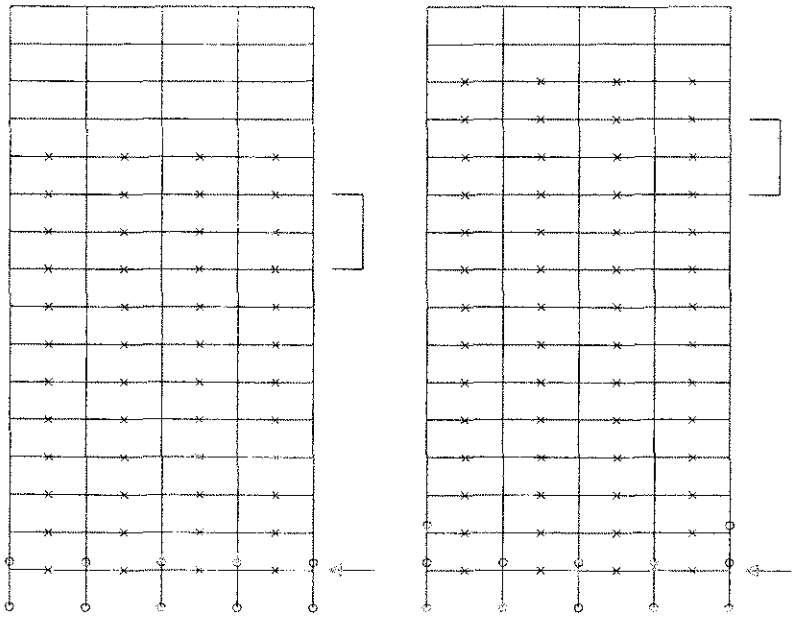

c) Uniform d) FEMA

Figure 3.4: Member Yielding in Regular 16-Story Frames at Mechanism, Static Analysis

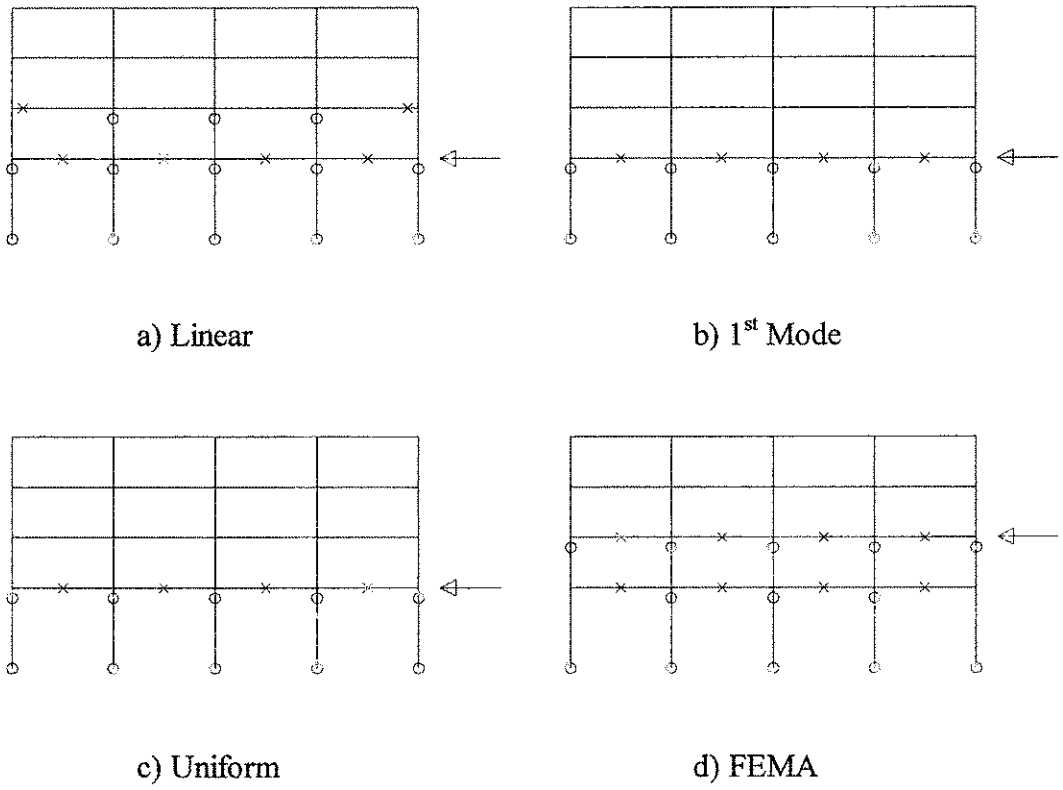

a) Linear

b) 1st Mode

c) Uniform

d) FEMA

Figure 3.5: Member Yielding in Tall First Story 4-Story Frames at Mechanism, Static Analysis

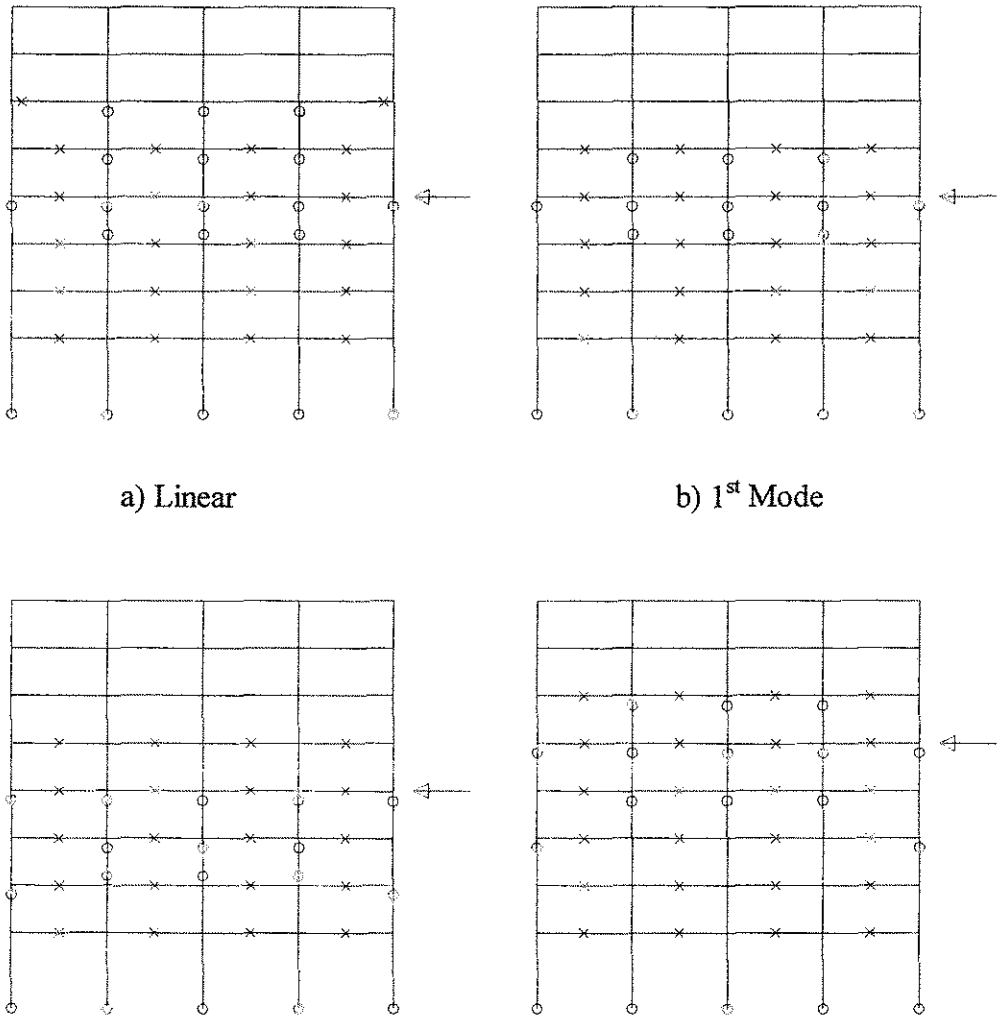

a) Linear

b) 1st Mode

c) Uniform

d) FEMA

Figure 3.6: Member Yielding in Tall First Story 8-Story Frames at Mechanism, Static Analysis

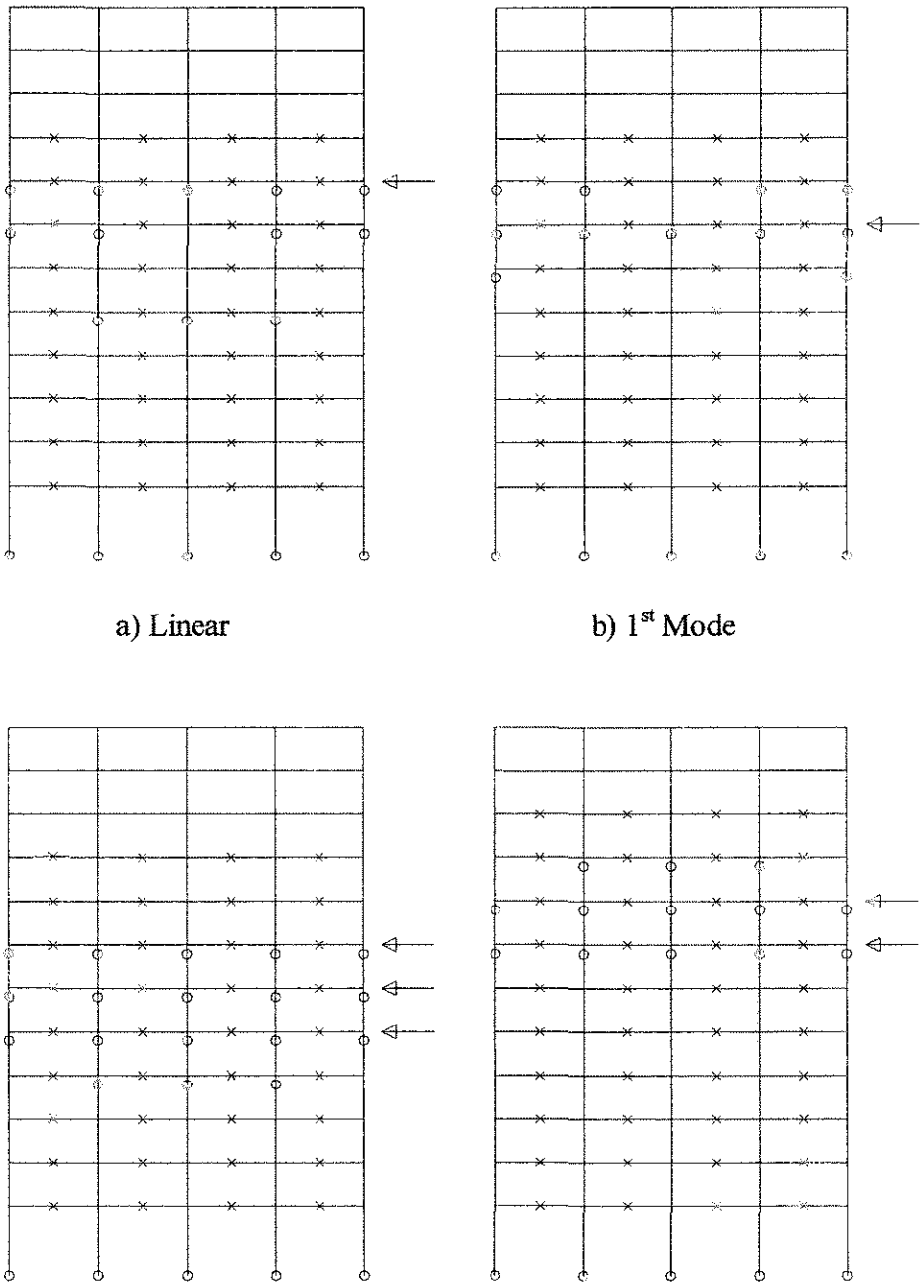

a) Linear

b) 1st Mode

c) Uniform

d) FEMA

Figure 3.7: Member Yielding in Tall First Story 12-Story Frames at Mechanism, Static Analysis

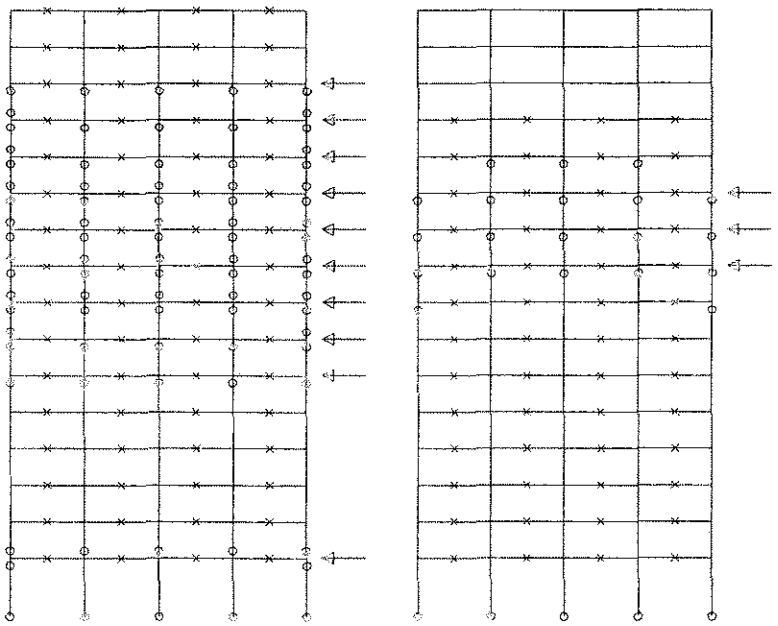

a) Linear b) 1st Mode

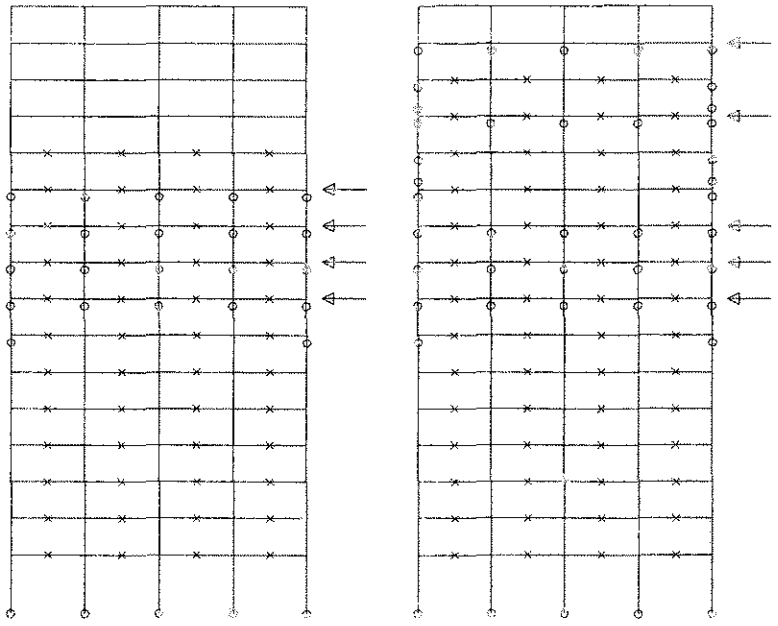

c) Uniform d) FEMA

Figure 3.8: Member Yielding in Tall First Story 16-Story Frames at Mechanism, Static Analysis

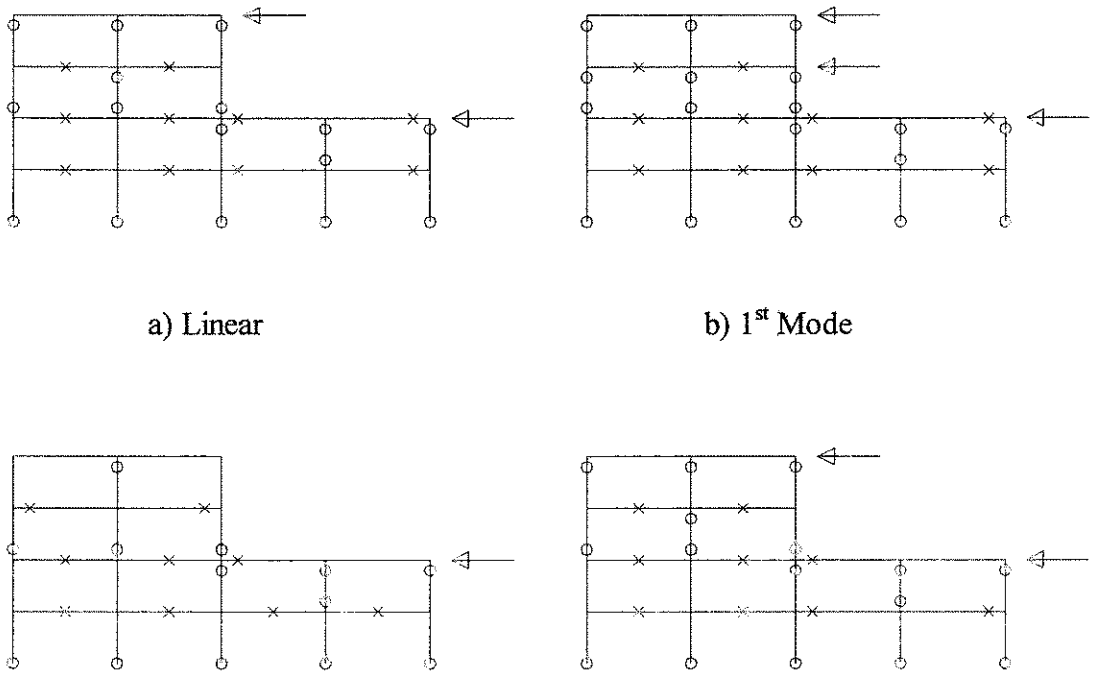

a) Linear

b) 1st Mode

c) Uniform

d) FEMA

Figure 3.9: Member Yielding in Irregular 4-Story Frames at Mechanism, Static Analysis

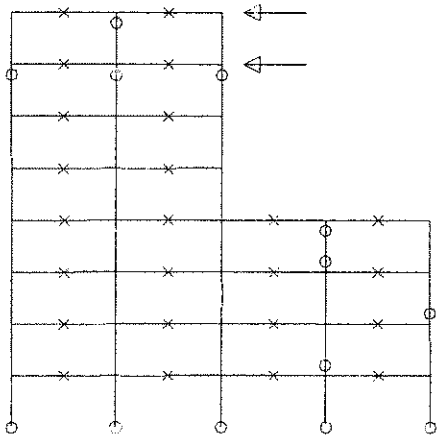

a) Linear

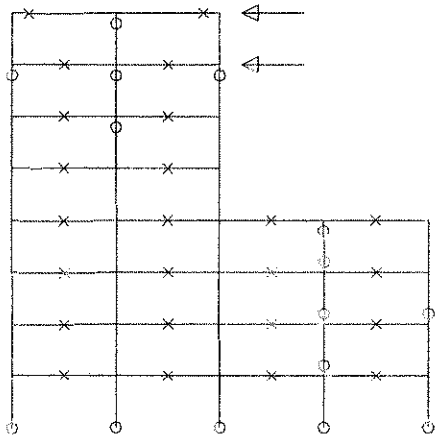

b) 1st Mode

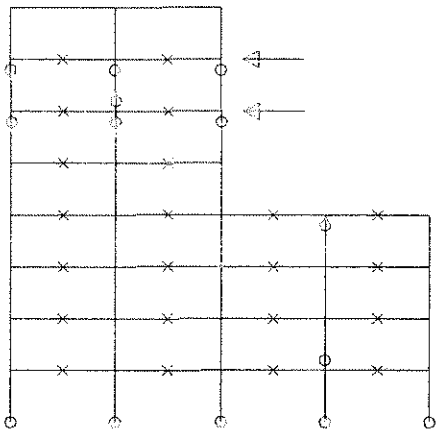

c) Uniform

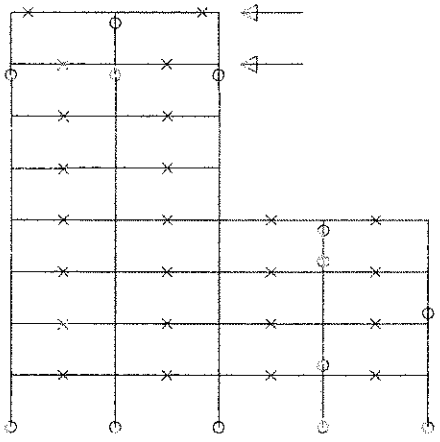

d) FEMA

Figure 3.10: Member Yielding in Irregular 8-Story Frames at Mechanism, Static Analysis

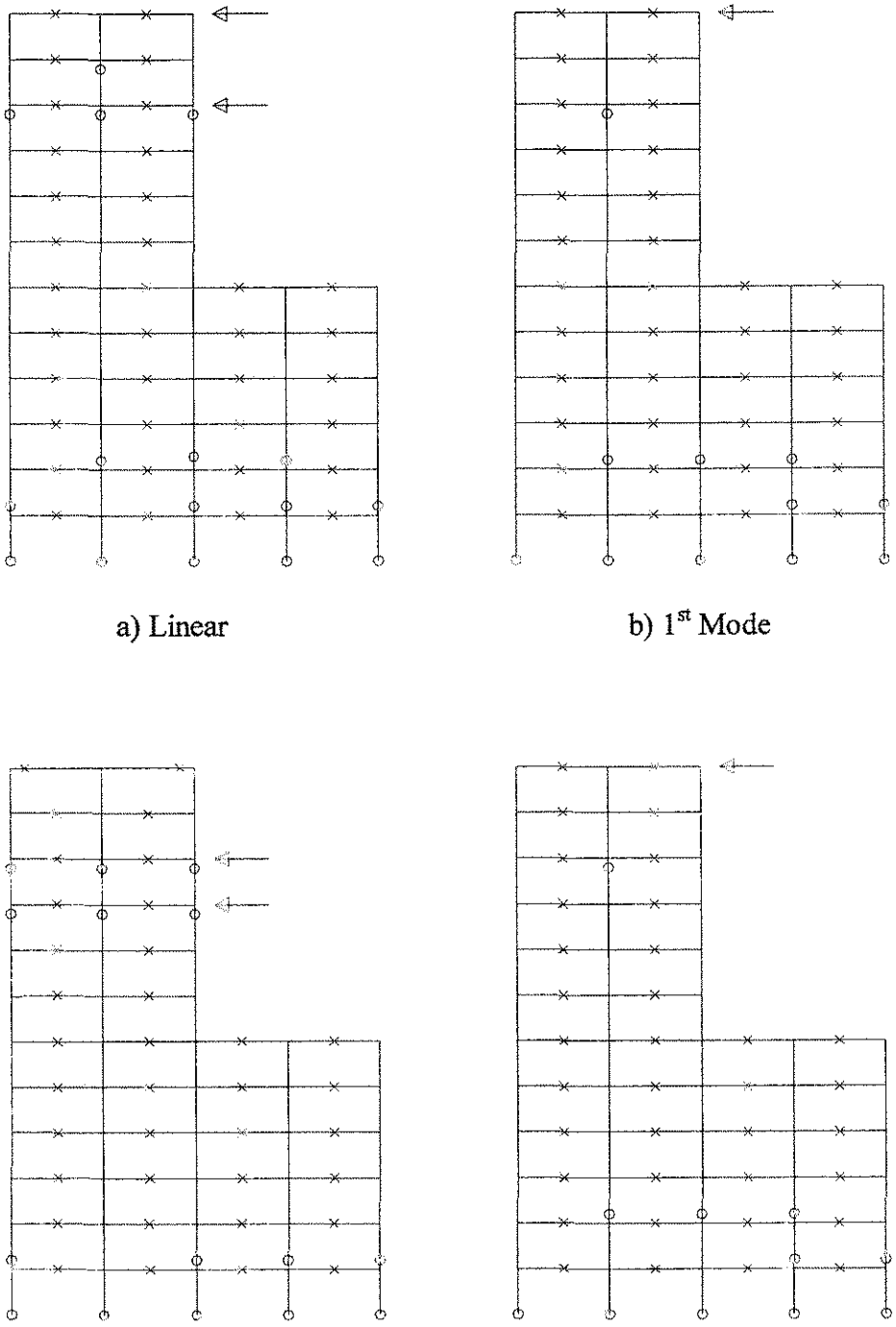

a) Linear

b) 1st Mode

c) Uniform

d) FEMA

Figure 3.11: Member Yielding in Irregular 12-Story Frames at Mechanism, Static Analysis

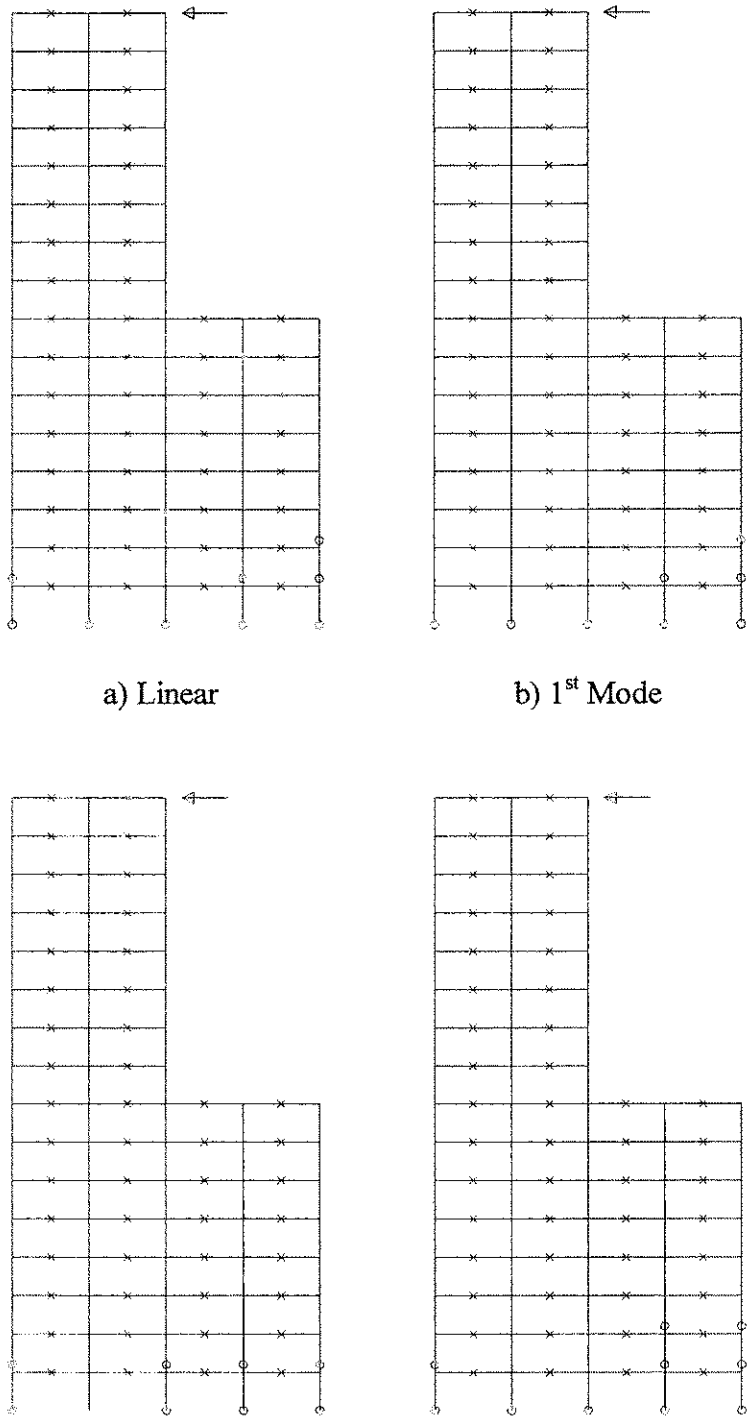

a) Linear b) 1st Mode

c) Uniform d) FEMA

Figure 3.12: Member Yielding in Irregular 16-Story Frames at Mechanism, Static Analysis

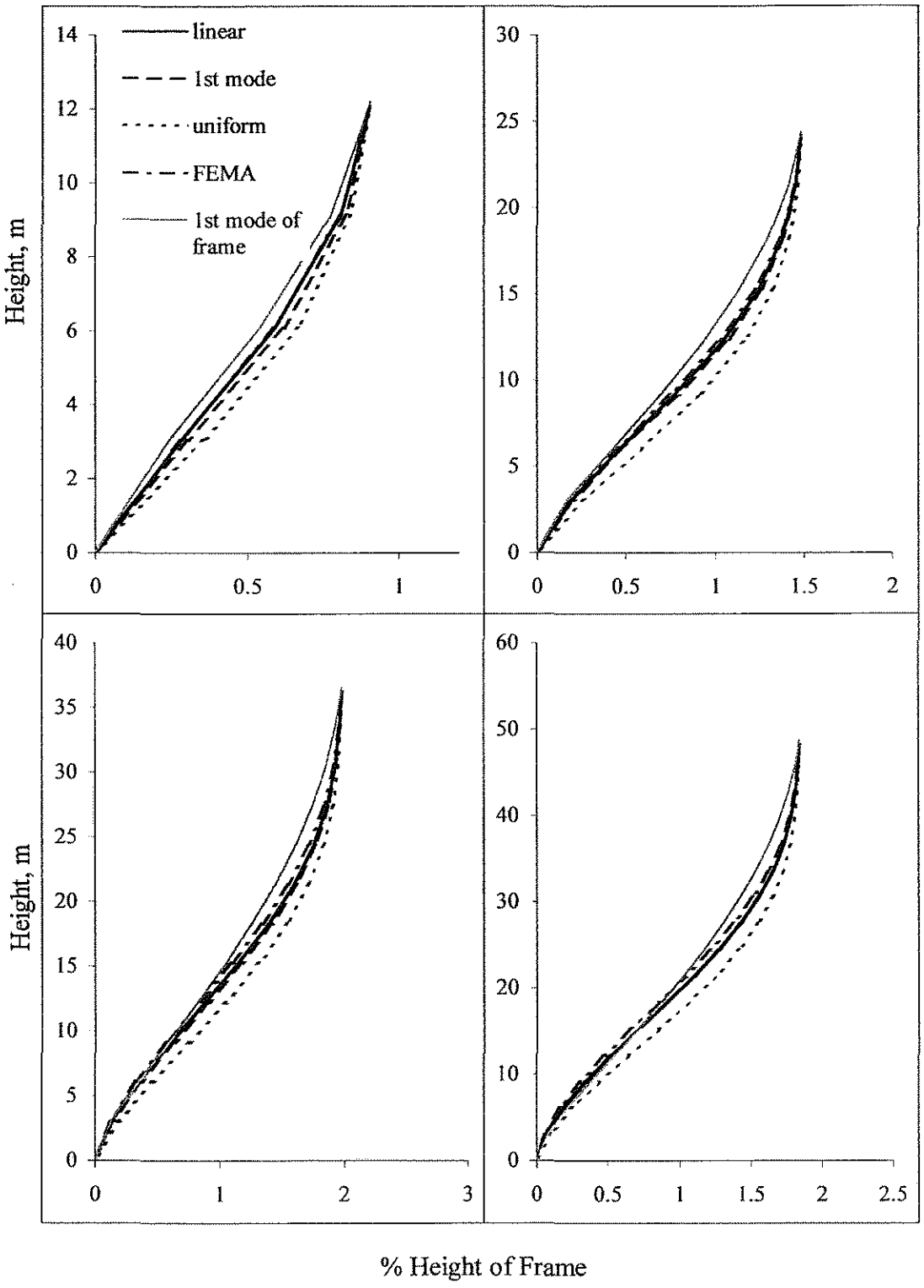


Figure 3.13: Distorted Shape of Regular Frames at Mechanism, Static Analysis Normalized to Average Roof Drift

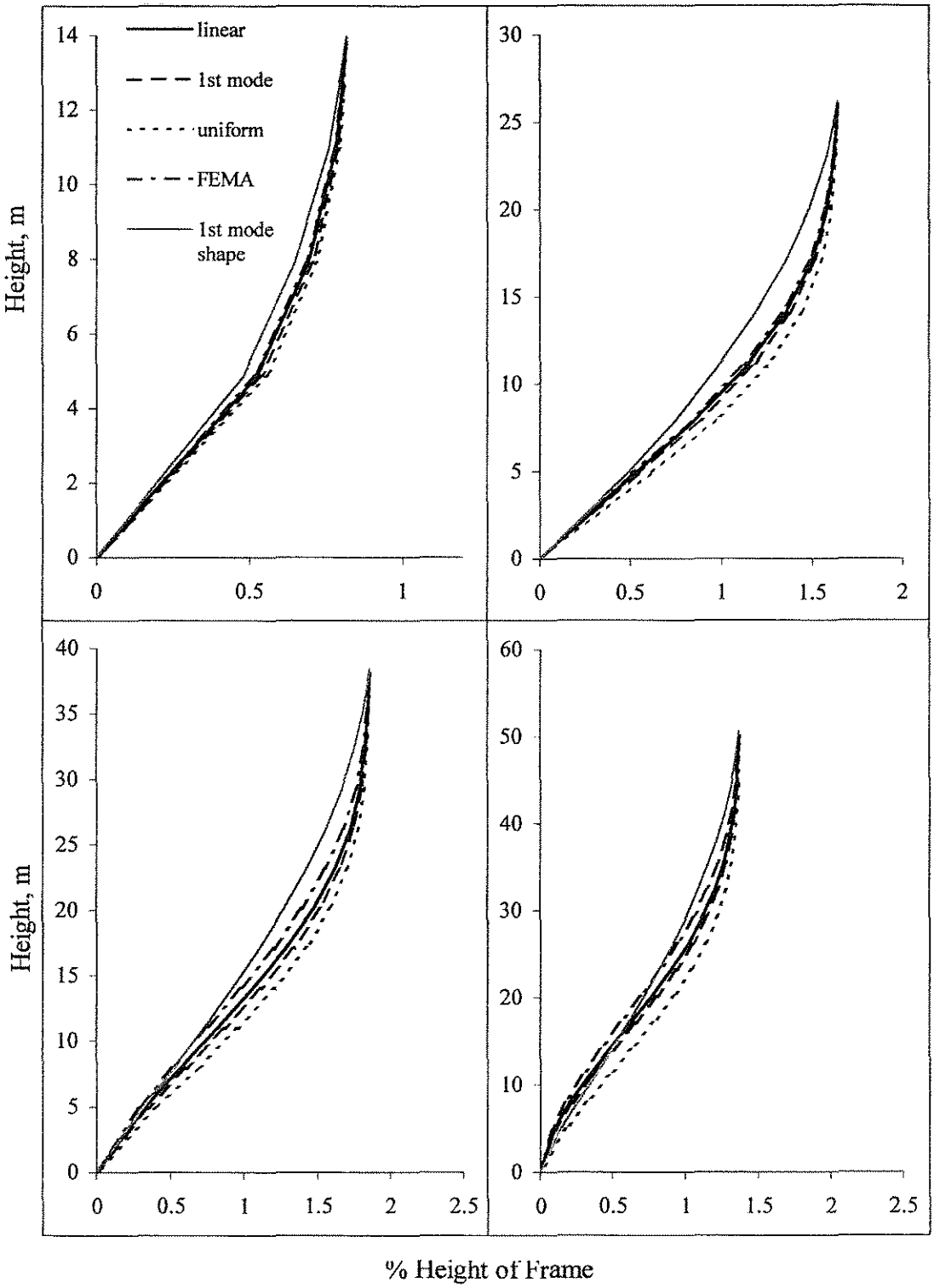


Figure 3.14: Distorted Shape of Tall First Story Frames at Mechanism, Static Analysis Normalized to Average Roof Drift

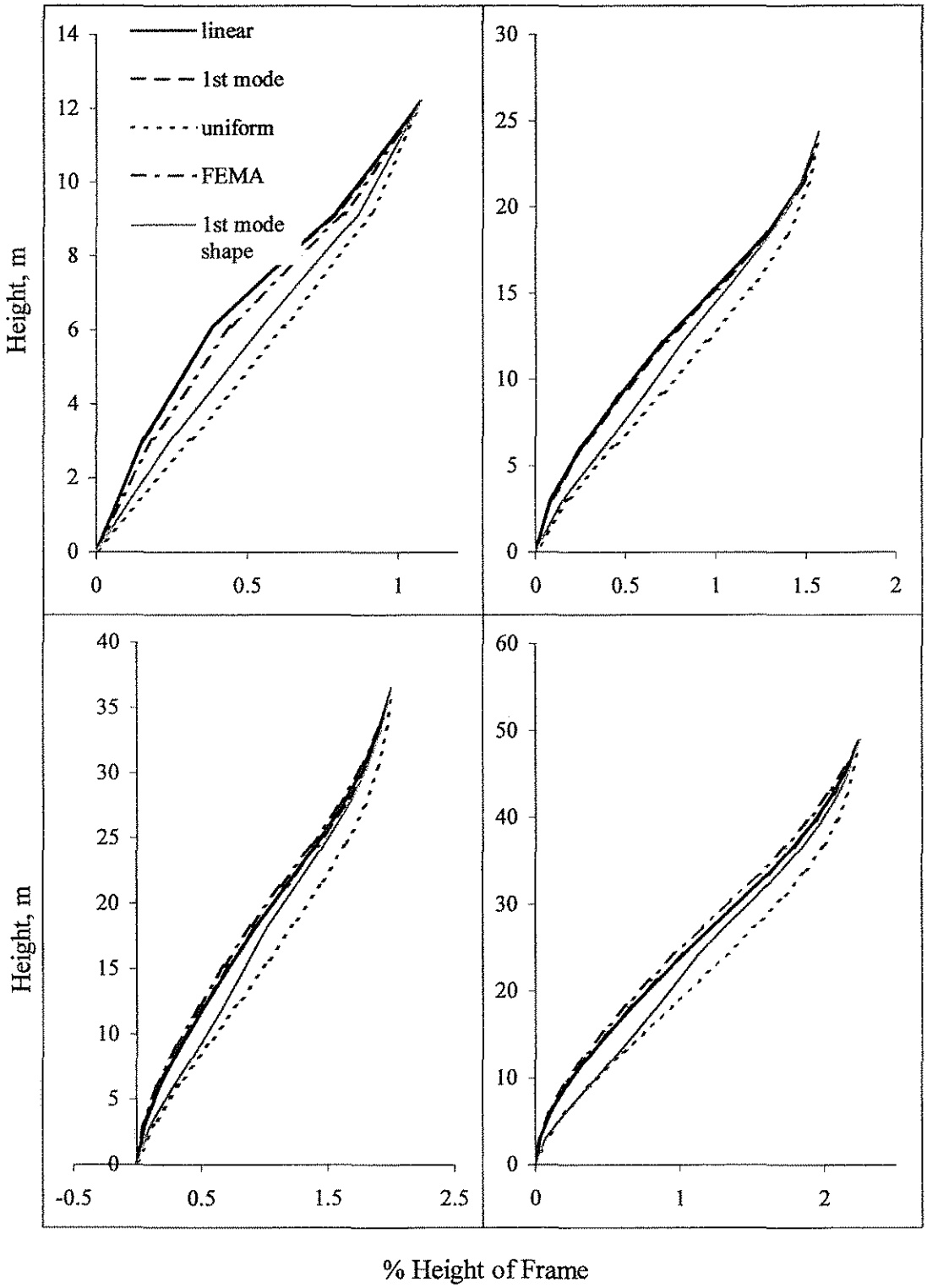


Figure 3.15: Distorted Shape of Irregular Frames at Mechanism, Static Analysis Normalized to Average Roof Drift

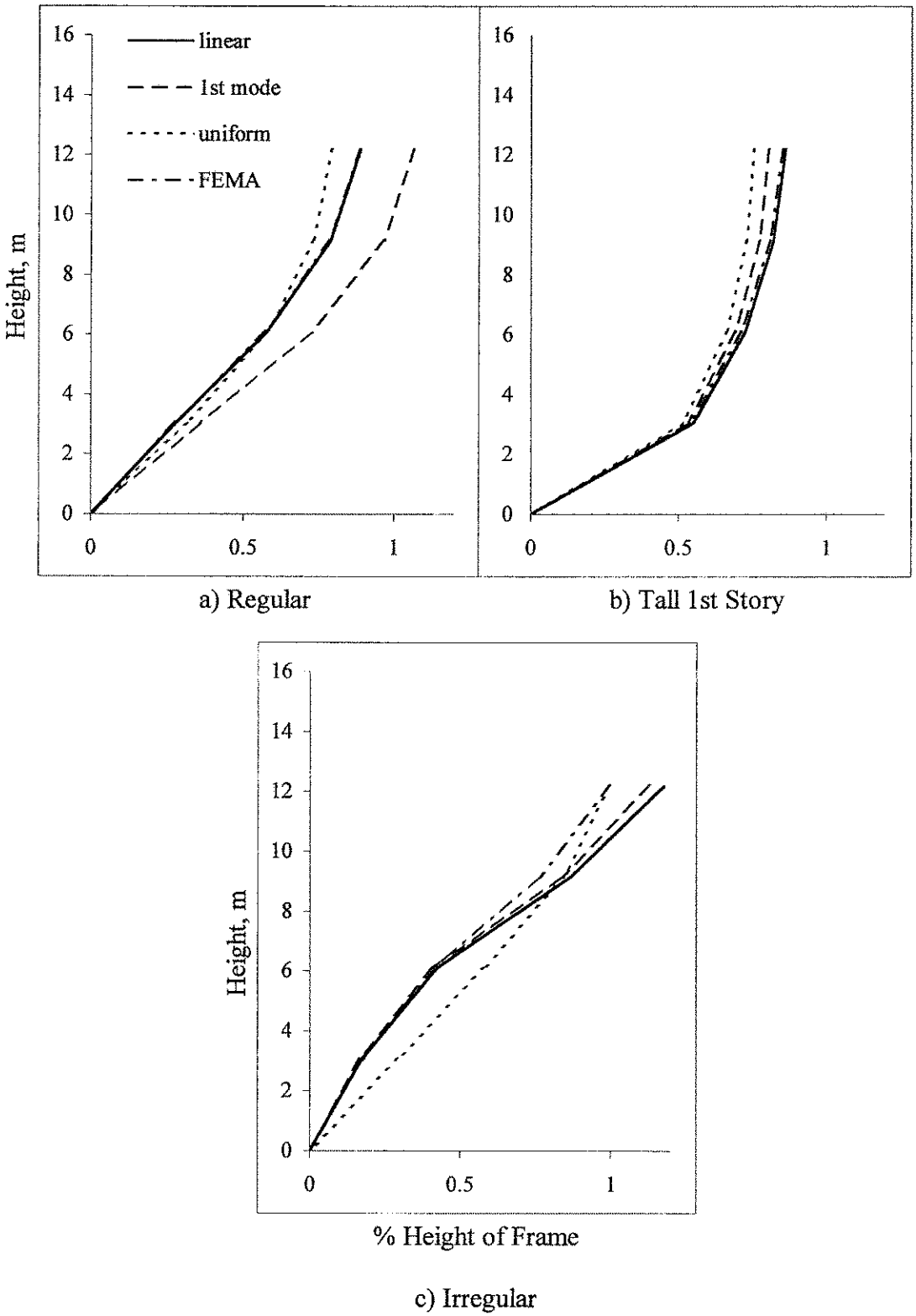


Figure 3.16: Distorted Shape of 4-Story Frames at Mechanism, Static Analysis

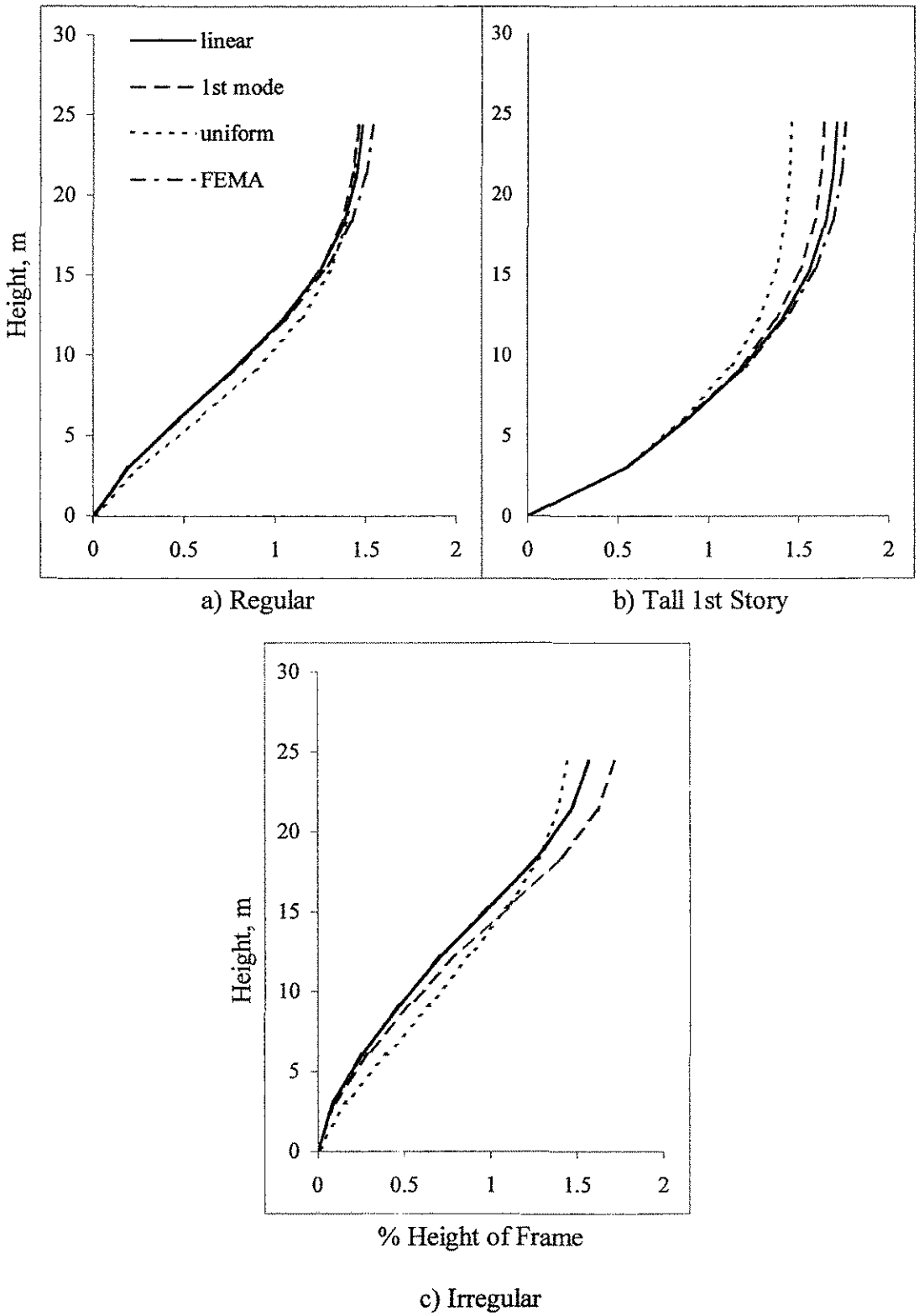


Figure 3.17: Distorted Shape of 8-Story Frames at Mechanism, Static Analysis

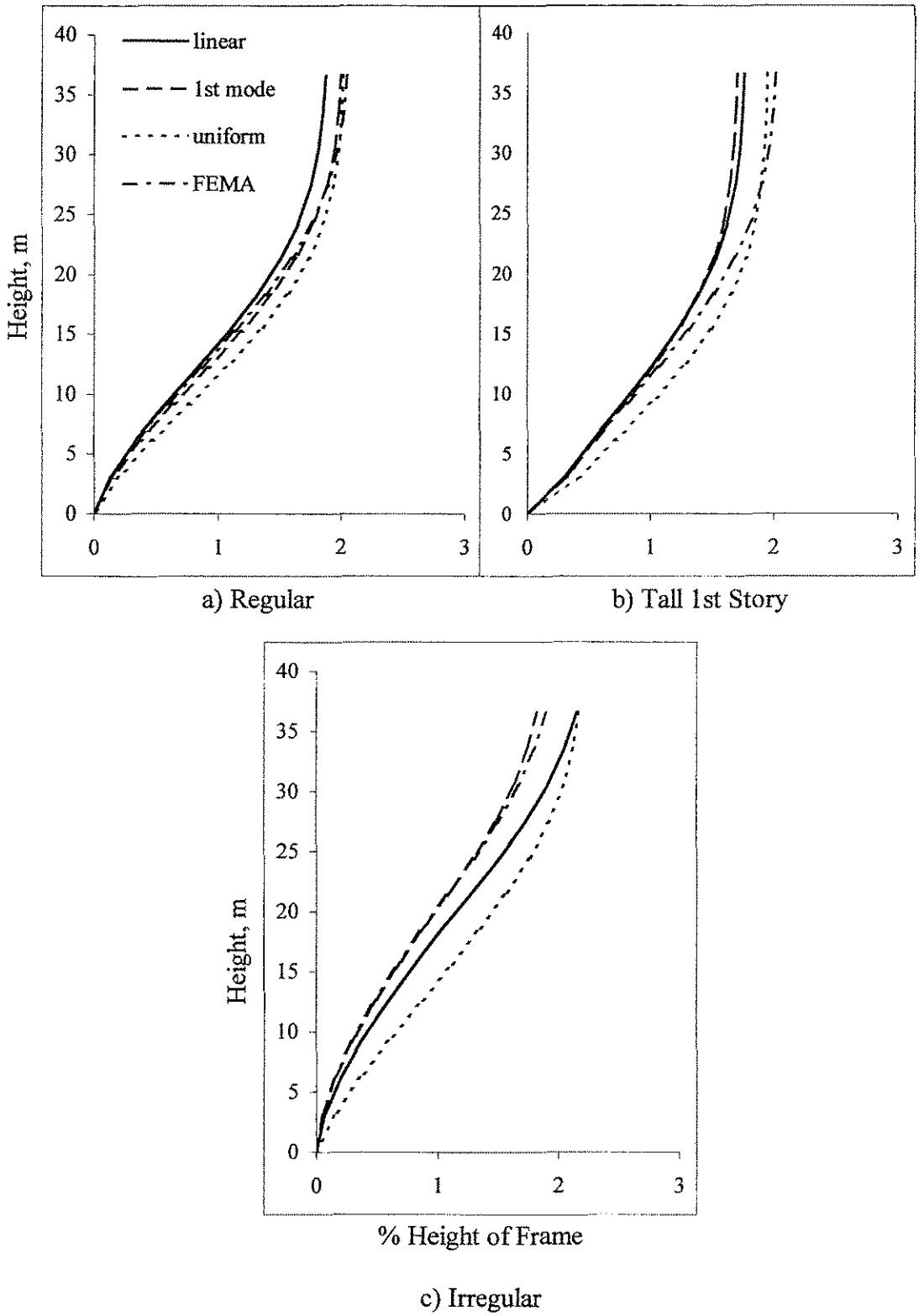


Figure 3.18: Distorted Shape of 12-Story Frames at Mechanism, Static Analysis

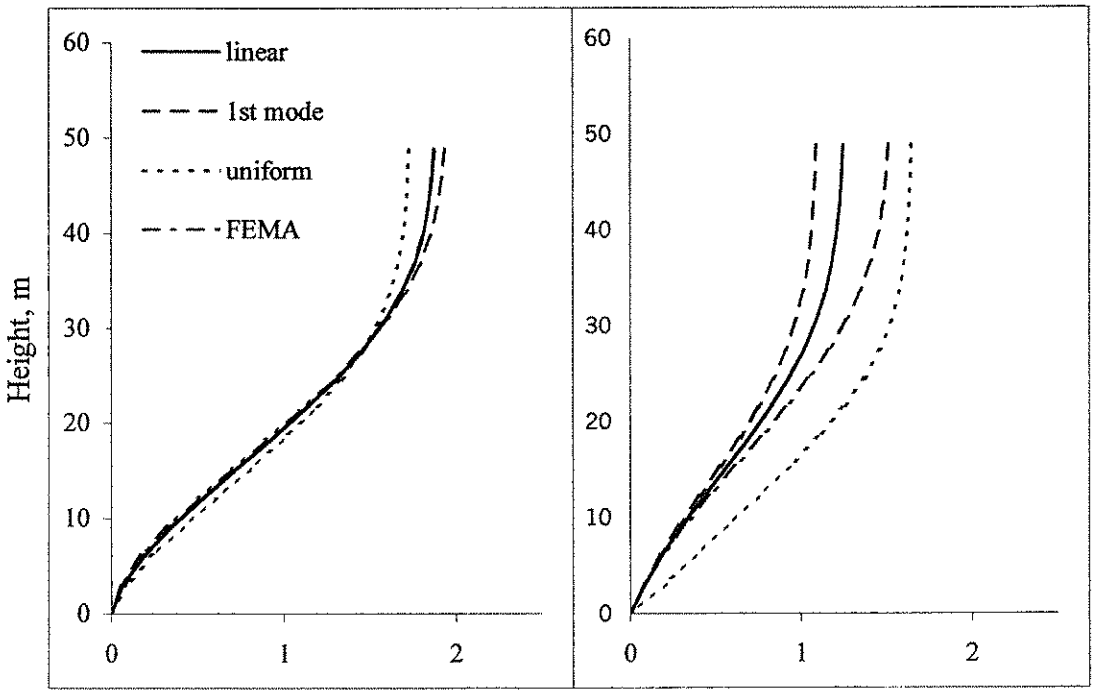


a) Regular b) Tall 1st Story

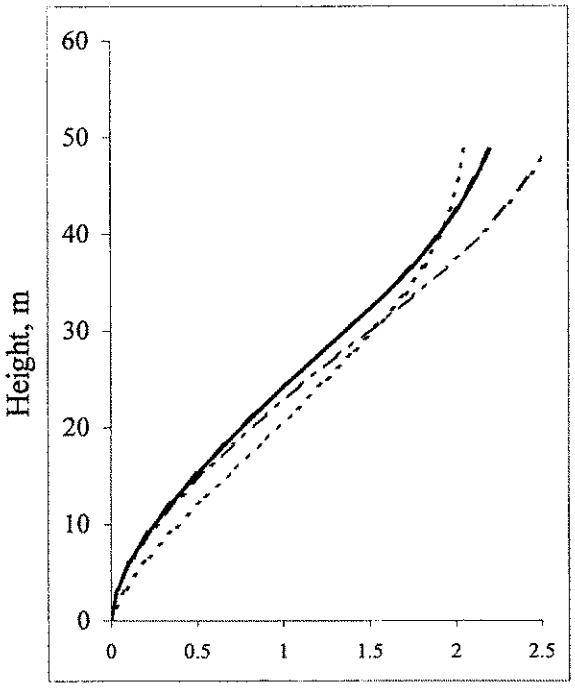


c) Irregular

Figure 3.19: Distorted Shape of 16-Story Frames at Mechanism, Static Analysis

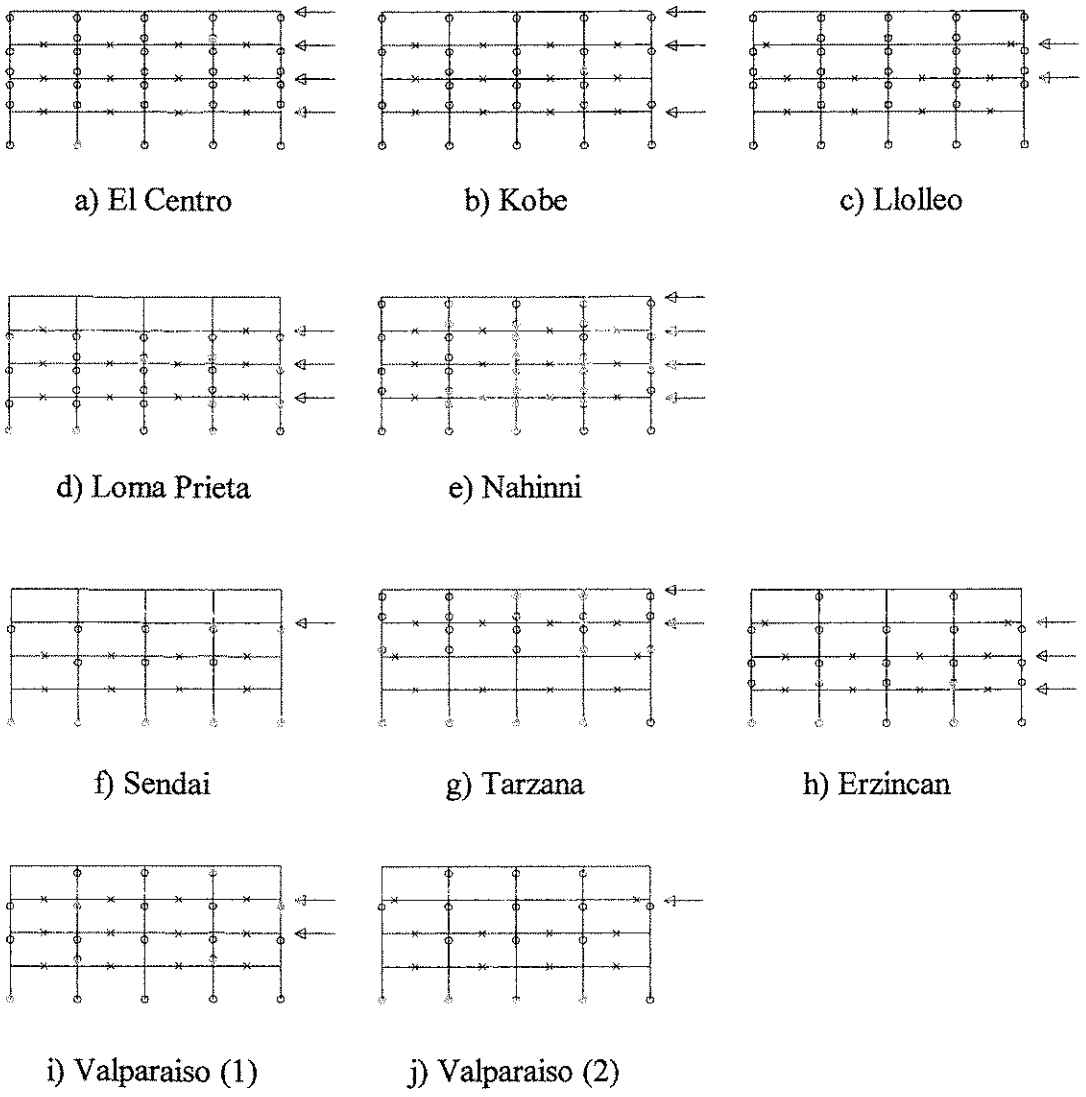


Figure 3.20: Member Yielding in Regular 4-Story Frames, Dynamic Analysis

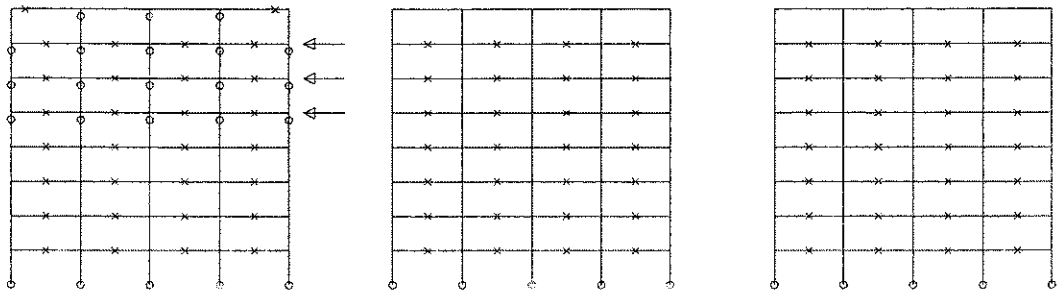

a) El Centro b) Kobe c) Llolleo

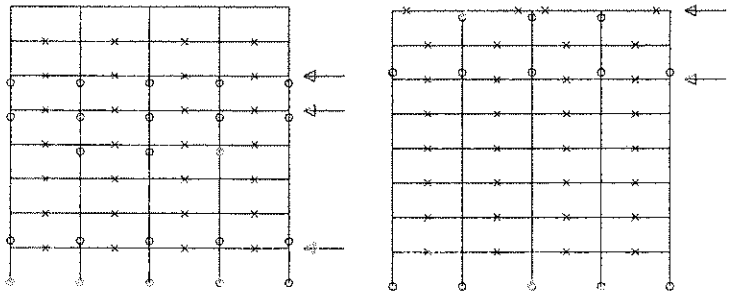

d) Loma Prieta e) Nahinni

Figure 3.21: Member Yielding in Regular 8-Story Frames, Dynamic Analysis

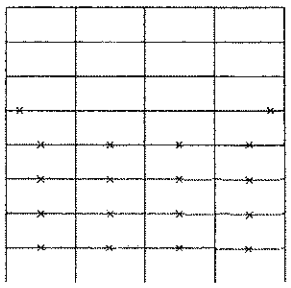

f) Sendai

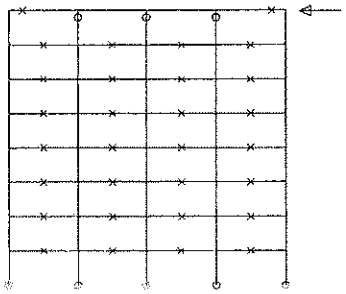

g) Tarzana

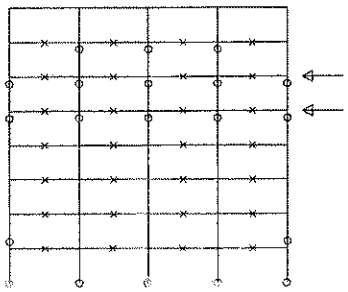

h) Erzincan

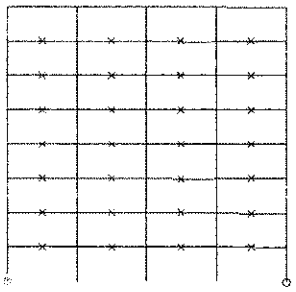

i) Valparaiso (1)

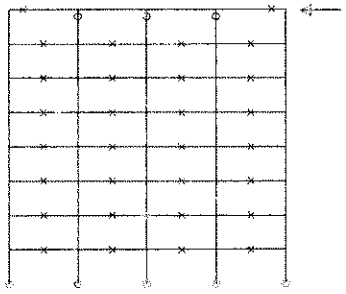

j) Valparaiso (2)

Figure 3.21: --Continued

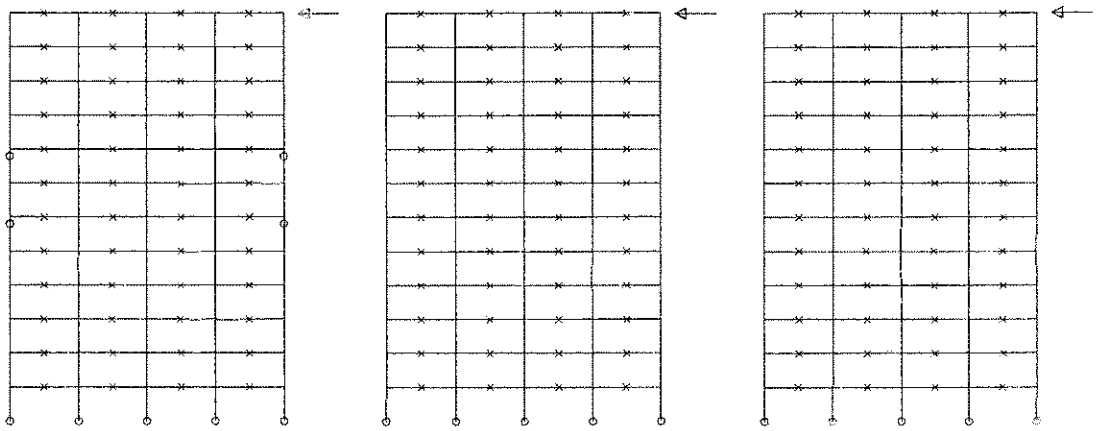

a) El Centro b) Kobe c) Llolleo

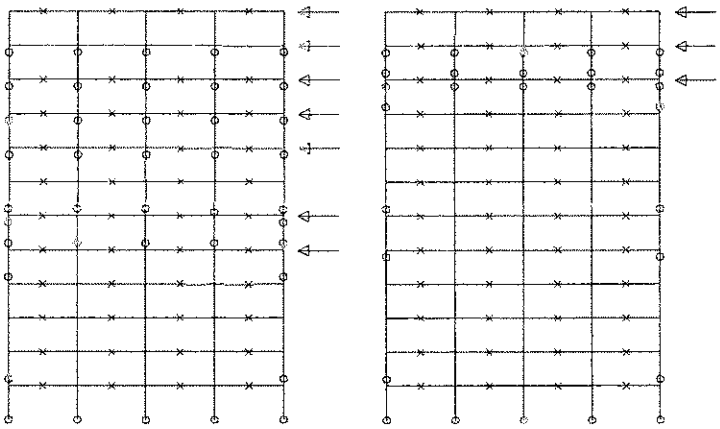

d) Loma Prieta e) Nahinni

Figure 3.22: Member Yielding in Regular 12-Story Frames, Dynamic Analysis

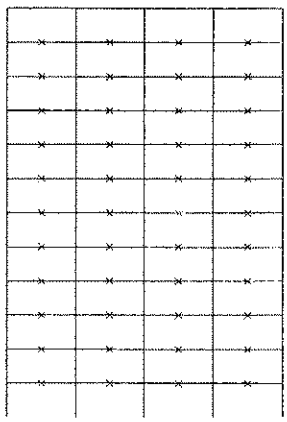

f) Sendai

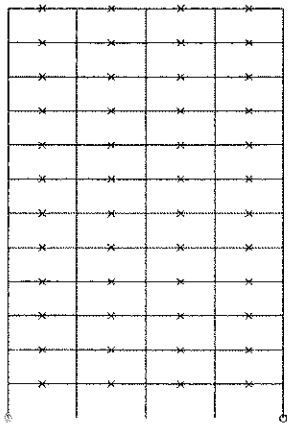

g) Tarzana

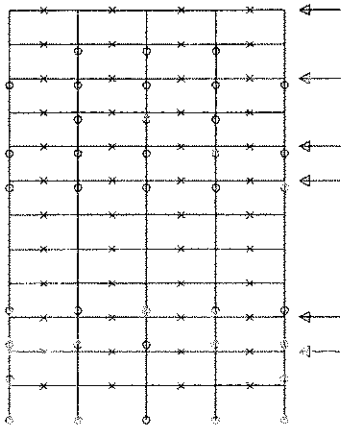

h) Erzincan

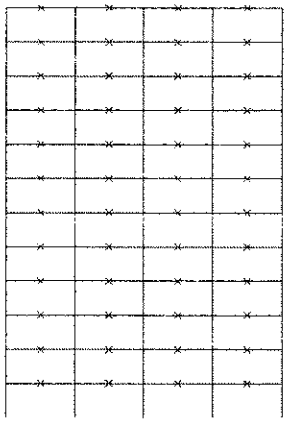

i) Valparaiso (1)

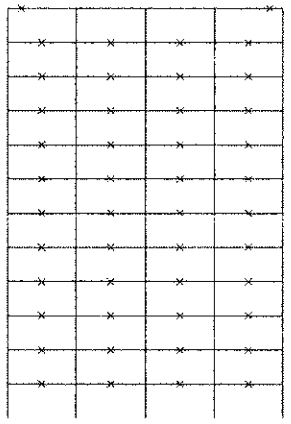

j) Valparaiso (2)

Figure 3.22: --Continued

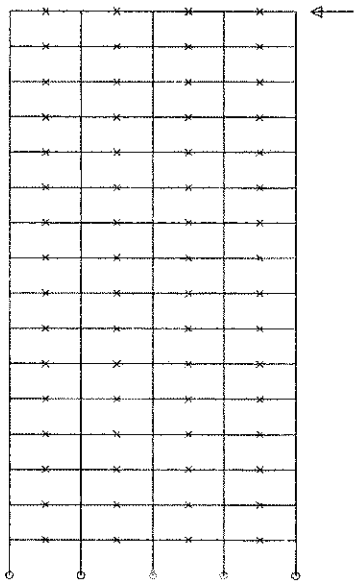

a) El Centro

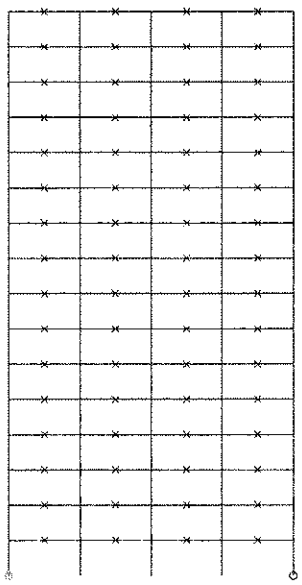

b) Kobe

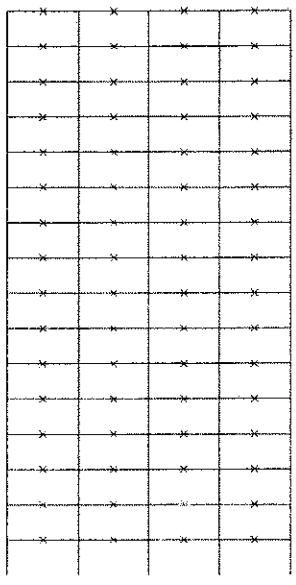

c) Llolleo

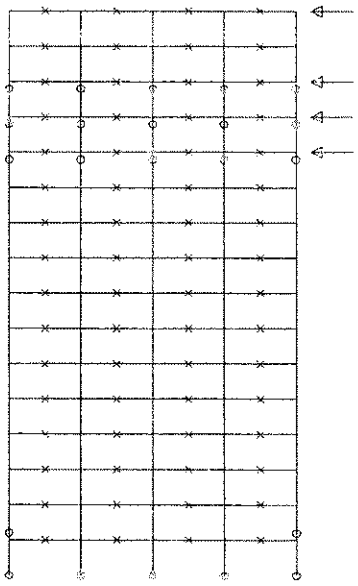

d) Loma Prieta

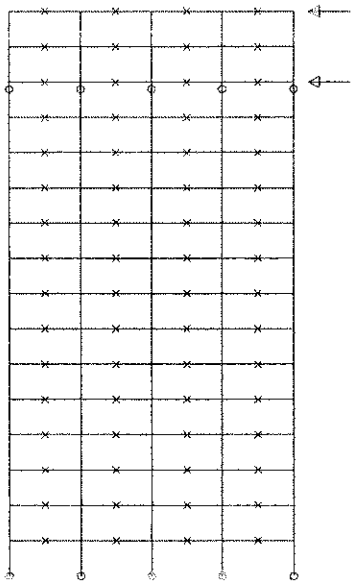

e) Nahinni

Figure 3.23: Member Yielding in Regular 16-Story Frames, Dynamic Analysis

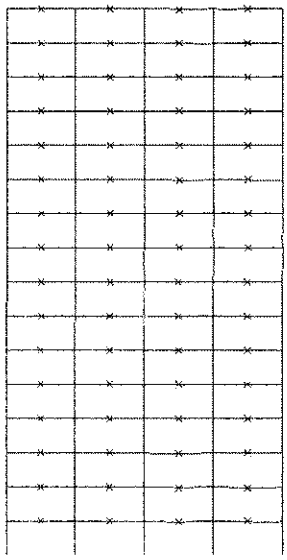

f) Sendai

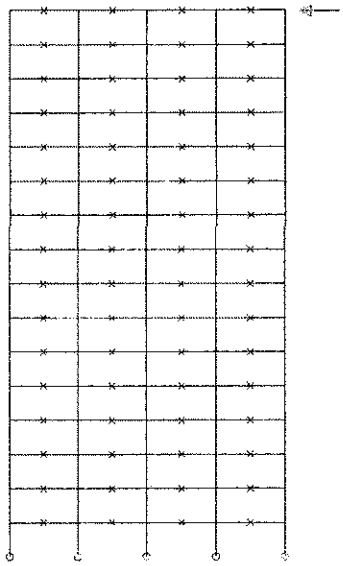

g) Tarzana

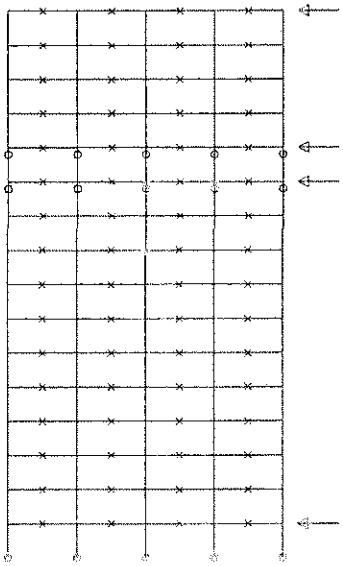

h) Erzincan

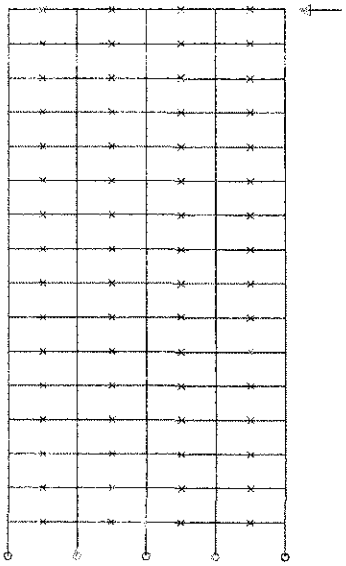

i) Valparaiso (1)

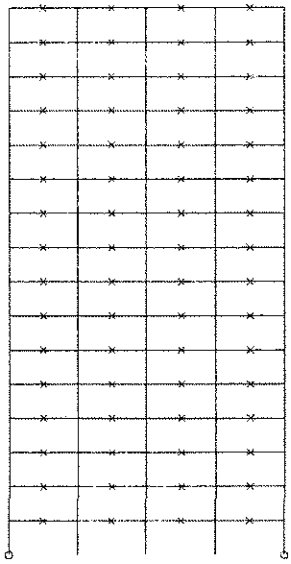

j) Valparaiso (2)

Figure 3.23: --Continued

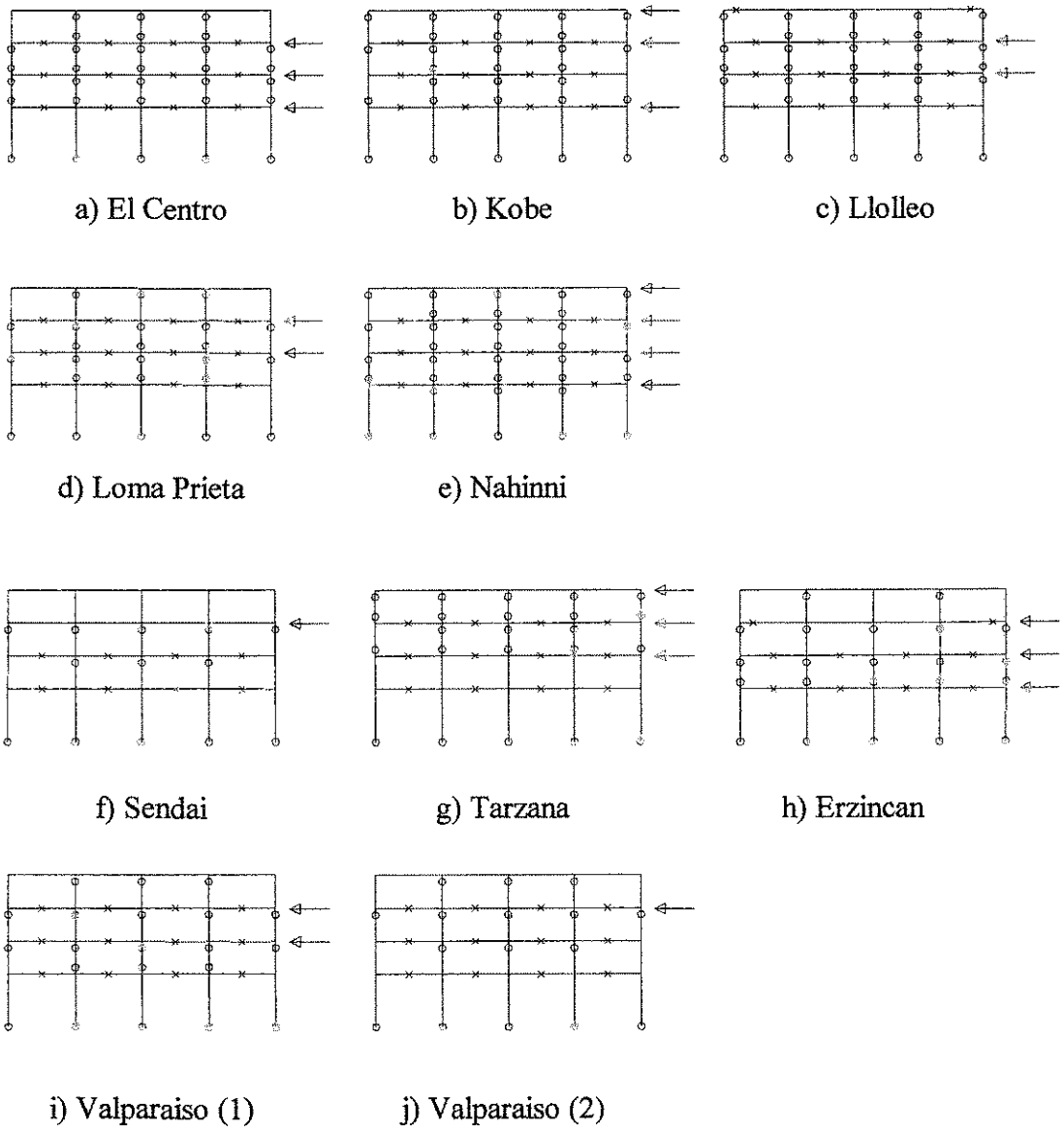


Figure 3.24: Member Yielding in Tall First Story 4-Story Frames, Dynamic Analysis

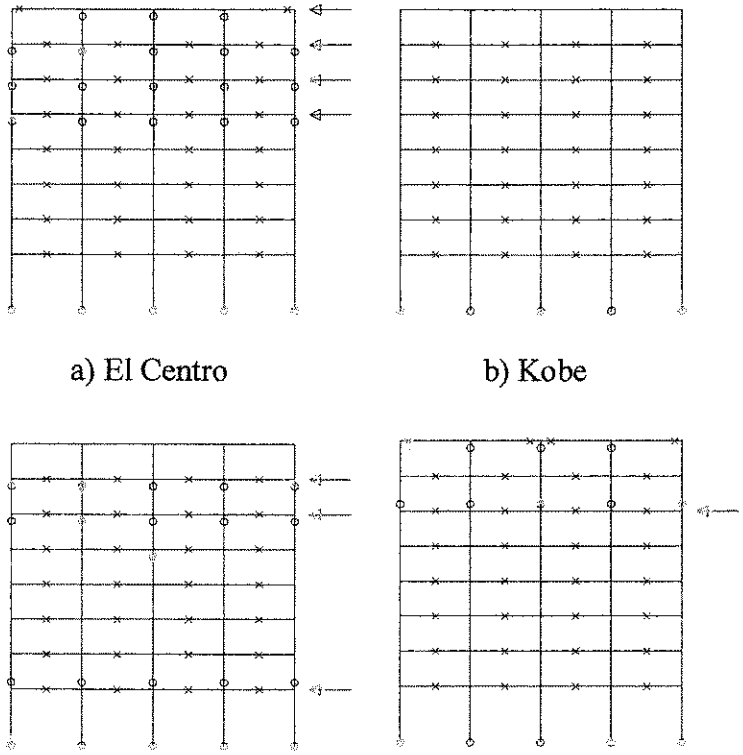


Figure 3.25: Member Yielding in Tall First Story 8-Story Frames, Dynamic Analysis

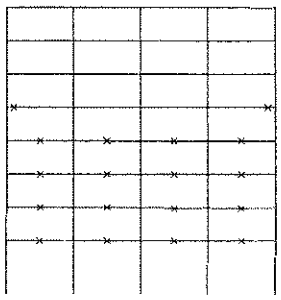

f) Sendai

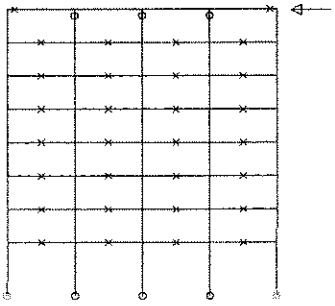

g) Tarzana

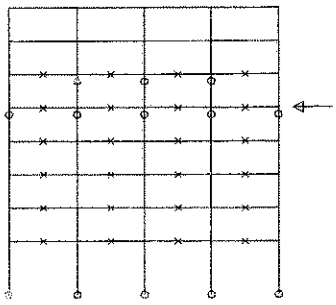

h) Erzincan

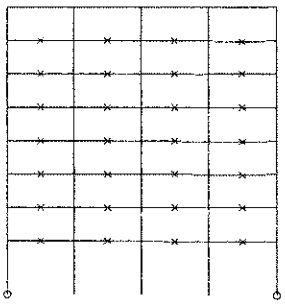

i) Valparaiso (1)

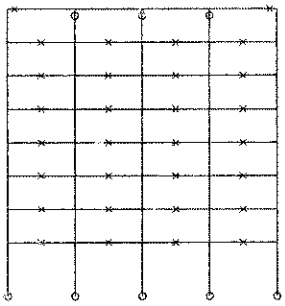

j) Valparaiso (2)

Figure 3.25: --Continued

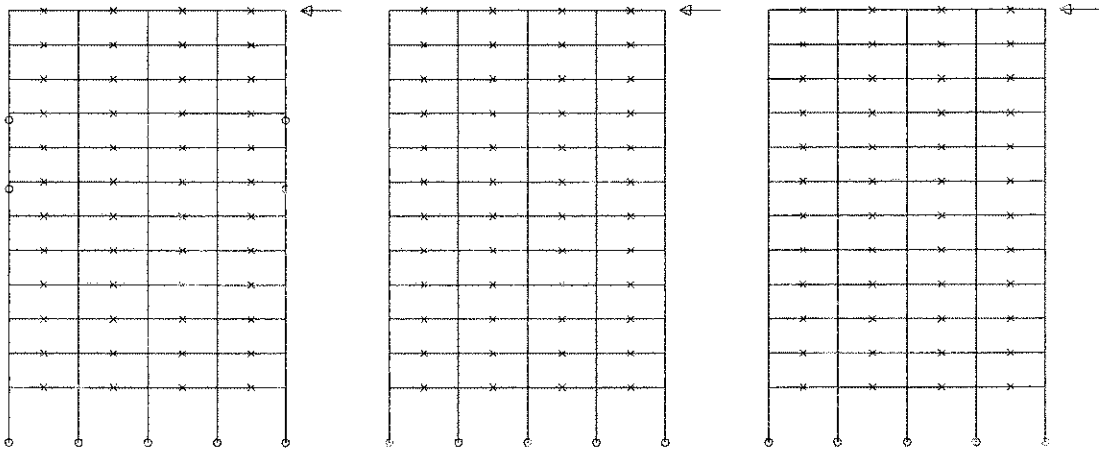

a) El Centro b) Kobe c) Llolleo

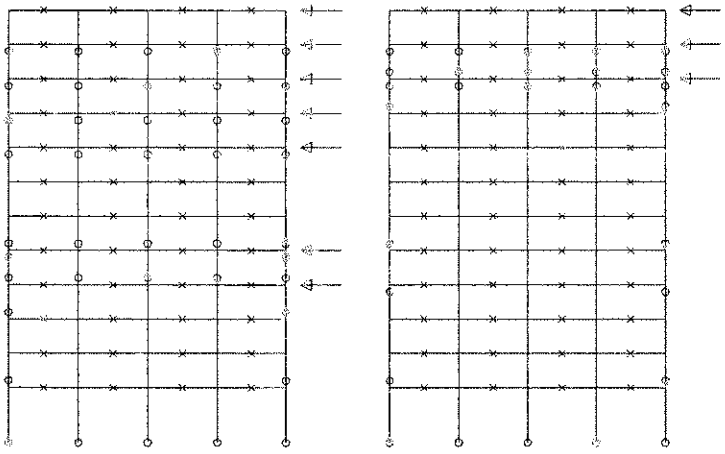

d) Loma Prieta e) Nahinni

Figure 3.26: Member Yielding in Tall First Story 12-Story Frames, Dynamic Analysis

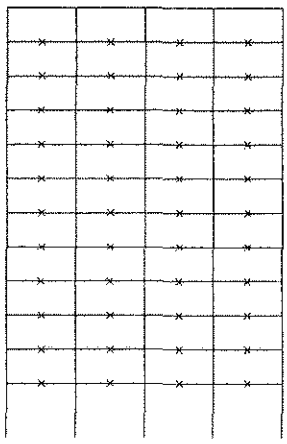

f) Sendai

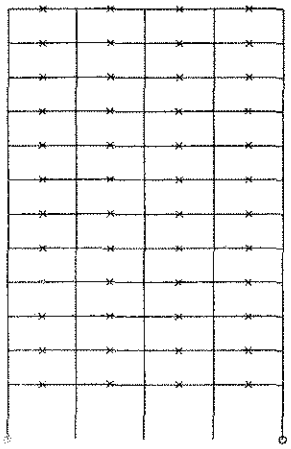

g) Tarzana

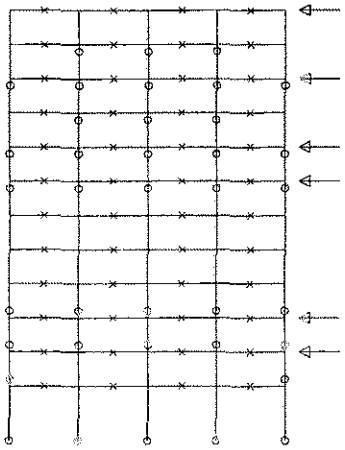

h) Erzincan

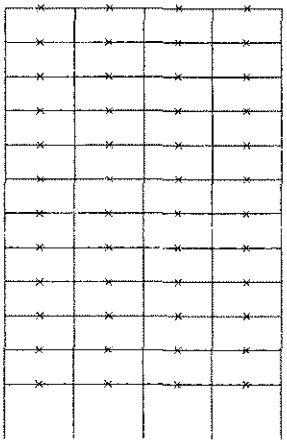

i) Valparaiso (1)

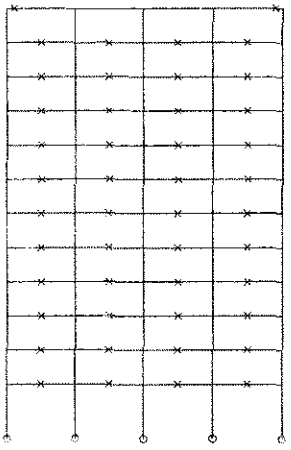

j) Valparaiso (2)

Figure 3.26: --Continued

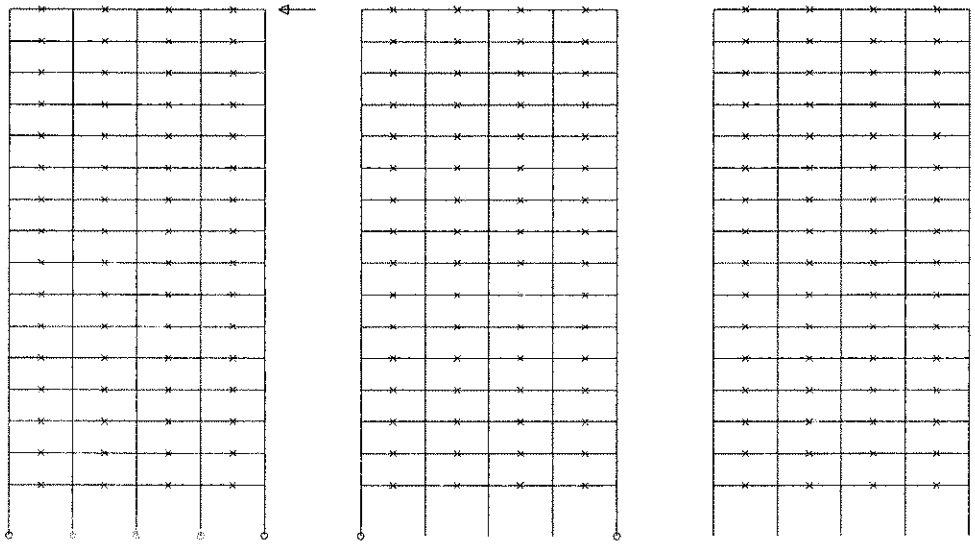

a) El Centro b) Kobe c) Llolleo

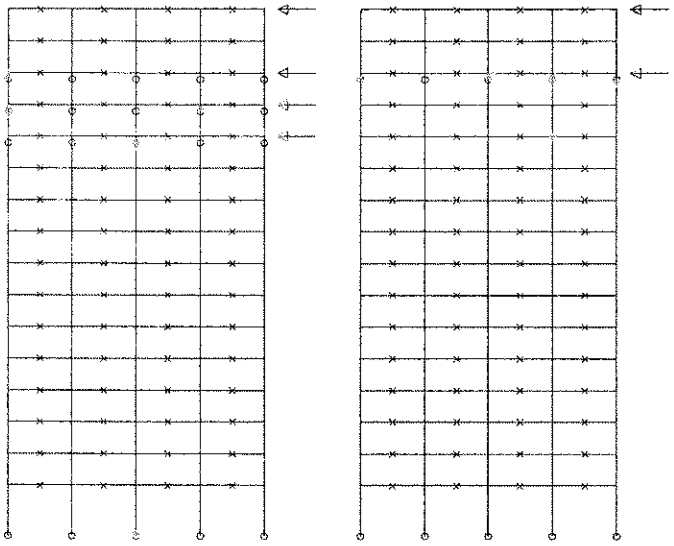

d) Loma Prieta e) Nahinni

Figure 3.27: Member Yielding in Tall First Story 16-Story Frames, Dynamic Analysis

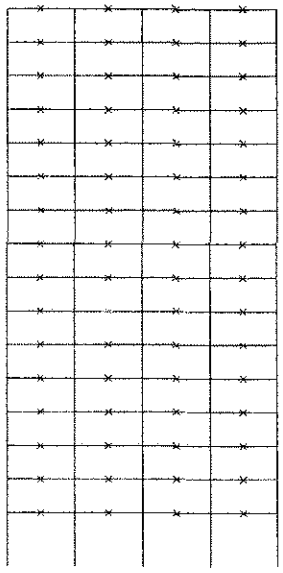

f) Sendai

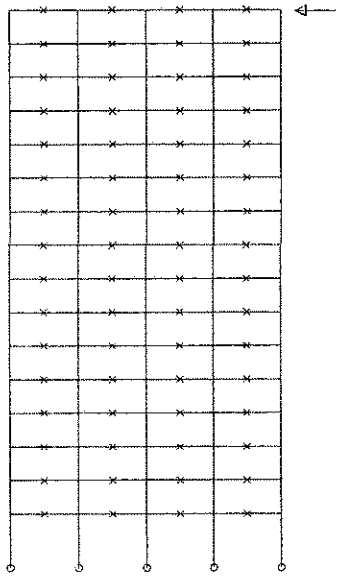

g) Tarzana

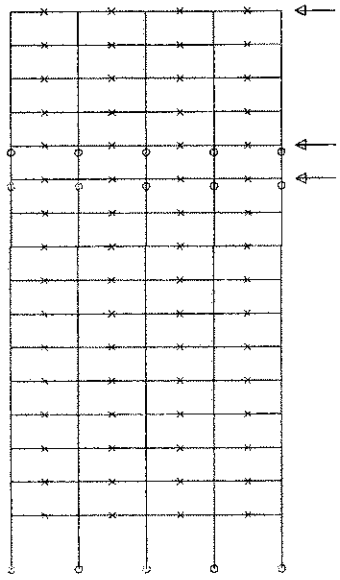

h) Erzincan

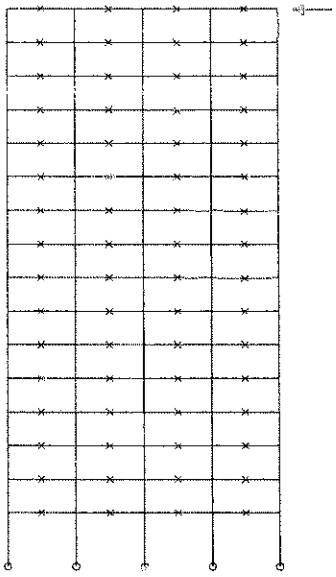

i) Valparaiso (1)

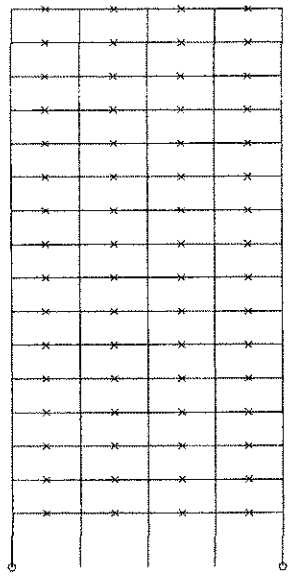

j) Valparaiso (2)

Figure 3.27: --Continued

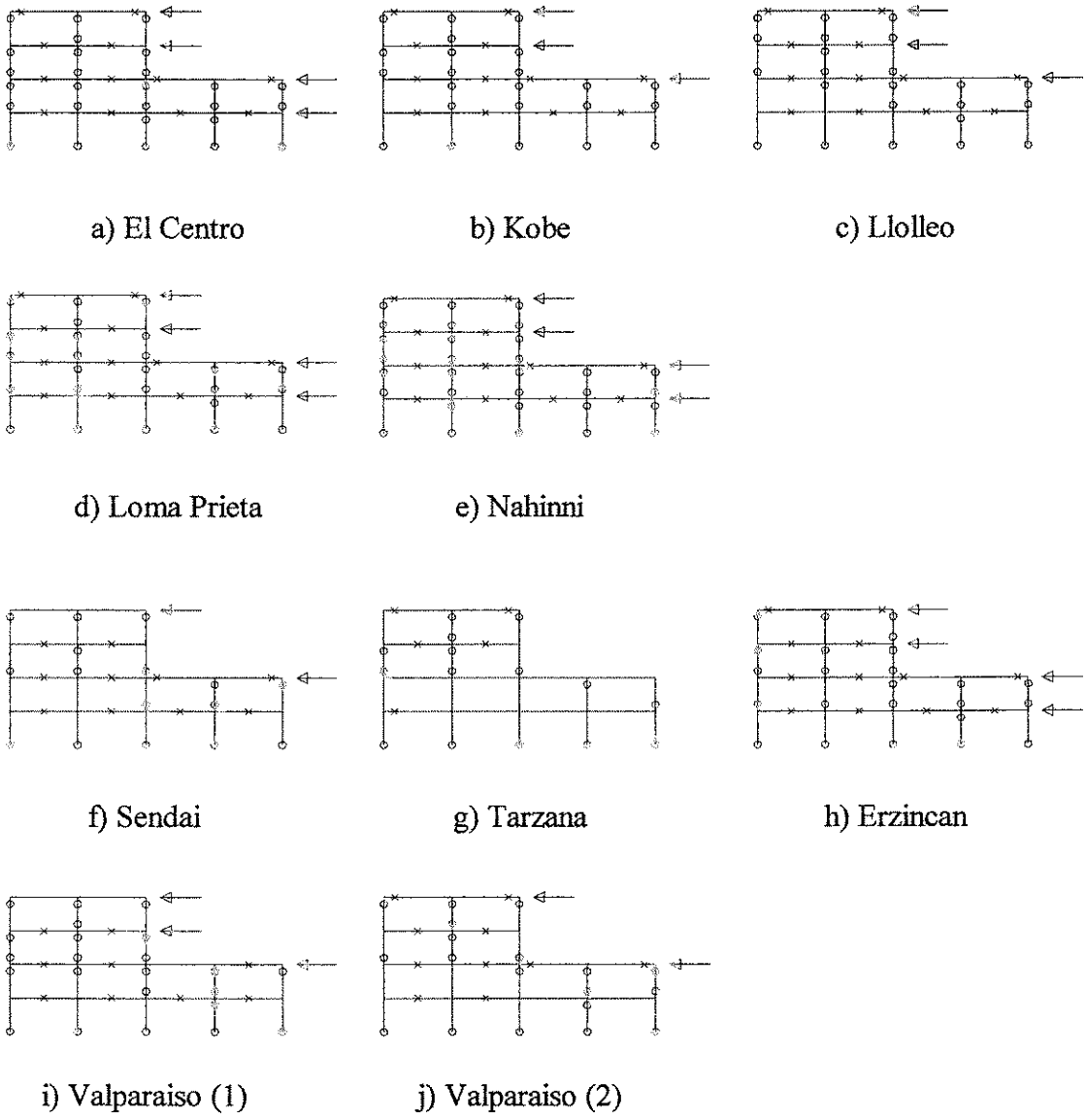


Figure 3.28: Member Yielding in Irregular 4-Story Frames, Dynamic Analysis

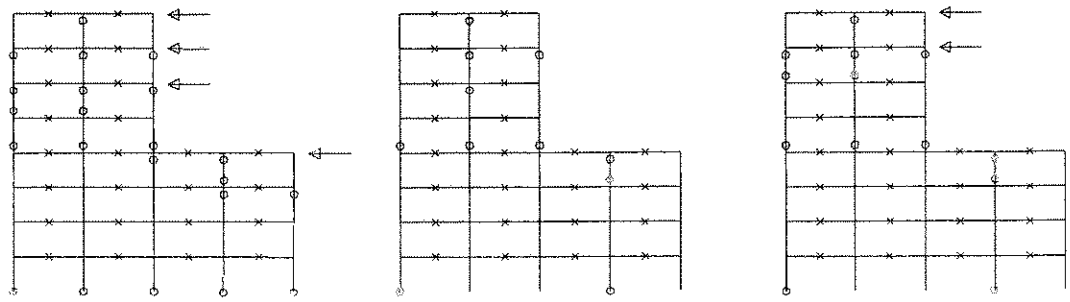

a) El Centro b) Kobe c) Llolleo

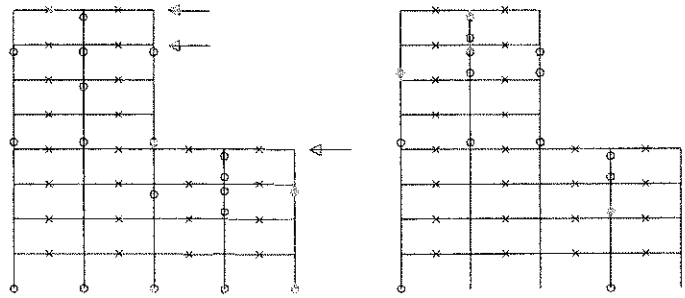

d) Loma Prieta e) Nahinni

Figure 3.29: Member Yielding in Irregular 8-Story Frames, Dynamic Analysis

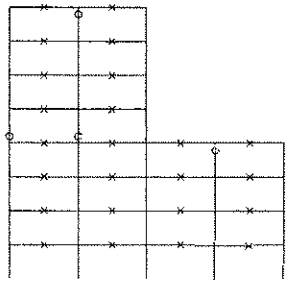

f) Sendai

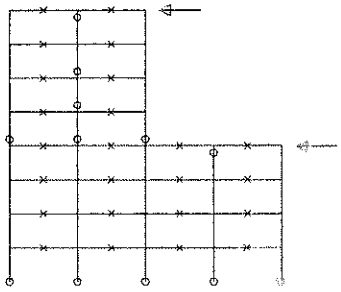

g) Tarzana

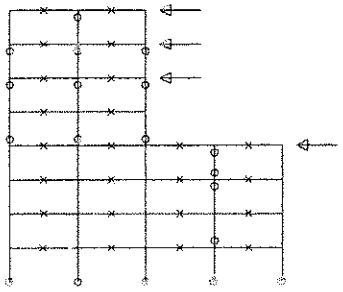

h) Erzincan

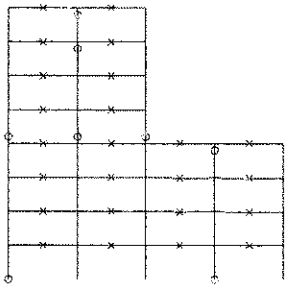

i) Valparaiso (1)

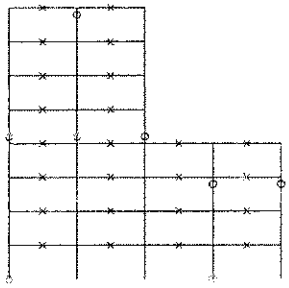

j) Valparaiso (2)

Figure 3.29: --Continued

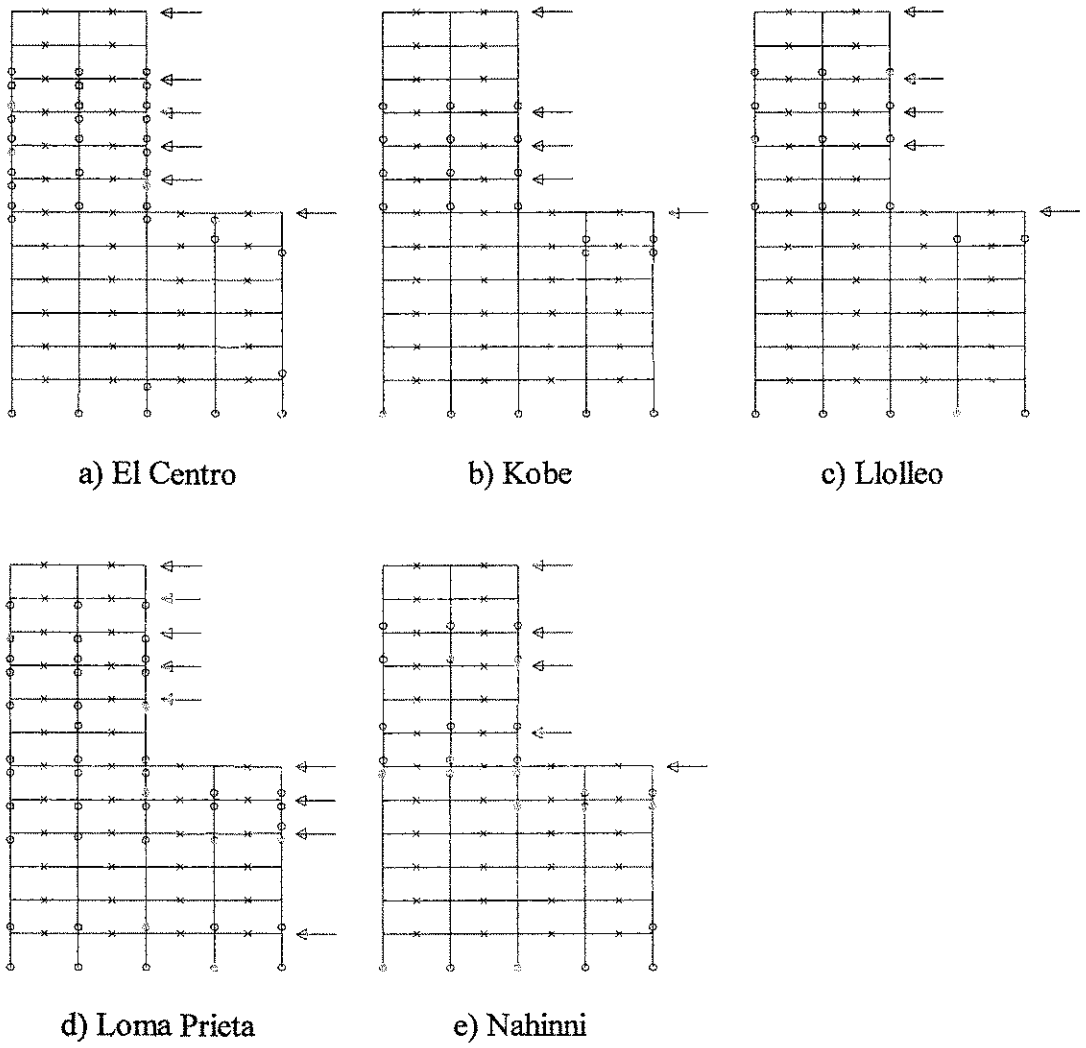


Figure 3.30: Member Yielding in Irregular 12-Story Frames, Dynamic Analysis

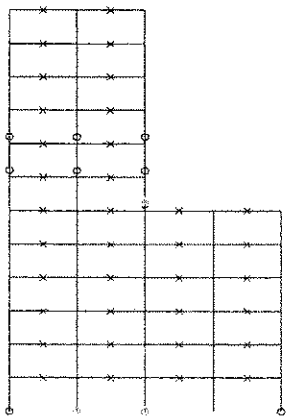

f) Sendai

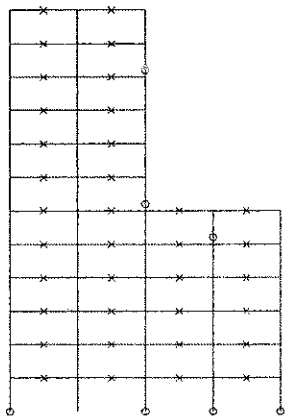

g) Tarzana

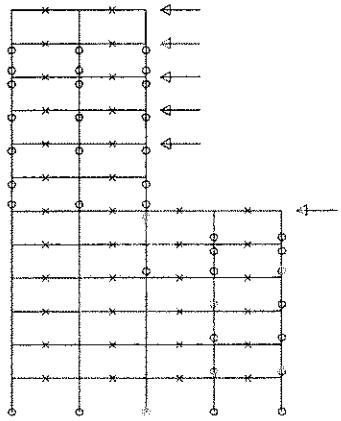

h) Erzincan

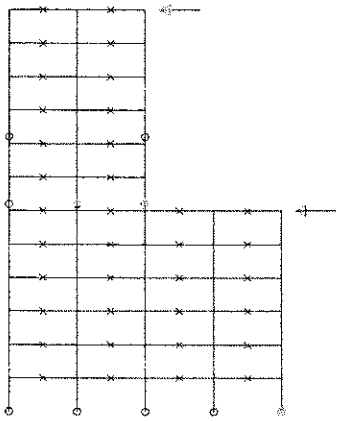

i) Valparaiso (1)

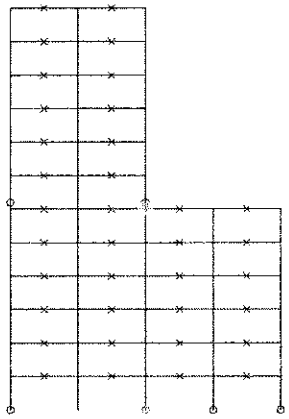

j) Valparaiso (2)

Figure 3.30: --Continued

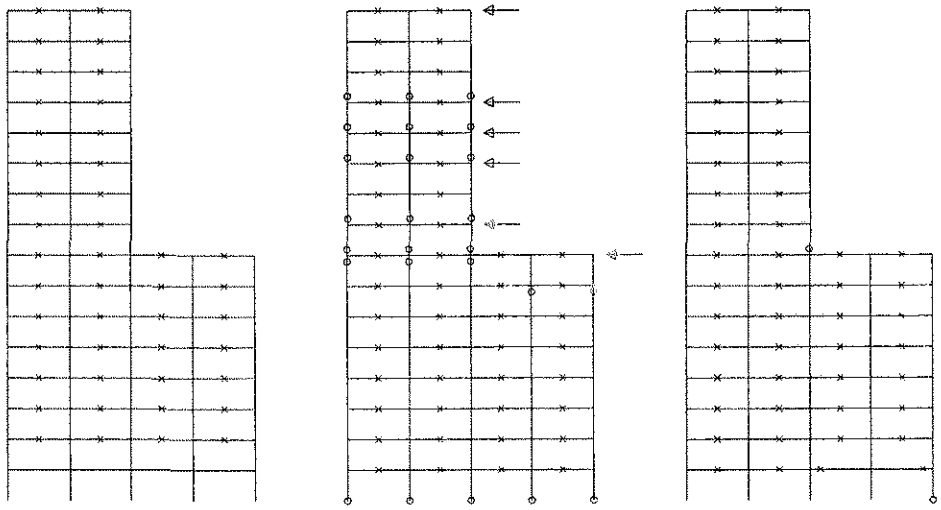

a) El Centro b) Kobe c) Llolleo

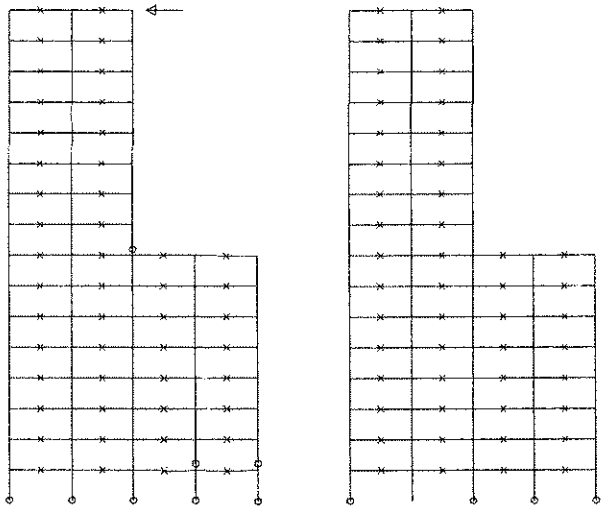

d) Loma Prieta e) Nahinni

Figure 3.31: Member Yielding in Irregular 16-Story Frames, Dynamic Analysis

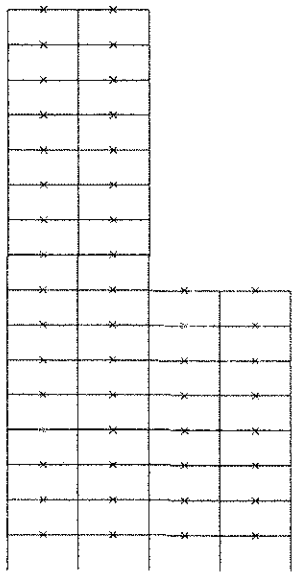

f) Sendai

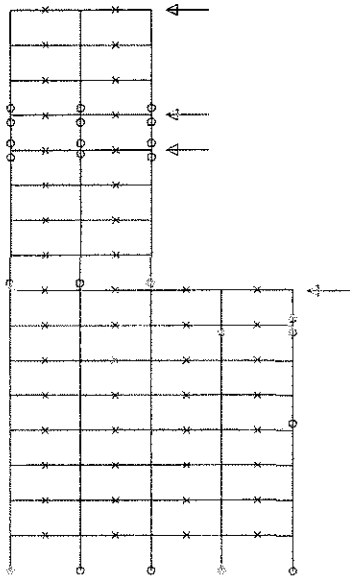

g) Tarzana

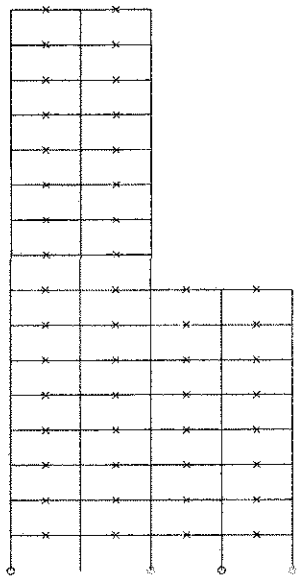

h) Erzincan

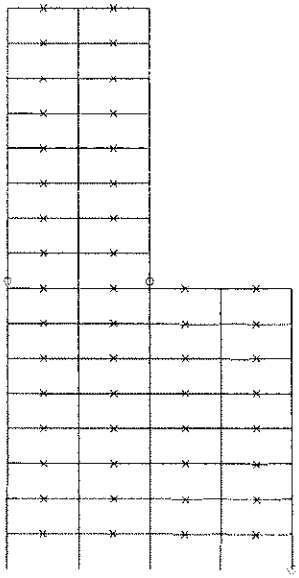

i) Valparaiso (1)

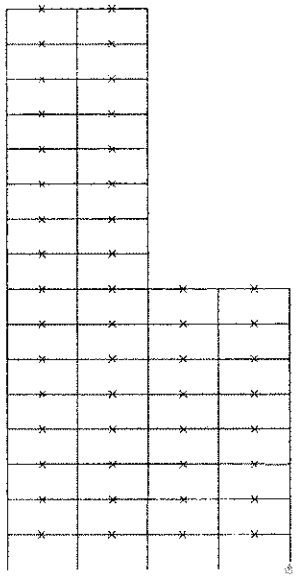

j) Valparaiso (2)

Figure 3.31: --Continued

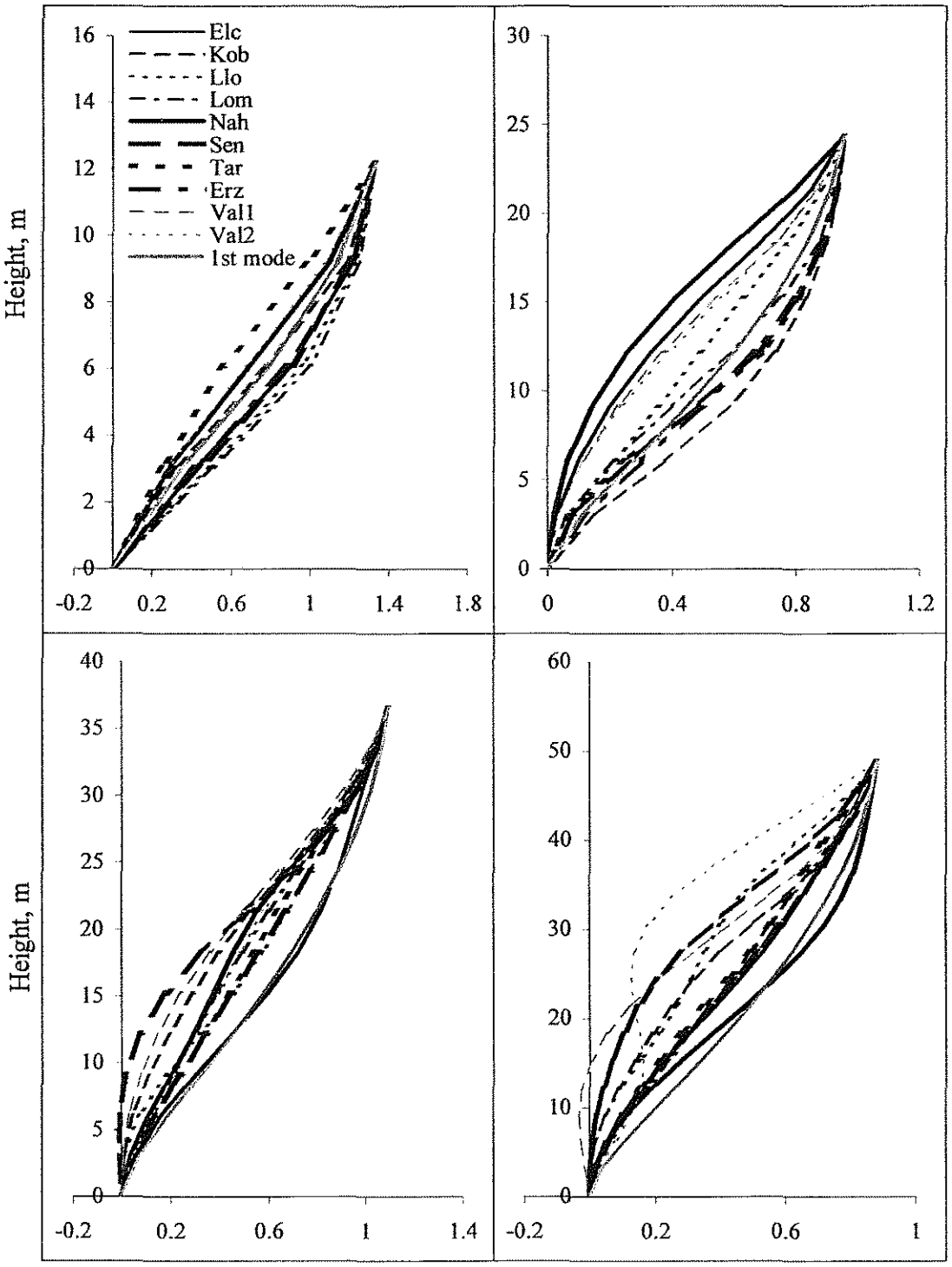


Figure 3.32: Distorted Shape of Regular Frames, Dynamic Analysis
Nomalized to Average Roof Drift

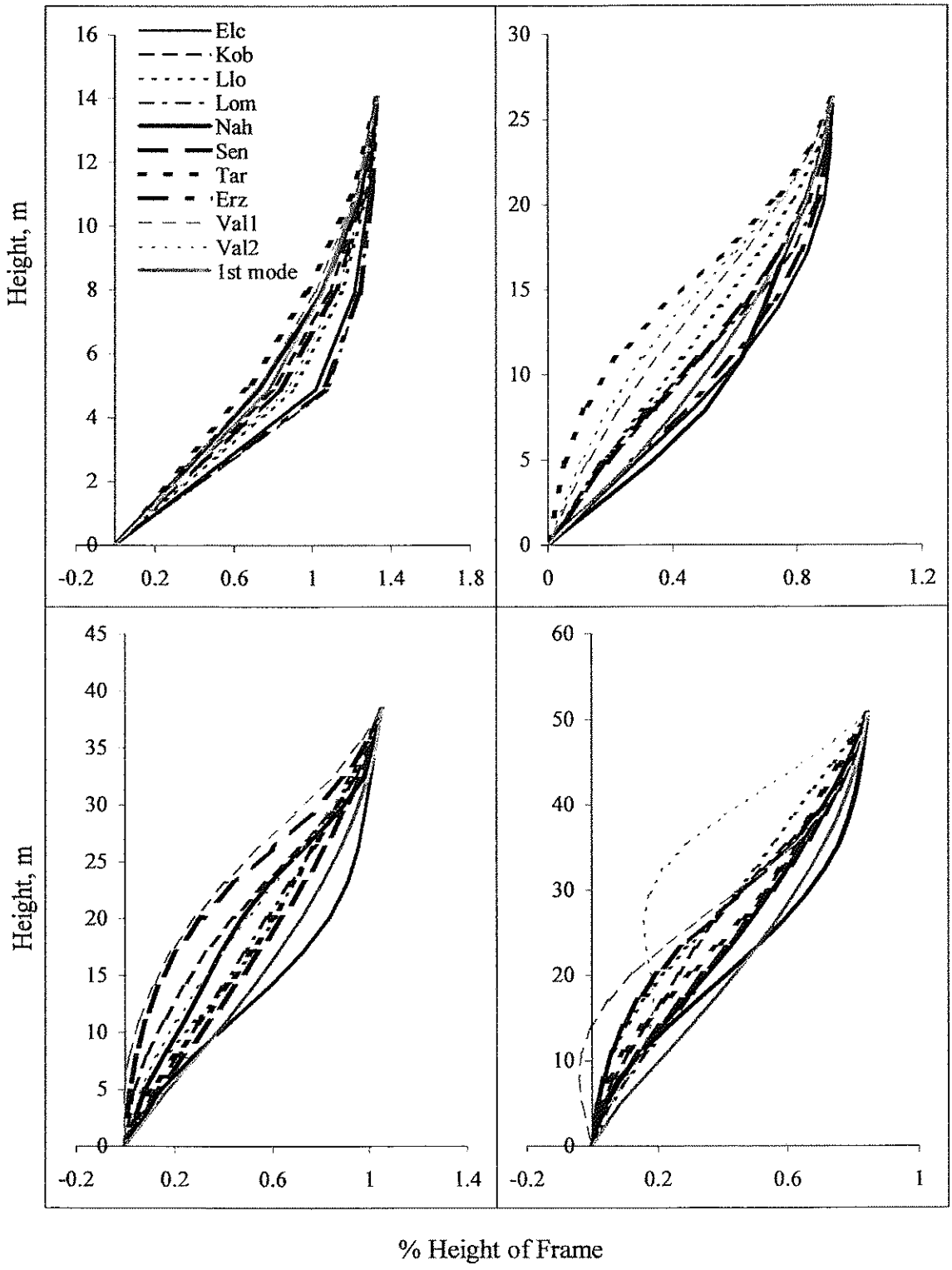


Figure 3.33: Distorted Shape of Tall First Story Frames, Dynamic Analysis Nomalized to Average Roof Drift

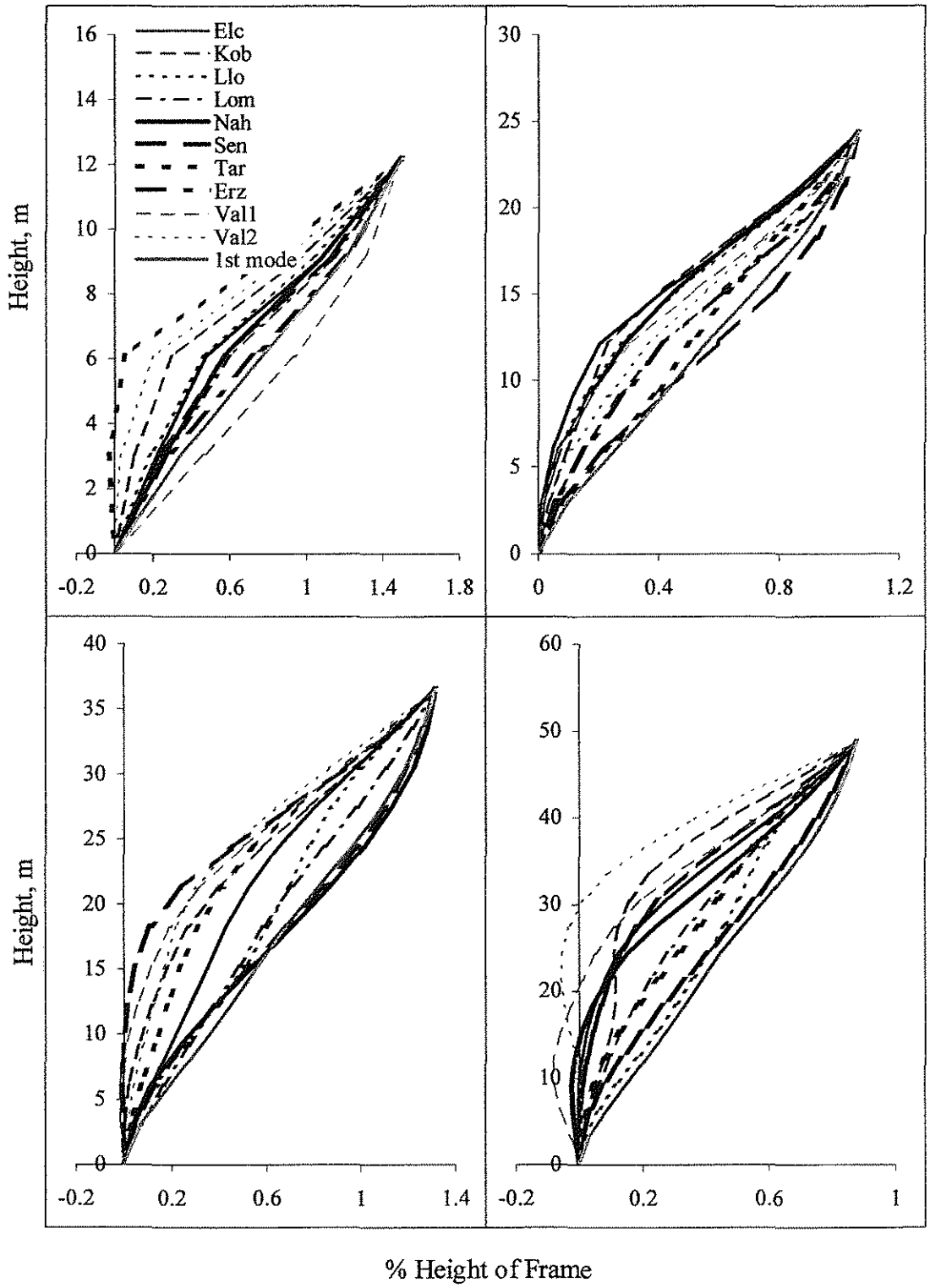


Figure 3.34: Distorted Shape of Irregular Frames, Dynamic Analysis
Nomalized to Average Roof Drift

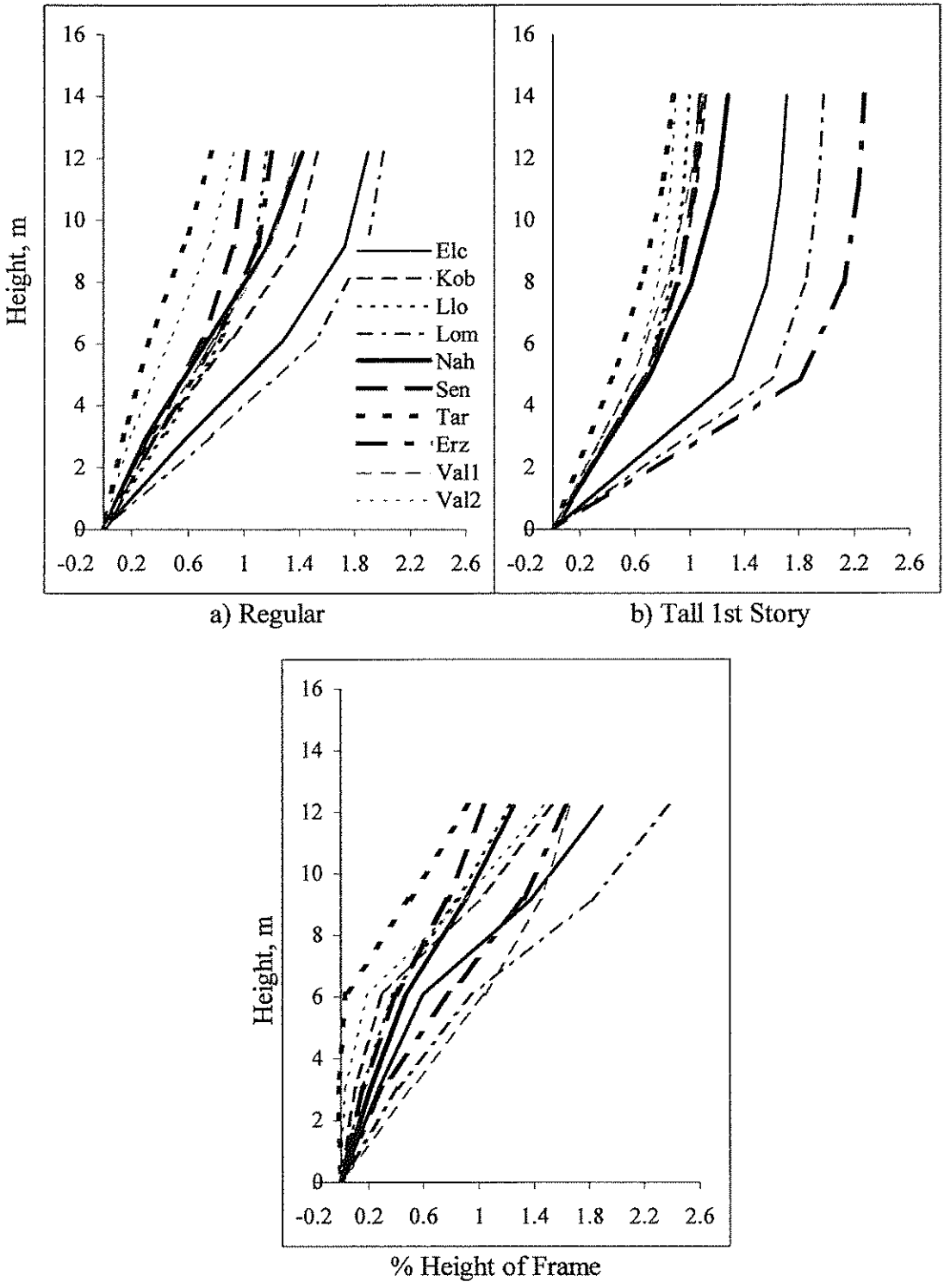


Figure 3.35: Distorted Shape of 4-Story Frames, Dynamic Analysis

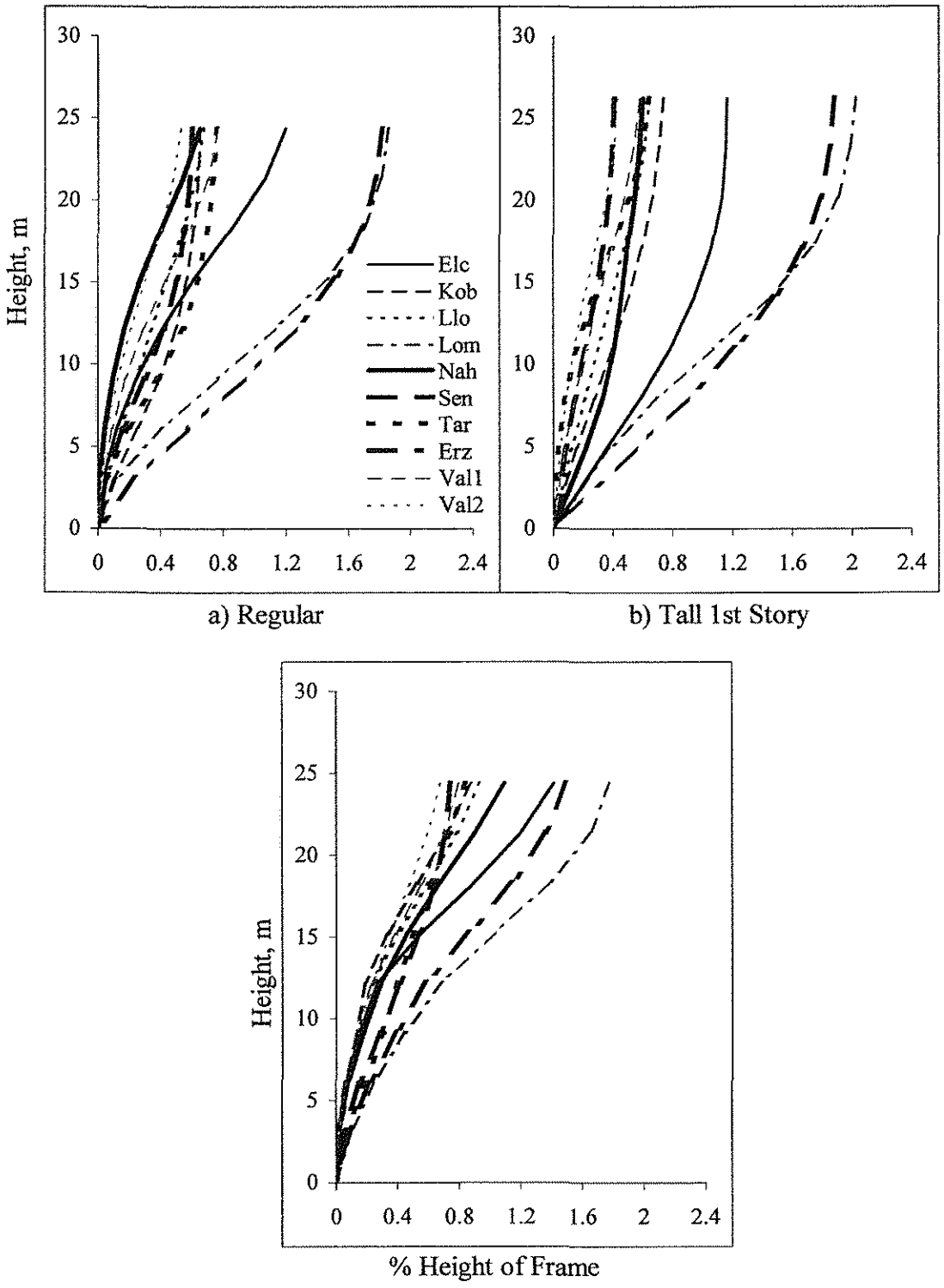


Figure 3.36: Distorted Shape of 8-Story Frames, Dynamic Analysis

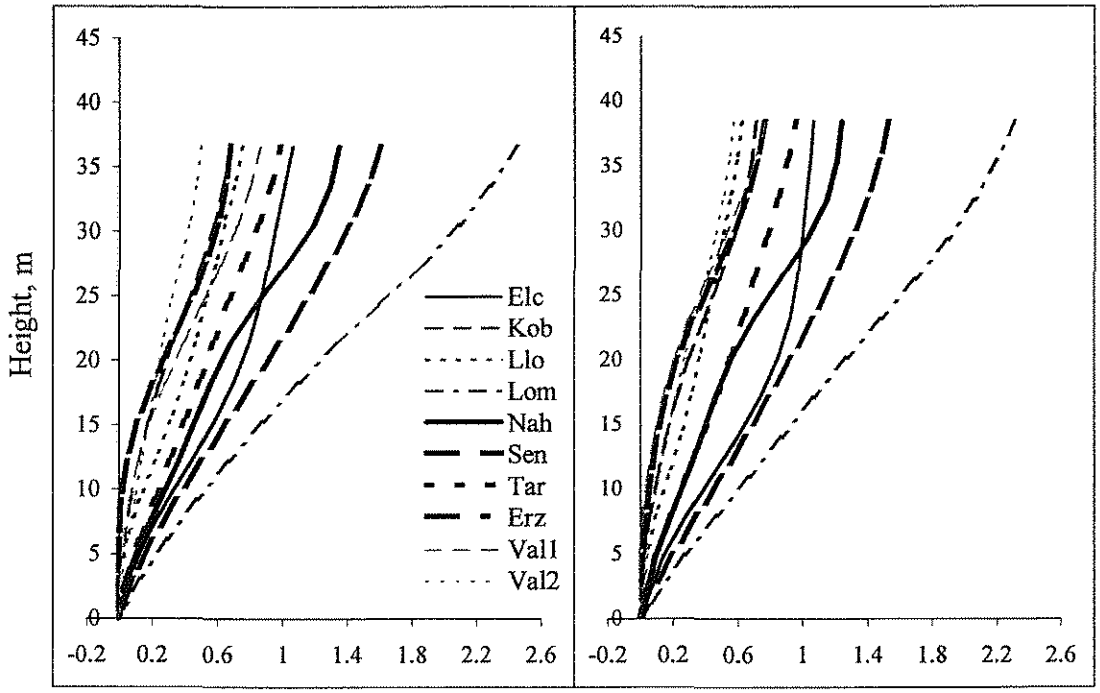


a) Regular

b) Tall 1st Story

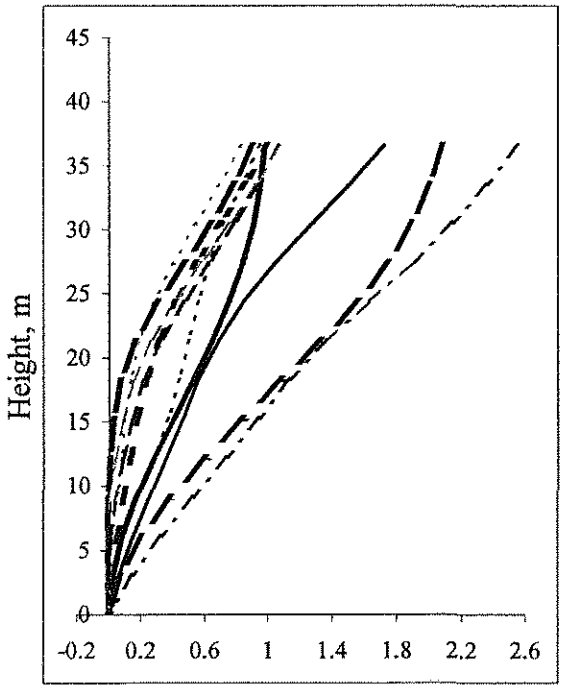


c) Irregular

Figure 3.37: Distorted Shape of 12-Story Frames, Dynamic Analysis

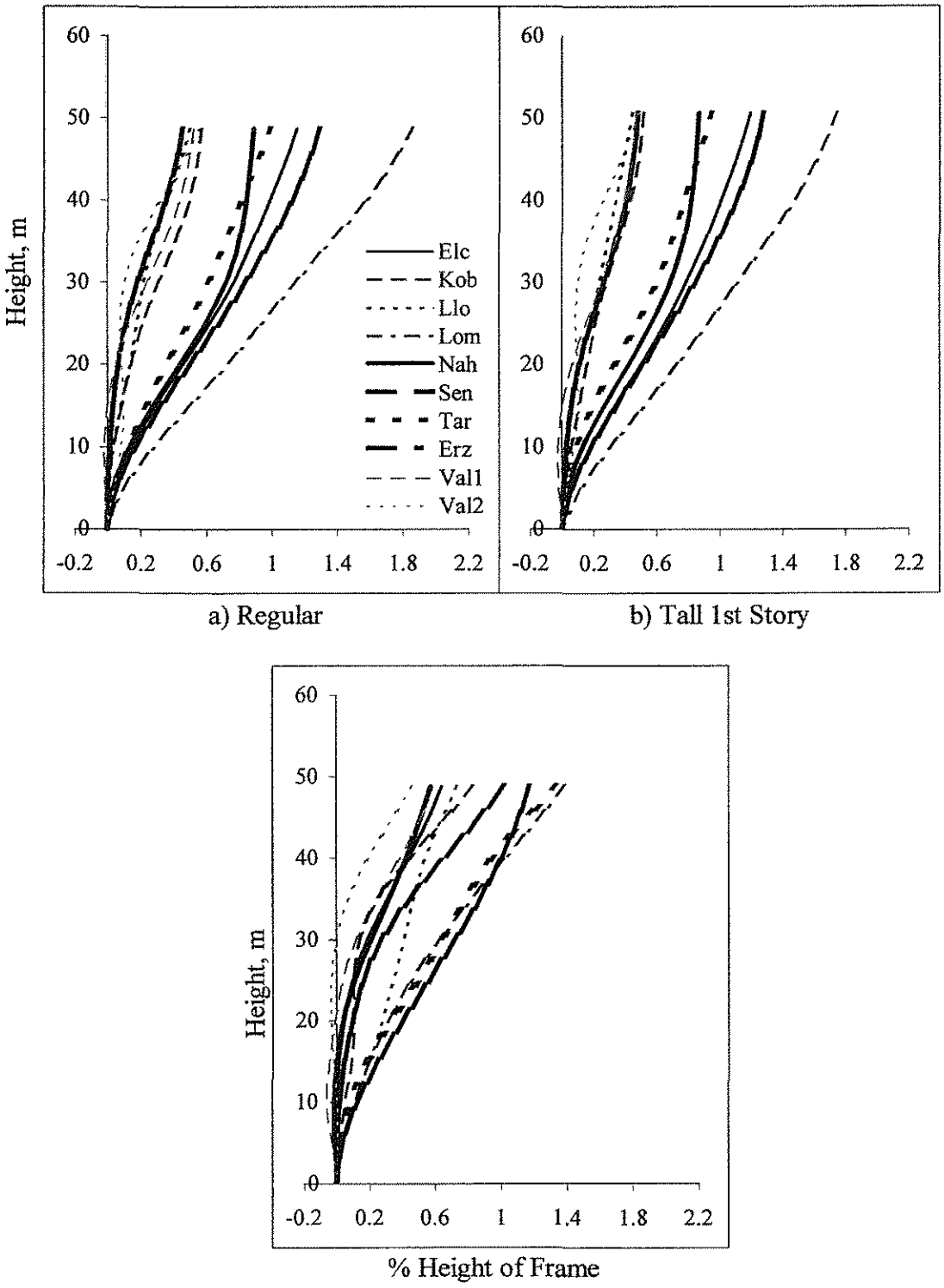


Figure 3.38: Distorted Shape of 16-Story Frames, Dynamic Analysis

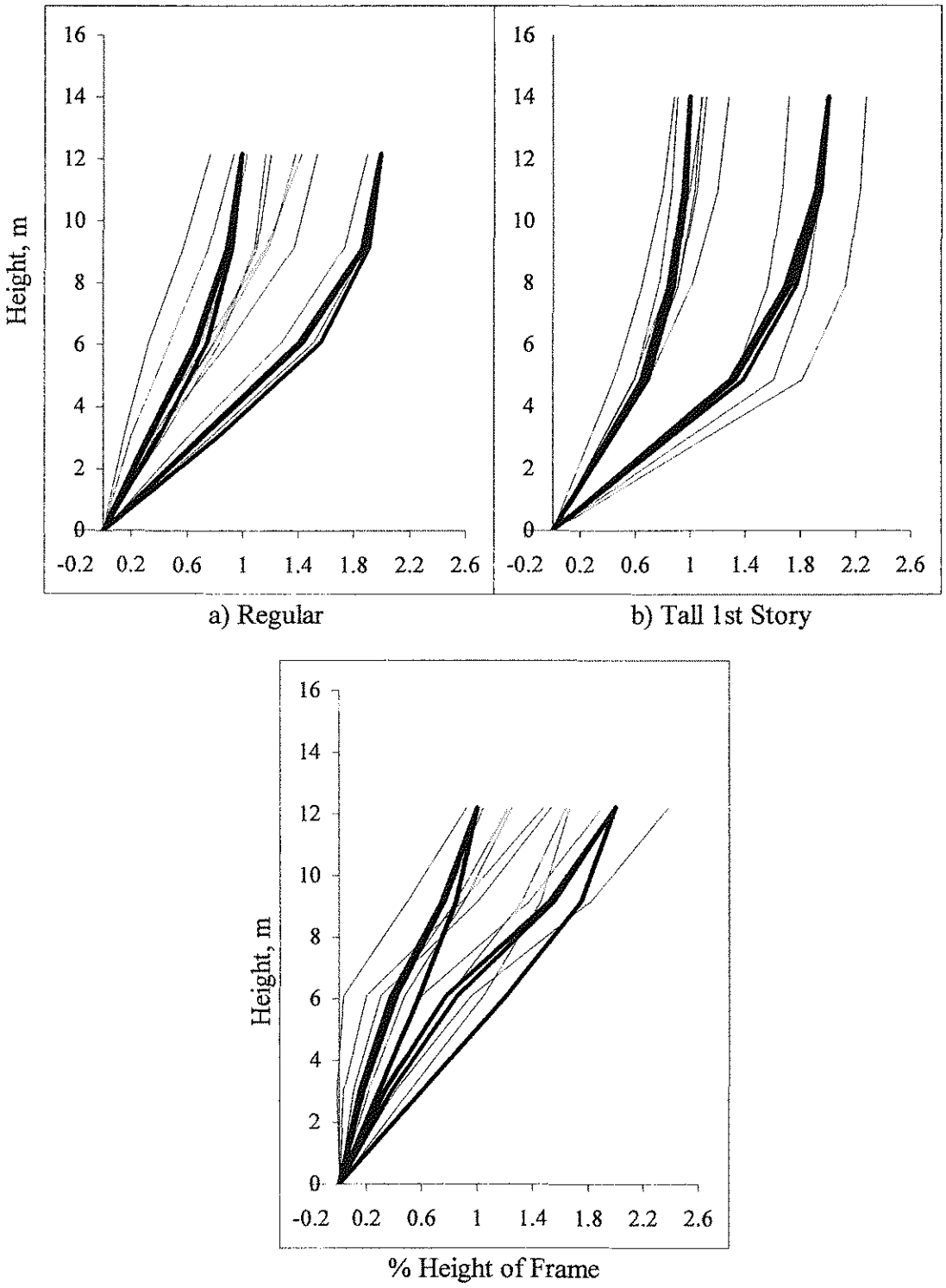


Figure 3.39: Distorted Shape of 4-Story Frames, Static and Dynamic Comparison

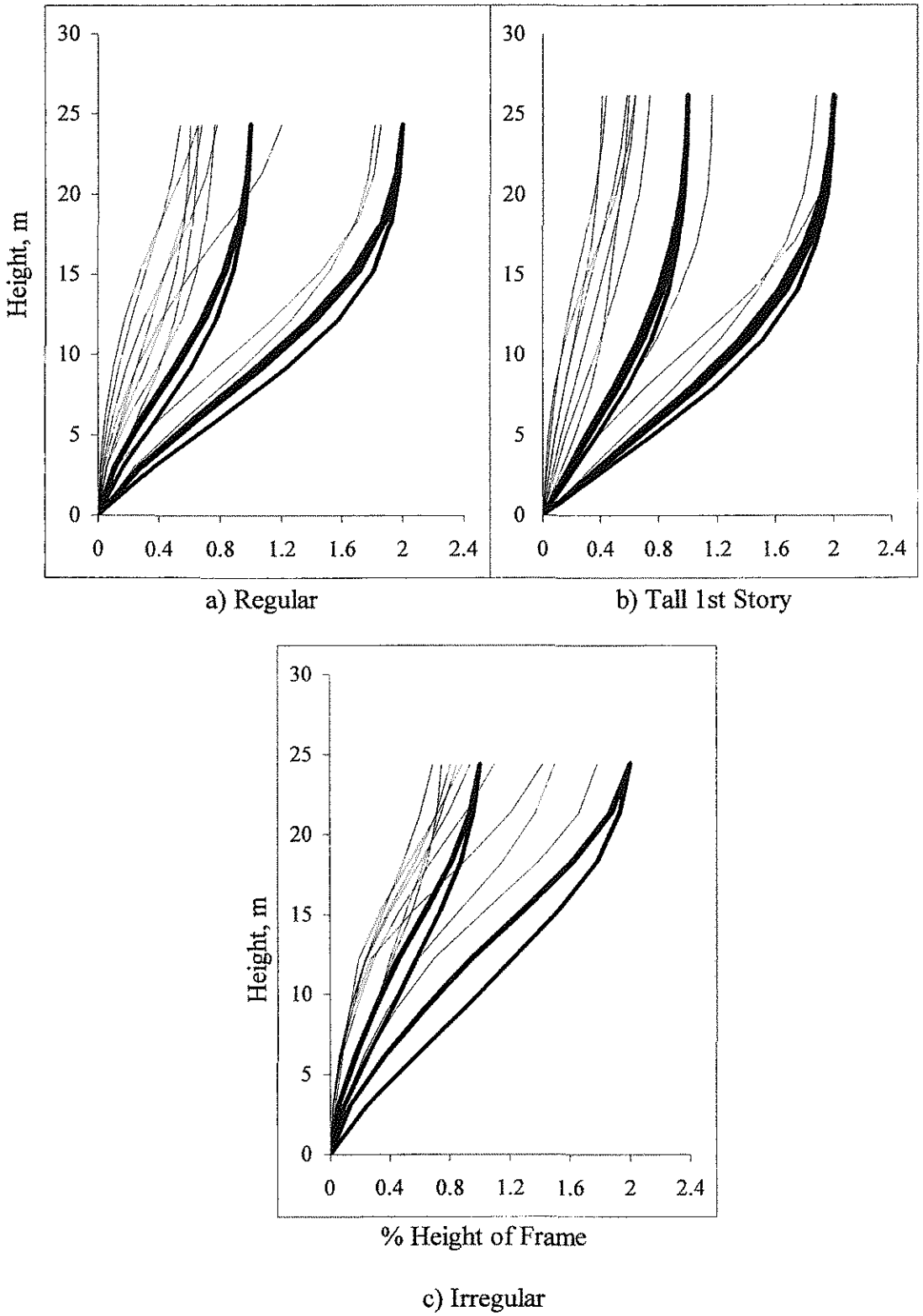


Figure 3.40: Distorted Shape of 8-Story Frames, Static and Dynamic Comparison

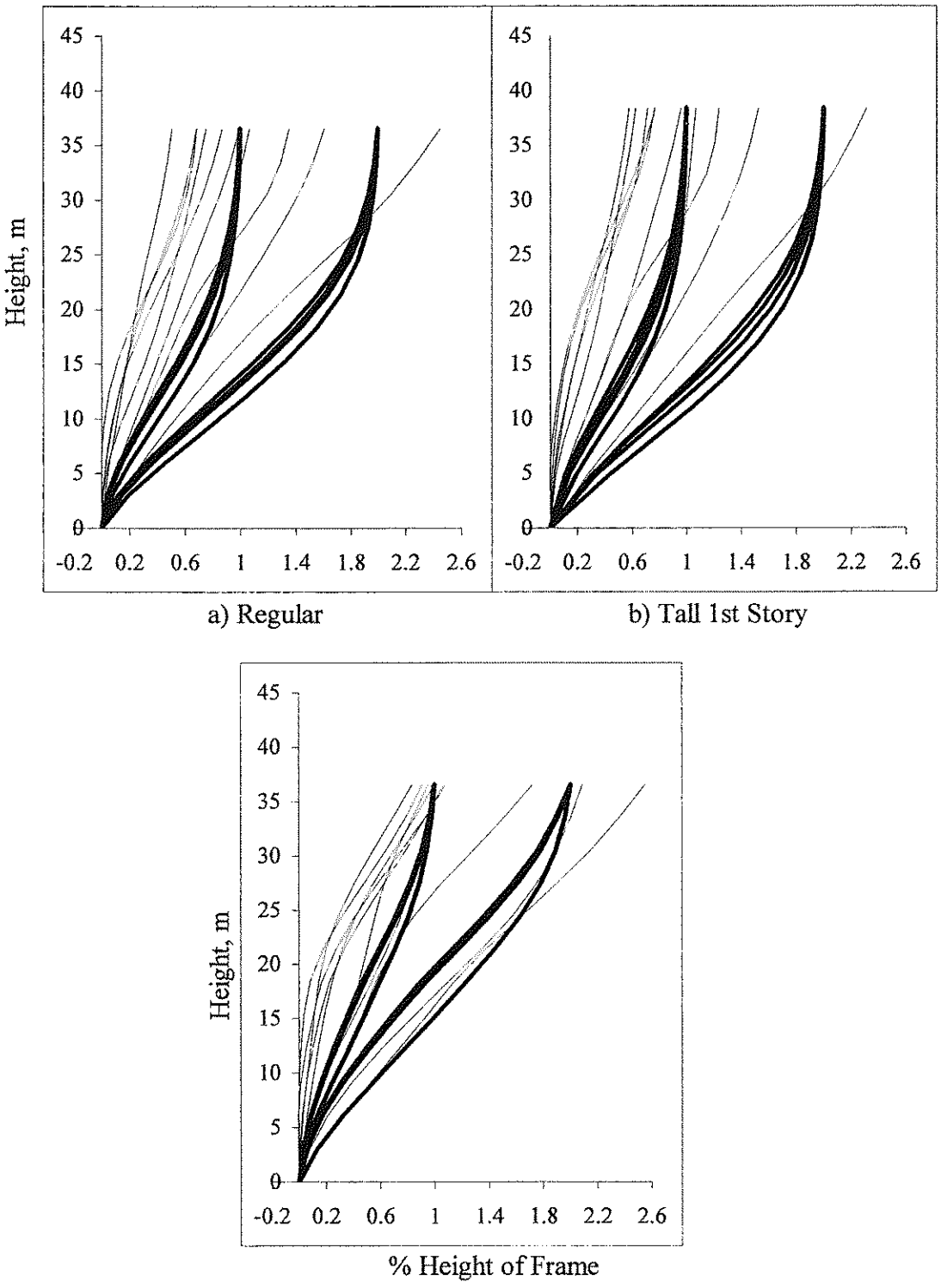


Figure 3.41: Distorted Shape of 12-Story Frames, Static and Dynamic Comparison

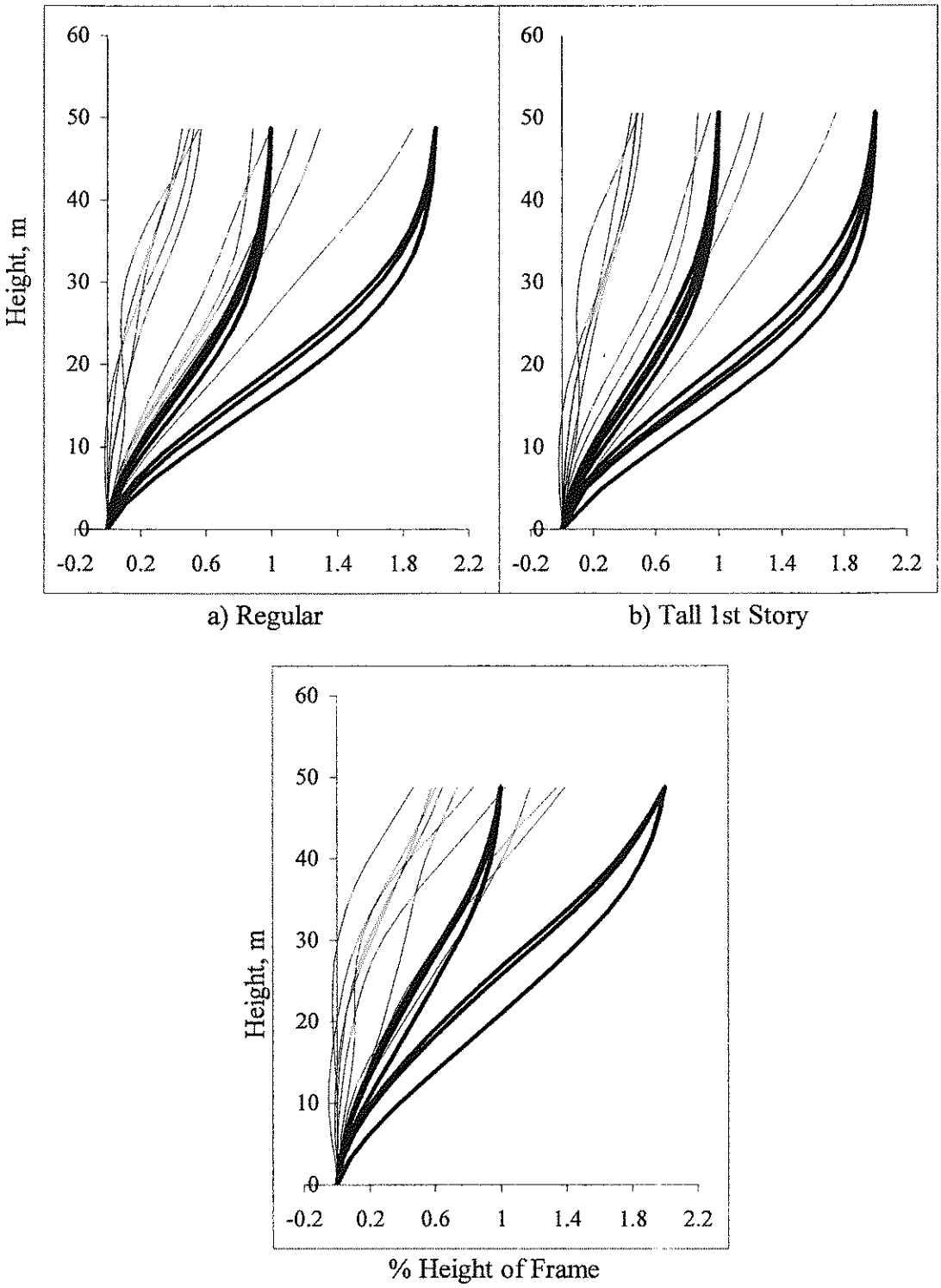


Figure 3.42: Distorted Shape of 16-Story Frames, Static and Dynamic Comparison